HIGHWAY RESEARCH RECORD

Number 119

Physical and Physico-Chemical Properties Of Soil, Processed Soil and Rock

8 Reports

Presented at the
44th ANNUAL MEETING
January 11-15, 1965

SUBJECT CLASSIFICATION
61 Exploration—Classification (Soils)
62 Foundations (Soils)
63 Mechanics (Earth Mass)
64 Soil Science

HIGHWAY RESEARCH BOARD
of the
Division of Engineering and Industrial Research
National Academy of Sciences—National Research Council
Washington, D. C.
1966

Department of Soils, Geology and Foundations

Eldon J. Yoder, Chairman
Joint Highway Research Project
Purdue University, Lafayette, Indiana

HIGHWAY RESEARCH BOARD STAFF

A. W. Johnson, Engineer of Soils and Foundations

J. W. Guinnee, Assistant Engineer of Soils and Foundations

DIVISION C

O. L. Lund, Chairman
Assistant Engineer of Materials and Tests
Nebraska Department of Roads, Lincoln

COMMITTEE ON SOIL AND ROCK PROPERTIES
(As of December 31, 1964)

G. A. Leonards, Chairman
Professor of Soil Mechanics, School of Civil Engineering
Purdue University, Lafayette, Indiana

George B. Clarke, Director of Research Center, School of Mines and Metallurgy, Rolla, Missouri
Robert W. Cunny, Chief, Soil Dynamics Branch, U. S. Army Engineer Waterways Experiment Station, Vicksburg, Mississippi
Robert C. Deen, Assistant Director of Research, Highway Research Laboratory, Kentucky Department of Highways, Lexington
Victor Dolmage, Consulting Geologist, Vancouver, British Columbia, Canada
Wilbur I. Duvall, Supervisory Physicist, Applied Physics Laboratory, U. S. Bureau of Mines, College Park, Maryland
Austin H. Emery, Associate Soils Engineer, Bureau of Soil Mechanics, New York State Department of Public Works, Albany
Charles L. Emery, Mining Engineering Department, Queens University, Kingston, Ontario, Canada
John A. Focht, Jr., Mc Clelland Engineers, Inc., Houston, Texas
Emmericus C. W. A. Geuze, Professor of Soil Mechanics and Foundation Engineering, Chairman, Civil Engineering Department, Rensselaer Polytechnic Institute, Troy, New York
Bernard B. Gordon, Staff Soils Engineer, California Department of Water Resources, Sacramento
James P. Gould, Associate, Mueser, Rutledge, Wentworth, Johnston, New York, New York
Ernest Jonas, Head, Soils and Foundations Department, Tippetts, Abbett, Mc Carthy, Stratton, New York, New York
Robert L. Kondner, Department of Civil Engineering, Northwestern University, Evanston, Illinois
Charles C. Ladd, Department of Civil Engineering, Massachusetts Institute of Technology, Cambridge
T. F. Mc Mahon, U. S. Bureau of Public Roads, Washington, D. C.
Victor Milligan, Associate, H. Q. Golder and Associates, Ltd., Toronto, Ontario, Canada
Roy E. Olson, Department of Civil Engineering, University of Illinois, Urbana
Shailer S. Philbrick, U. S. Army Engineer District of Pittsburgh, Pittsburgh, Pennsylvania

Ronald F. Scott, Division of Engineering and Applied Science, California Institute of Technology, Pasadena
T. H. Wu, Department of Civil Engineering, Michigan State University, East Lansing

COMMITTEE ON PHYSICO-CHEMICAL PHENOMENA IN SOILS

(As of December 31, 1964)

Hans F. Winterkorn, Chairman
Professor of Civil Engineering
Princeton University, Princeton, New Jersey

Gail C. Blomquist, School of Civil Engineering, Michigan State University, East Lansing
James H. Havens, Director of Research, Kentucky Department of Highways, Lexington
J. B. Hemwall, The Dow Chemical Company, Chemicals Laboratory, Midland, Michigan
Earl B. Kinter, U. S. Bureau of Public Roads, Washington, D. C.
Joakim G. Laguros, Department of Civil Engineering, University of Oklahoma, Norman
Philip F. Low, Department of Agronomy, Purdue University, Lafayette, Indiana
R. C. Mainfort, Michigan State Highway Department, Lansing
Edward Penner, Division of Building Research, National Research Council of Canada, Ottawa
Elmer A. Rosauer, Engineering Experiment Station, Iowa State University, Ames
J. B. Sheeler, Associate Professor of Civil Engineering, Engineering Experiment Station, Iowa State University, Ames
Mehmet A. Sherif, Department of Civil Engineering, University of Washington, Seattle
F. L. D. Wooltorton, Truffles, Pigbush Lane, Loxwood, Billingshurst, Sussex, England

COMMITTEE ON ENGINEERING GEOLOGY

(As of December 31, 1964)

Ernest Dobrovolny, Chairman
U. S. Geological Survey
Engineering Geology Branch, Federal Center
Denver, Colorado

Louis J. Circeo, Jr., Plowshare Division, Lawrence Radiation Laboratory, Livermore, California
A. C. Dodson, Chief Geologist, North Carolina State Highway Commission, Raleigh
Duncan J. Mc Gregor, State Geologist, Science Center, University of South Dakota, Vermillion
John D. Mc Neal, Research Engineer, State Highway Commission of Kansas, Topeka
Shailer S. Philbrick, U. S. Army District of Pittsburgh, Pittsburgh, Pennsylvania
Charles S. Robinson, Engineering Geology Branch, U. S. Geological Survey, Federal Center, Denver, Colorado
David L. Royster, Chief, Soils and Geological Section, Tennessee Department of Highways, Nashville
Rockwell Smith, Research Engineer—Roadway, Association of American Railroads, Chicago, Illinois
Travis W. Smith, Assistant Materials and Research Engineer—Foundation, California Division of Highways, Sacramento

Foreword

Highway Research Record No. 119 presents 8 papers that give the results of both basic and applied research. Most of these papers are presented in abridged form.

Soils that exhibit high volume change, with changes in moisture content or in environmental conditions have frequently caused pavements to heave in the order of ¾ to 1 foot and have shown excessive shrinkage on drying. Two papers, Ring and Budge, et al., report the results of studies that provide practicable solutions to sampling, testing, and analysis for control of the behavior of those soils on new constructions.

Two papers concern widely differing considerations of soil stabilization. Demirel, et al. report on the successful use of an ammonium chloride as a means for increasing the stability in the order of 60 percent for a slightly plastic clay-bearing limestone sand. Laguros' paper concerns a property of stabilized soil that has received increasing attention in recent years. Many nontreated and some treated subgrade soils and bases for pavements have settled in the wheeltrack area due to further compaction under service conditions. These shallow ruts interfere with drainage of pavement surfaces. Laguros reports on the reduction in consolidation of soils stabilized by various methods.

Three of the four remaining papers constitute a group that add markedly to our basic knowledge of the behavior of soil. The early stages of consolidation of a saturated soil under load, a time-dependent phenomenon in which the soil mass decreases in volume as water escapes from the pores of the soil, are fairly well understood and a workable theory exists which permits translation of test data to good estimates of actual fill subsidences due to the consolidation of foundation soil. However, a better understanding is needed of consolidation as it continues to decrease with time and occurs at a slower rate. Perloff, Johnson and DeGroff have added to the knowledge of this phenomenon, known as secondary consolidation, through the use of cyclic loading during the test. They have produced time-consolidation curves from controlled laboratory tests that are believed to be representative of what actually occurs in the field.

Clayey soils that swell and shrink have a strong affinity for water and are said to develop high values of suction or negative pore pressures. Yong and Chahal describe the techniques used for measurement of this soil property and the difficulties encountered in making this determination when air is trapped in the soil.

A great portion of the literature on soil mechanics deals with soil strength. Concepts of means for determining, analyzing, and expressing soils strength, particularly for clays, have changed some since the time of the earliest reports. As new knowledge has been developed changes have been made in the expressions for the shear strength of soils. Sherif reviews and analyzes some of the basic theories concerning shear strength of soils and investigations in the field of shear strength of cohesive soils. He explains the engineering properties from a modern point of view and proposes a new and complete failure criterion for shear strength of clays.

An example of how modern means for measuring certain properties of soil and rock and applying them directly to the solution of construction and maintenance problems is given in the paper by Goodman and Blake who detected, amplified, recorded, and measured subaudible sounds that are associated with strains in rock in unstable slopes (including landslides) and used this means to detect impending movements in landslide zones.

Contents

EFFECT OF LOAD CYCLING ON THE CONSOLIDATION PROCESS FOR A COHESIVE SOIL

W. H. Perloff, Jr., H. P. Johnson, and W. L. DeGroff 1

SHRINK-SWELL POTENTIAL OF SOILS

George W. Ring, III 17

A METHOD OF DETERMINING SWELL POTENTIAL OF AN EXPANSIVE CLAY

W. D. Budge, E. Sampson, Jr., and R. L. Schuster 22

DEFORMATION AND FLOW PROPERTIES OF CLAY SOILS FROM THE VIEWPOINT OF MODERN MATERIAL SCIENCE

Mehmet A. Sherif 24

ROCK NOISE IN LANDSLIDES AND SLOPE FAILURES

Richard E. Goodman and Wilson Blake 50

TREATMENT OF CRUSHED STONE WITH QUATERNARY AMMONIUM CHLORIDE

T. Demirel, M. H. Farrar, and J. M. Hoover 61

CONSOLIDATION CHARACTERISTICS OF STABILIZED CLAYEY SOILS

J. G. Laguros. 63

ENTRAPPED AIR EFFECTS ON SOIL SUCTION MEASUREMENTS

R. N. Yong and R. S. Chahal 64

Effect of Load Cycling on the Consolidation Process For a Cohesive Soil

W. H. PERLOFF, JR., Assistant Professor of Civil Engineering, Ohio State University;
H. P. JOHNSON, Captain, U. S. Corps of Engineers, Fort Belvoir, Virginia; and
W. L. DEGROFF, Senior Laboratory Technician, Department of Civil Engineering, Ohio State University

One-dimensional consolidation tests, in which the load was cycled between fixed values, were performed on a sensitive Maine clay. Load cycling, up to 13 times, caused increased settlement with each cycle, but application of a pressure in excess of that applied during cycling caused a return to the original virgin curve. Both primary and secondary compression were reduced by load cycling. Pore water pressures measured at the base of single-drained specimens were of measurable magnitude during secondary compression.

•CONSOLIDATION of a saturated soil is the time-dependent decrease of soil volume due to the escape of water from the void in the soil mass. The classical analysis of one-dimensional consolidation (Terzaghi, 16) based on hydrodynamic principles, is the most commonly applied predictive method for handling consolidation problems. The consolidation experienced by a soil under a particular applied pressure increment is shown in Figure 1. The time-settlement curve in this figure is typical for one-dimensional consolidation tests on many cohesive soils. The dash line shows the time-settlement relation predicted by the classical consolidation theory. The portion of the consolidation predicted by the classical theory is commonly referred to as primary consolidation, and the additional portion is usually called secondary compression. Gray (4), Buisman (1), Taylor (15), Leonards and Girault (8) and Wahls (18) are among the many investigators who have examined secondary compression. Many hypotheses about its causes have been advanced although no generally accepted explanation has yet been proposed.

BACKGROUND

Effect of Secondary Compression on Time-Settlement Relation

The characteristic features of secondary compression and its influence on the time-settlement curve are shown in Figure 1. This curve is typical of results reported by many investigators. The theoretical and experimental curves usually agree quite well until approximately 60 to 70 percent of the theoretical consolidation has occurred. At that point the theoretical curve frequently falls below the experimental curve and then crosses the experimental curve again when almost 100 percent of the theoretical consolidation has occurred. For relatively large values of the time, the experimental curve becomes linear with the logarithm of time. Although exceptions to linearity have been reported (Hanrahan, 6; Palmer and Thompson, 13), Haefeli and Schaad (5) observed secondary compression to be linear with logarithm of time for load durations of about 3 yr.

The quantitative description of secondary compression is usually given by the amount of secondary compression occurring over one logarithmic cycle of time. When the

Paper sponsored by Committee on Soil and Rock Properties.

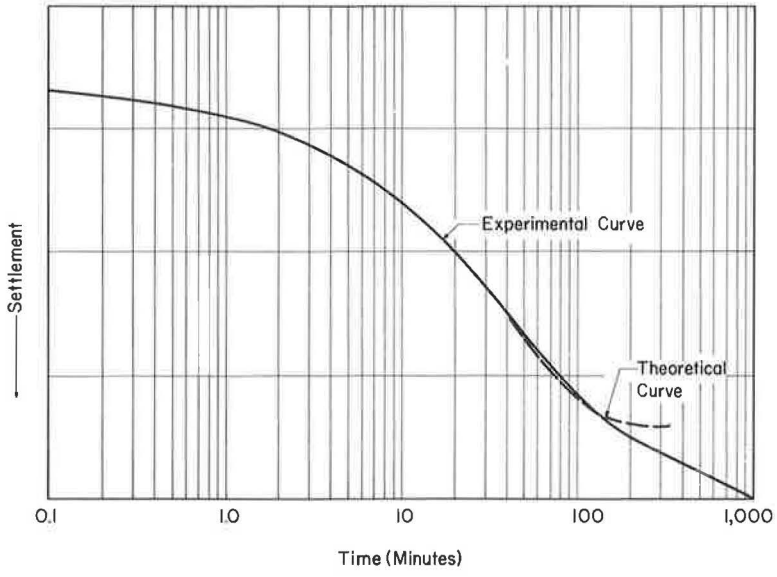

Figure 1. Typical time-settlement curve for one-dimensional consolidation test on cohesive soil.

consolidation curve is expressed in terms of void ratio change, the secondary compression is expressed by the coefficient of secondary compression, C_α, equal to the void ratio change occurring over one logarithmic cycle of time. When the consolidation curve is expressed in terms of settlement, secondary compression can be represented by the coefficient of secondary settlement, R_s, the settlement occurring over one logarithmic cycle of time. For one-dimensional compression, these two quantities are proportional, and will be used interchangeably hereafter.

Factors Affecting C_α (R_s)

Considerable research effort has been devoted to the study of the coefficient of secondary compression, and the factors affecting it. Moran et al. (10), Leonards and Girault (8), and Wahls (18) found that C_α varied with the total pressure applied to the soil specimen. A similar result was observed by Ray (14) for three-dimensional consolidation in a triaxial compression chamber. However, Taylor (15) and Newland and Allely (11) observed that C_α was independent of the total consolidation pressure. Girault (3), Newland and Allely (11), and Wahls (17) all agree that C_α is independent of the pressure increment ratio (the ratio of the applied pressure increment to the previous total pressure). Girault (3) inferred this from the fact that the ratio of secondary compression to primary consolidation, R_s/R_{100} (where R_{100} is the amount of settlement occurring during primary consolidation), depended on the pressure increment ratio in the same way as $1/R_{100}$.

It has been suggested in the past (Moran, et al., 10; Leonards and Ramiah, 9) that preloading reduces secondary compression. It was felt that if preloading once would reduce secondary compression, perhaps cycling of the load a sufficient number of times would completely eliminate it. To shed some additional light on the foregoing factors, a laboratory investigation was undertaken to examine the influence of load cycling on the consolidation process.

LABORATORY INVESTIGATION

Description of Soil

The soil tested was a sensitive gray, silty clay with black streaks from Clinton, Maine. Undisturbed samples of the soil were taken with 3½-in. diameter Shelby tubes

from a depth of 9 to 11 ft beneath the surface. The results of routine laboratory tests indicate the following properties:

Specific gravity of solids	2.77
Liquid limit	33.0 percent
Plasticity index	13.0 percent
Dry unit weight	91.4 pcf
Field water content	30.4 percent
Organic content	0.7 by weight (ignition method)
Sensitivity	7

The clay appears to have been deposited under marine conditions and subsequently uplifted, undergoing some leaching of salts from the pore fluid; it was normally consolidated and fully saturated.

Apparatus and Testing Procedures

All soil specimens were extruded from the 3½-in. diameter Shelby tubes and trimmed to fit snugly into consolidation rings. Fixed-ring consolidometers were used for all tests. The brass rings were liberally coated with Dow-Corning silicone grease to reduce the effects of side friction. All samples were 2½ in. in diameter and 1 in. thick before consolidation.

Three specimens were consolidated with drainage permitted at both top and bottom of the specimens. These tests were carried out in a standard manner using dial gages with 0.0001-in. divisions to measure settlements. In addition, one specimen was consolidated in a specially modified fixed-ring consolidometer in which drainage was permitted only at the top, so that pore water pressure could be measured at the base of the specimen. The special consolidometer (Fig. 2) consists of a standard fixed-ring type of consolidometer with the bottom porous stone replaced by a brass plug with a smaller porous stone inserted in it. Two outlets are provided for the water at the base leading into temperature-compensated electrical pressure transducers, a Dynisco PT 25 with a range of pressure from 0 to 100 psi, and a Dynisco PT 85 with a range from 0 to 1 psi. This special low pressure transducer was isolated from the system by a valve to protect it from overloading. Excitation of the pressure transducers was accomplished with B and F model 110-T input conditioners with zener diode regulated voltage outputs. In addition, a thermistor (temperature sensitive resistance) was mounted inside the consolidometer underneath the specimen to permit observation of temperature.

Settlement of the specimen was measured by Daytronic 103C-200 linear variable differential transformer (LVDT). Outputs from the pressure transducers and the LVDT were fed into Varian G-14 strip-chart recorders, and recorded continuously as a function of time. It was possible to record accurately pressure changes as small as that created by ¼ mm of water when using the PT 85. Settlements of 5×10^{-6} in. could also be observed. Temperature changes were recorded on a Bausch and Lomb V. O. M. 5 strip-chart recorder and could be observed with an accuracy of 0.05 C.

Accuracy of the recorded variables was continually checked. The zero setting of the pressure transducers was checked daily. Correct calibration of the pressure transducers was verified every second or third day. The LVDT and thermistor circuits were calibrated before the test started and checked at the end of the test. No variations were observed in the response of the various transducers of sufficient magnitude to influence the results.

Description of Tests

The cyclic loading was accomplished by applying pressure increments to the soil to some predetermined pressure on the virgin curve. The soil was rebounded in the standard manner to a predetermined pressure, with each rebound increment remaining at least 24 hr. Pressure increments were then reapplied, in the same manner as for the initial loading until the previous maximum pressure was reached. In this way, one cycle was completed. The process was repeated for all additional cycles.

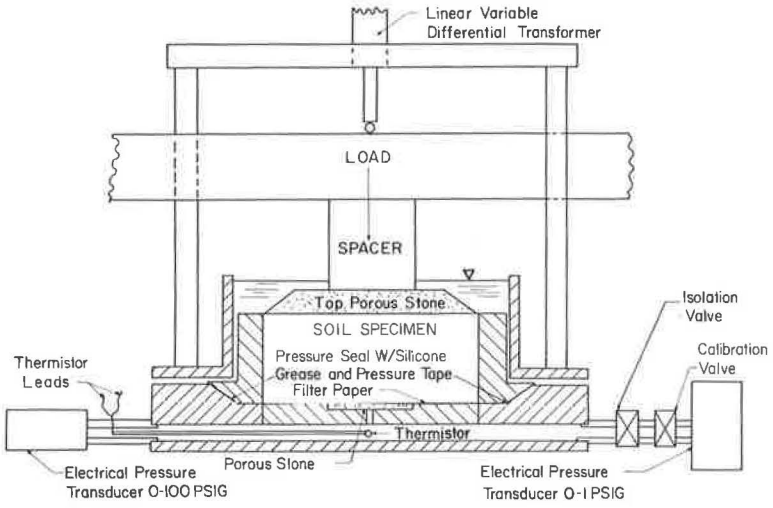

Figure 2. Single-drained consolidometer with provisions for pore water pressure and temperature measurement.

TABLE 1

SUMMARY OF TESTS

Specimen No.	Max. Press. Before Cycling (kg/cm^2)	Cyclic Loading		No. of Recomp. Cycles	Duration of Test (days)
		Min. Press. (rebound to) (kg/cm^2)	Max. Press. (reload to) (kg/cm^2)		
1[a]	11.50	1.44	11.50	13	215
2[a]	22.99	2.87	22.99	13	211
3[a]	5.75	0.719	5.75	13	213
4[b]	7.54	0.228	7.54	3	80

[a]Double drained.
[b]Single drained.

A pressure increment ratio of approximately 1 was used for all tests. On all initial loadings and for the first few reloadings, the pressure increment duration was 48 hr. During later load cycles, when the time to 100 percent consolidation was very short, the time was reduced to 24 hr. Each of the specimens was cycled over a different range of pressure to obtain an indication of the influence of the magnitude of pressure on the results.

Table 1 gives a summary of the tests reported. At the end of 13 recompression cycles, specimens 1 and 3 were loaded to a total pressure of 22.99 kg/sq cm before the final rebound. Specimen 4 was loaded to 15.05 kg/sq cm after 3 recompression cycles.

TEST RESULTS

Settlement-Pressure Relationships

The relationship between settlement and pressure after 24 hr under a given load increment is shown in Figures 3 through 5 for specimens 1-3. (Figure 3c also shows the effect of load cycling on time-settlement curves for double-drained specimen 1.) The curve in Figure 6, for specimen 4, is for settlements at the Casagrande 100 percent consolidation point. Results of the cyclic loading are shown in detail in Figures 3b,

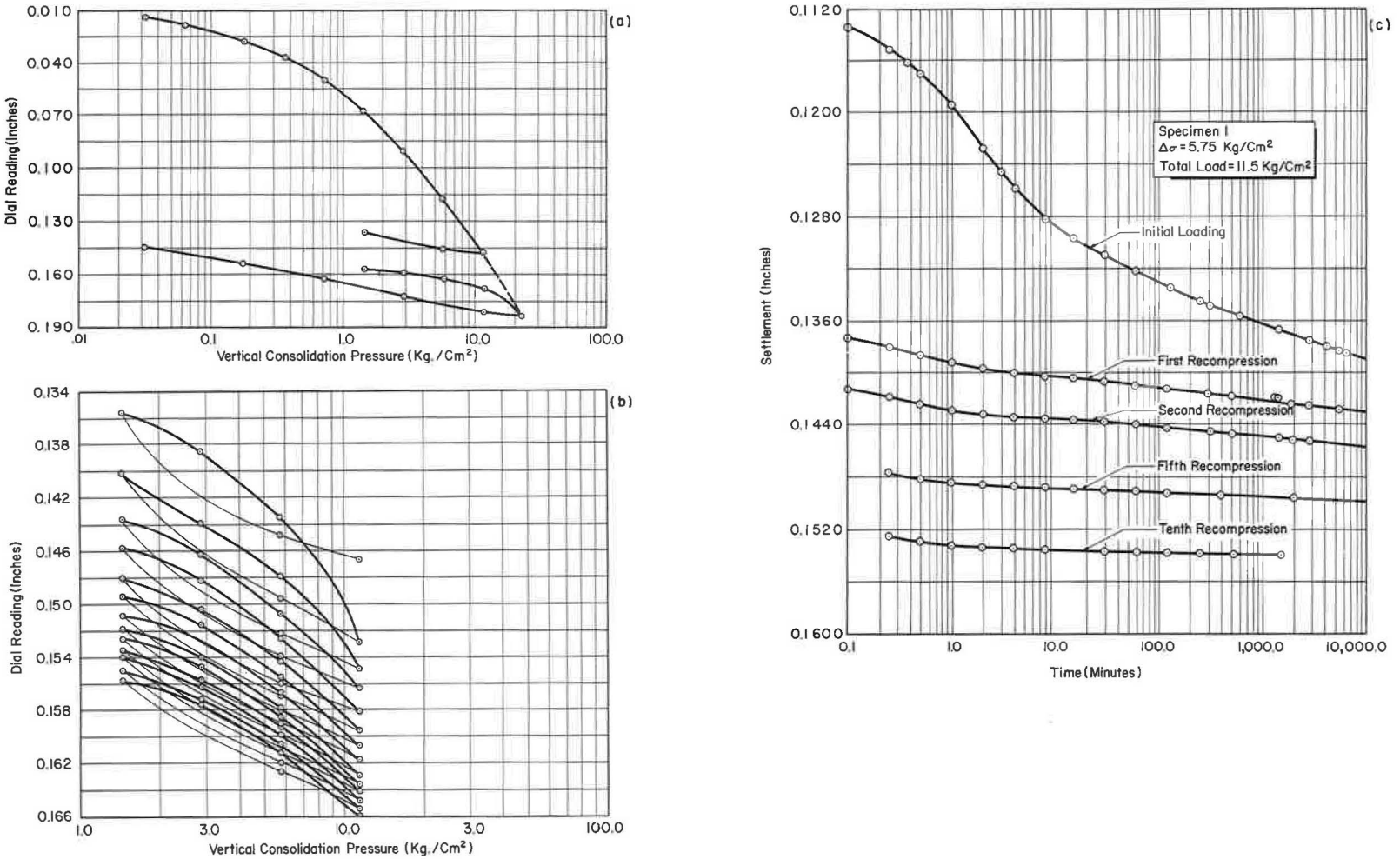

Figure 3. Relationship between consolidation pressure and settlement for specimen 1: (a) initial and final loading; (b) load cycling; (c) effect of load cycling on the time-settlement curves for a double drained specimen.

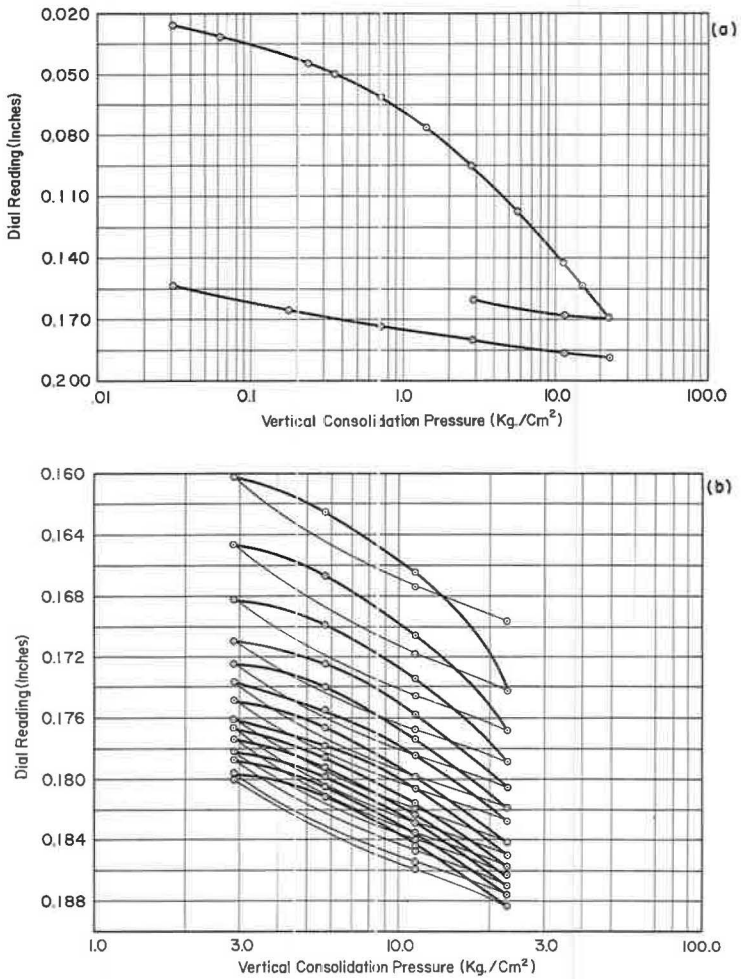

Figure 4. Relationship between consolidation pressure and settlement for specimen 2: (a) initial and final loading, and (b) load cycling.

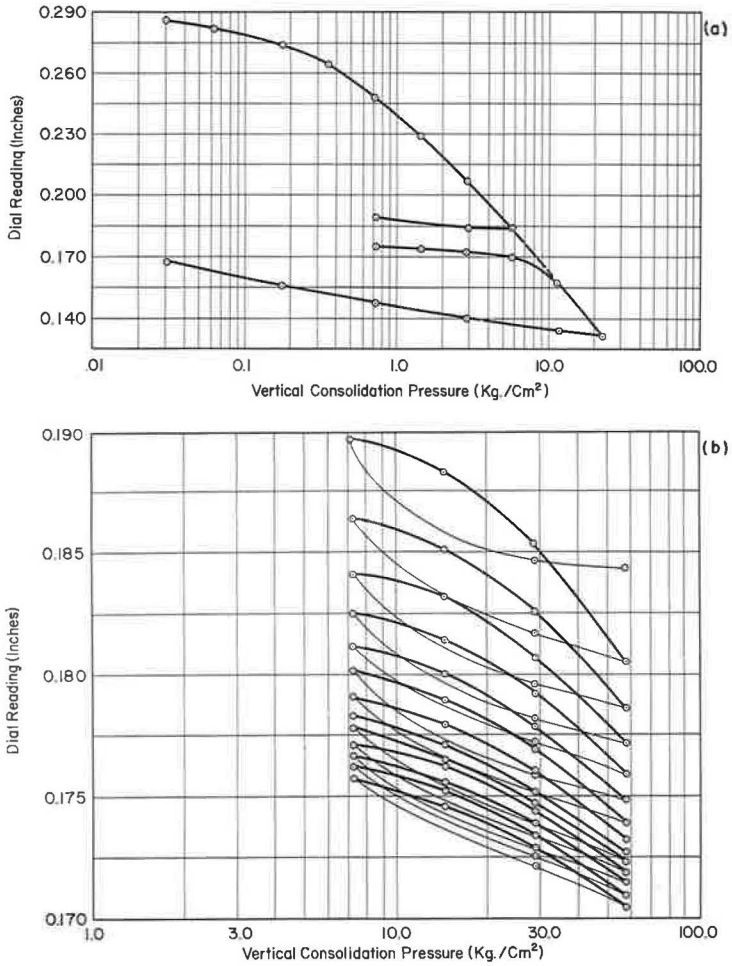

Figure 5. Relationship between consolidation pressure and settlement for specimen 3: (a) initial and final loading, and (b) load cycling.

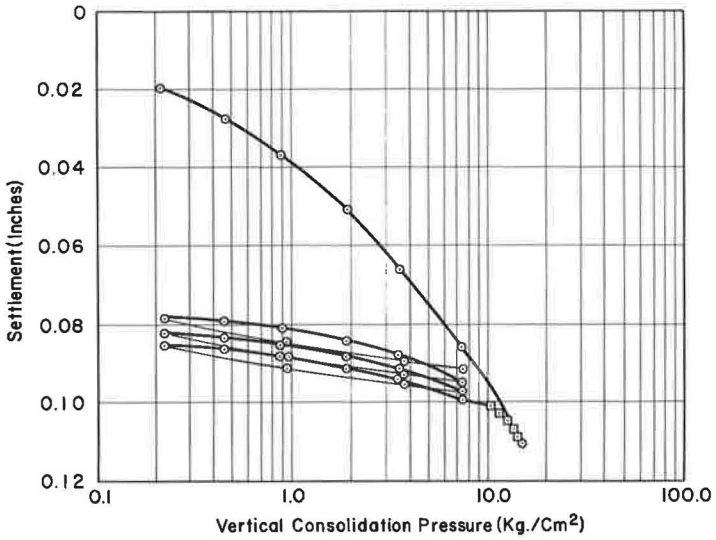

Figure 6. Relationship between consolidation pressure and settlement for specimen 4.

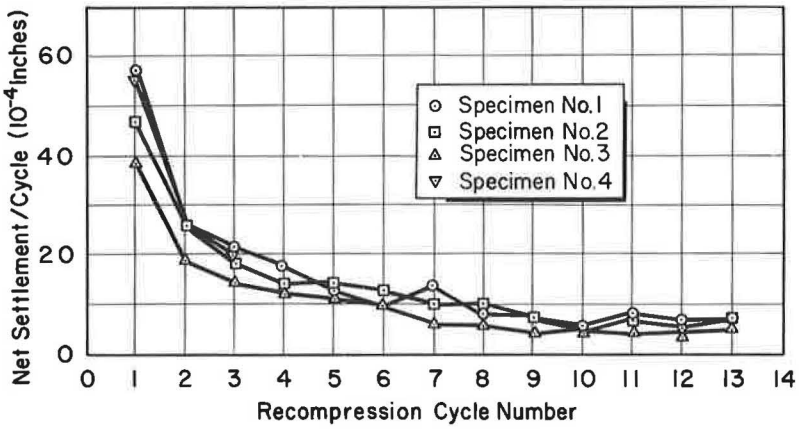

Figure 7. Effect of number of recompression cycles on net settlement.

4b, 5b, and 6 for the four specimens, where the reloading curves are shown as heavy lines and the rebound curves as lighter lines to facilitate interpretation. The net displacement for each hysteresis loop decreases as the number of cycles increases. In addition, there is a decrease in the size of the hysteresis loops for each successive cycle of loading.

The net reduction in sample thickness for each load cycle is shown as a function of the number of recompression cycles in Figure 7. The results do not definitely indicate whether the net settlement will approach zero after some large number of cycles. Tentative extrapolation of the results suggests that at least 50 cycles would be required to reduce the net settlement to zero.

At the end of 13 load cycles for specimens 1 through 3, and three load cycles for specimen 4, the specimens were loaded to the next higher pressure. Figures 3a, 5a, and 6 show that the settlement-pressure relationship returns to the virgin compression

curve. Since continuous pore water pressure measurements were made at the base of specimen 4, it was possible to estimate the average effective consolidation pressure at each point during the increment. This was done using the expressions presented by Perloff et al. (12) for the pore water pressure distribution throughout a consolidating specimen which include the influence of flexibility of the pressure measuring system on this distribution. The method by which these equations have been used to determine the average effective consolidation pressure is given in the Appendix. With the average effective consolidation pressure known, the shape of the settlement-pressure curve between the end points can be determined for the last applied pressure increment, and is shown in Figure 6 as the portion of the curve indicated by the small rectangles. It appears that load cycling has a prestressing effect on the soil, since the preconsolidation pressure determined from this curve is distinctly higher than the previously applied maximum pressure. This is not surprising since the void ratio is less than that on the virgin curve under the initial loading. This effect appears similar to the "quasi-preconsolidation pressure" reported by Leonards and Ramiah (9) and Leonards and Altschaeffl (7) for consolidation tests in which a given pressure has remained on a specimen much longer than the ordinary time increment.

Coefficient of Secondary Settlement (R_s)

The coefficients of secondary settlement, R_s, are shown in Figure 8 as a function of the effective consolidation pressure for the initial loading for the four specimens. The magnitude of R_s increases as the effective consolidation pressure increases to a pressure of approximately three times the preconsolidation pressure, at which point the magnitude of R_s remains more or less constant. This result is consistent with data presented by Leonards and Girault (8) and Wahls (18) for one-dimensional consolidation tests, and data presented by Ray (14) for triaxial consolidation tests.

These data imply that the magnitude of R_s is independent of the length of the drainage path for a given specimen thickness because the values of R_s are the same for specimen 4 as for the other three specimens, even though specimen 4 was single-drained and the others were double-drained.

The influence of load cycling on the magnitude of R_s is shown in Figure 9, where the ratio of R_s at the end of the nth load cycle, R_{sn}, to R_s for the initial loading at that pressure, R_{si}, is a function of number of recompression cycles. The magnitude of R_s is reduced to about 36 to 38 percent of its initial value in the first recompression cycle. As the number of recompression cycles increases, R_s decreases to approximately 5 to 8 percent of its initial value, at which point it remains essentially constant with continued load cycling, at least for the number of cycles observed in the study. The curves appear quite similar even though each curve corresponds to a different magnitude of load. Furthermore, there does not seem to be any effect of length of drainage path, for a given specimen thickness, on the ratio R_{sn}/R_{si}.

The effect of load cycling on the ratio of the coefficient of secondary settlement, R_s, to the amount of settlement occurring during primary consolidation, R_{100}, was introduced by Girault (3) as an indicator of the shape of the time-settlement curve. A small value of R_s/R_{100} indicates a curve which approximates the theoretical curve. A large value of R_s/R_{100} indicates substantial deviation from the Terzaghi curve, particularly at times near and after the 100 percent point. Girault found that R_s/R_{100} was a function of the pressure-increment ratio. He reported results of tests on Mexico City and Bedford clays and showed that R_s/R_{100} varied from 0.8 to 1.0 at a pressure-increment ratio of approximately 0.15. The ratio R_s/R_{100} decreased rapidly as the pressure-increment ratio increased, with values as small as 0.05 to 0.1 at a pressure-increment ratio of 3. At a pressure-increment ratio of one, Girault (3) found that R_s/R_{100} varied from approximately 0.05 to 0.15. Table 2 gives the magnitude of R_s/R_{100} at each pressure for the initial and recompression cycles for specimen 4, tested at a pressure-increment ratio of approximately 1. Due to the hydraulic loading arrangement used for testing this specimen, the actual pressure-increment ratio varied from 0.87 to 1.12. Almost all of the values of R_s/R_{100} lie between 0.1 and 0.2, indicating that the shape of the time settlement curve is essentially the same after cycling of the load as before.

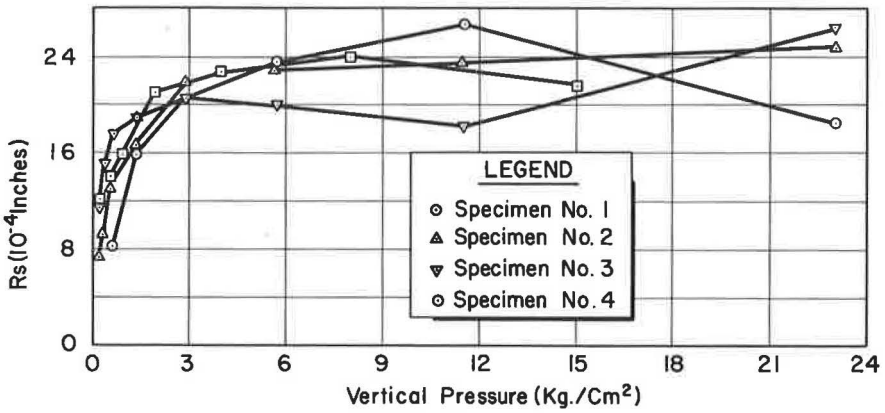

Figure 8. Effect of consolidation pressure on coefficient of secondary settlement (R_s).

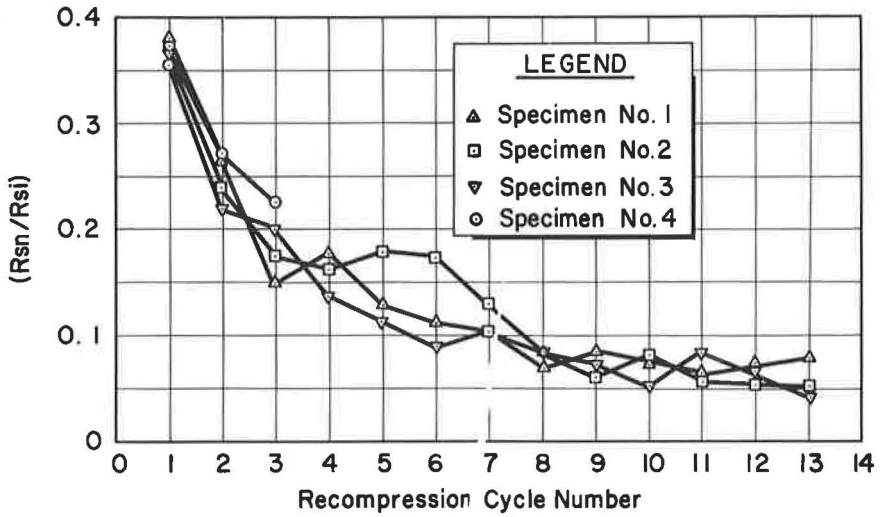

Figure 9. Effect of number of recompression cycles on the coefficient of secondary settlement.

TABLE 2

EFFECT OF LOAD CYCLING ON R_s/R_{100} FOR SPECIMEN 4

Pressure (kg/cm^2)	Initial Increment	Cycle 1	Cycle 2	Cycle 3
0.216	0.071			
0.465	0.062	0.114	0.110	0.133
0.903	0.230	0.112	0.090	0.114
1.918	0.185	0.099	0.081	0.094
3.580	0.206	0.114	0.100	0.095
7.540	0.160	0.186	0.157	0.151
15.050	0.191			

It appears that whatever prestress effects are induced by cycling of the load, the secondary compression is affected in essentially the same way as the magnitude of primary consolidation.

Pore Water Pressure Dissipation as a Function of Time

The classical consolidation theory is formulated in terms of pore water pressure dissipation. Void ratio changes are inferred from the assumption that volume changes of the soil mass are proportional to the pressure dissipation. According to the classical theory, pore water pressure dissipates to zero at the end of primary consolidation. Many investigators have attempted to determine if, in fact, this is the case. Hanrahan (6) and Girault (3) presented data indicating that the pore water pressure approaches zero shortly after primary consolidation has ceased. Crawford (2) showed results suggesting that pore water pressure at the base dissipated to zero after about 1 day for specimens which reached 100 percent consolidation (as determined by the Casagrande construction) in 100 to 200 min.

Curves of pore water pressure dissipation as a function of time are shown in Figures 10-13 for a typical initial pressure increment and the three corresponding recompression increments, along with the time-settlement curves. The theoretical pore water pressure dissipation curves were determined using the expression presented by Perloff et al. (12) to account for the effect of system flexibility on pore water pressure measurement at the base of one-dimensional consolidation specimens. System flexibility is especially important when the soil has been highly precompressed by cyclic loading because the stiffness of the measuring system relative to that of the soil structure is substantially reduced. The reason for the extremely low peak pore water pressure in Figure 10 is that the hydraulic loading arrangement used in these tests experienced some lag in following the specimen deformation for the initial increment when deformations were relatively large. This did not seem to be as much of a problem in the recompression increments as indicated by the relative agreement between the peak magnitude measured and theoretical pore water pressures shown in Figures 11 through 13.

The pore water pressure at the base of the specimen does not decrease to zero, for the time duration shown in Figures 10-13, even though the theoretical 100 percent consolidation points for the recompression increments occur at approximately 10 min. Increments have been carried out for as long as 72 hr without observation of zero pore water pressure. However, at very long periods of time, when the excess pore water pressure has dissipated to less than 2 cm of water, small variations in temperature cause variations in the magnitude of pressure greater than the magnitude of the pressure itself. Figure 14 shows the variations in temperature at the base of the specimen, pore water pressure at the base, and settlement over a 4-hr period starting approximately 35 hr after the application of the pressure increment. A moderately rapid reduction in temperature causes a corresponding reduction in pore water pressure and a slackening of the settlement curve. With moderately rapid temperature fluctuations (Fig. 14), the pressure may even become negative for very small values of pressure until the temperature decrease occurs at a reduced rate, ceases, or becomes a temperature increase. Although the general trends of the time-settlement and time-pore water pressure curves are unchanged, it is obvious that at very small pressures, small temperature variations tend to mask the results. It seems likely that these changes occurring over short time spans are probably due to expansion and contraction of the water in the specimen and in the cavity underneath the porous stone. It appears here that not only the temperature but the rate of temperature change is particularly significant. This can be seen by observing the close correspondence of the breaks in the pressure and settlement curves with changes in rate of temperature change. Present tests are being conducted in a specially prepared constant temperature chamber which will insure constant specimen temperature within ± 0.05 C.

In spite of the influence of temperature changes at very small pressures, the data indicate that the pore water pressure at the base does not dissipate to zero, at least over the time span measured.

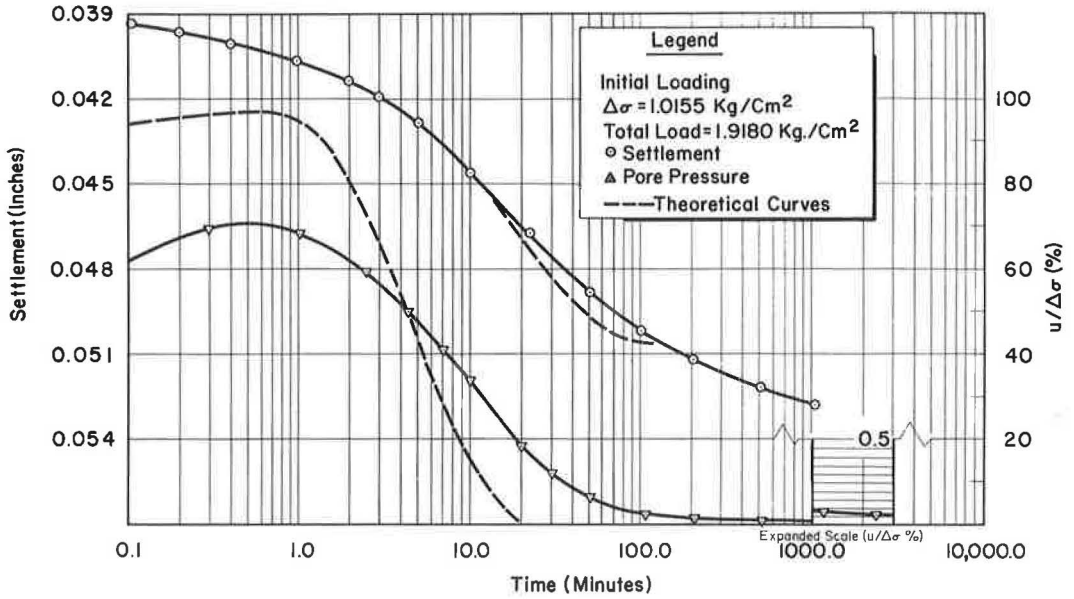

Figure 10. Consolidation behavior of single-drained specimen (specimen 4) for typical pressure increment.

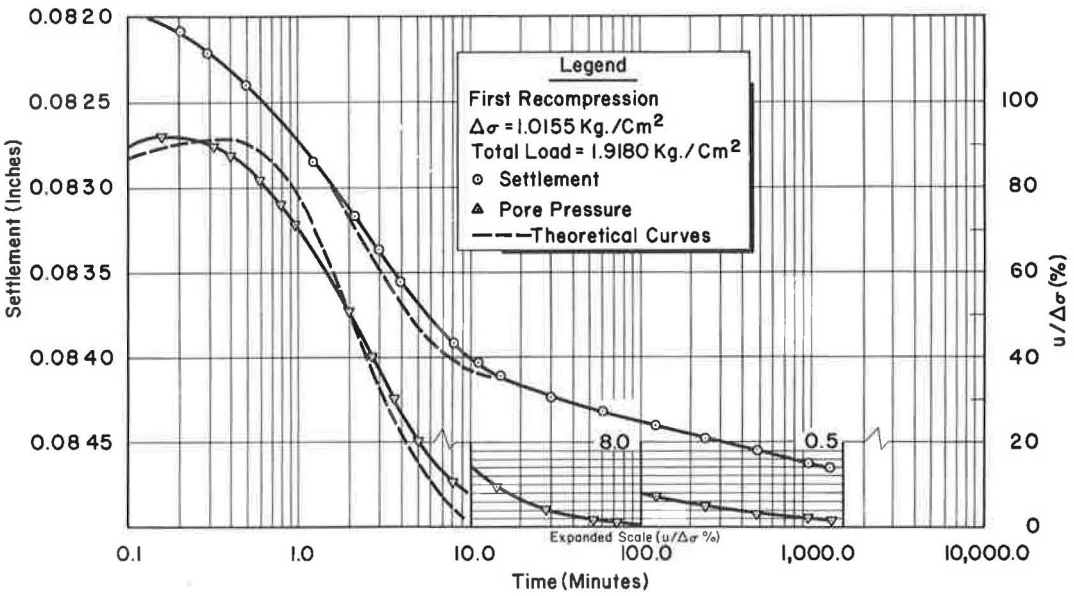

Figure 11. Consolidation behavior of single-drained specimen (specimen 4) for typical pressure increment.

CONCLUSIONS

Based on the foregoing results, the following conclusions can be drawn, at least for one-dimensional consolidation tests on a sensitive undisturbed clay:

1. Pore water pressures exist and are of measurable magnitude during secondary compression. The pressure at the base did not go to zero for as long as the tests were conducted.

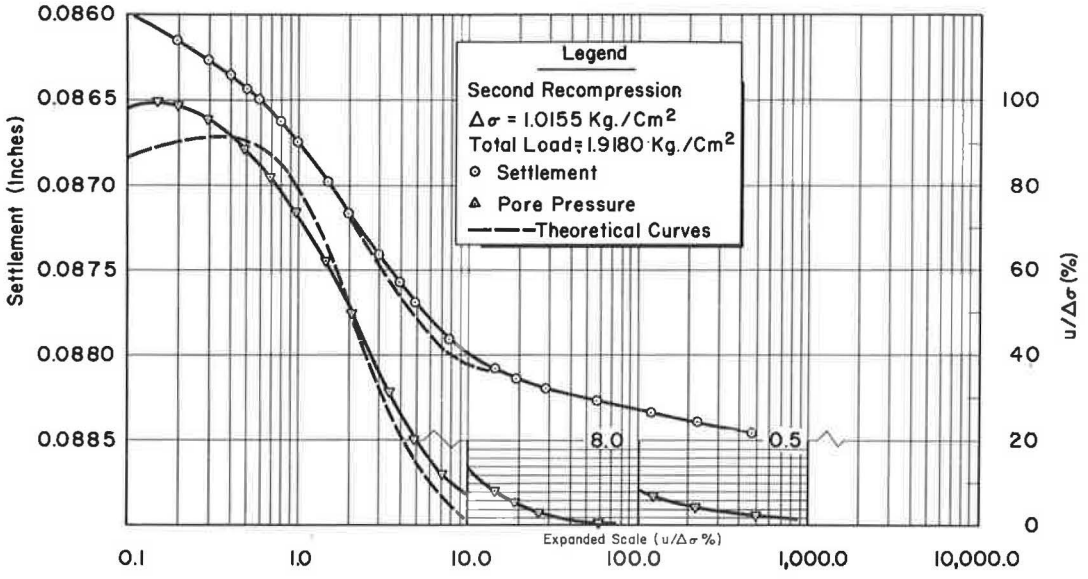

Figure 12. Consolidation behavior of single-drained specimen (specimen 4) for typical pressure increment.

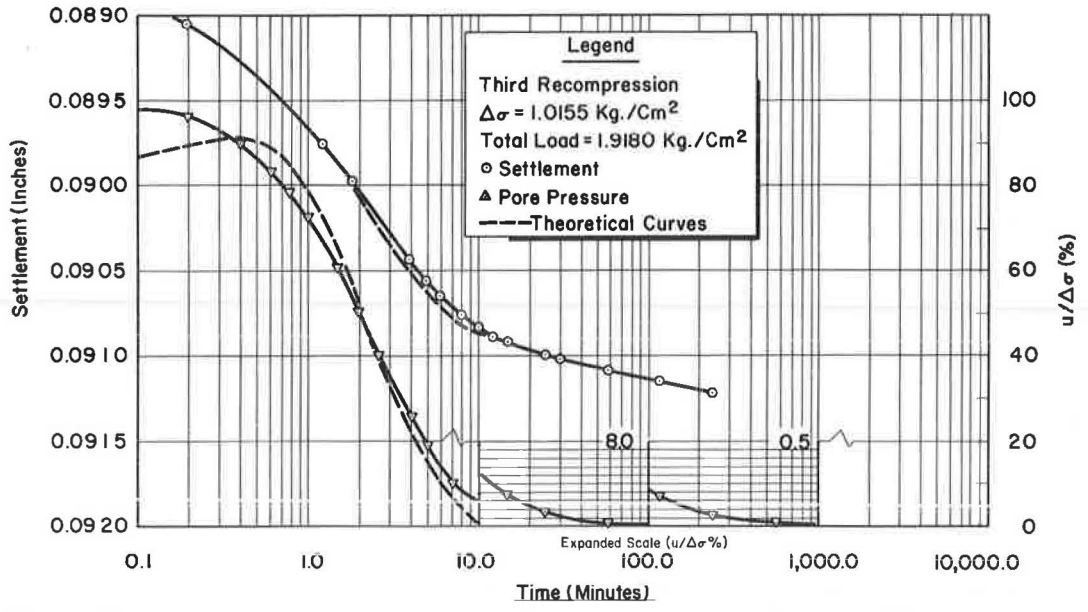

Figure 13. Consolidation behavior of single-drained specimen (specimen 4) for typical pressure increment.

2. Cyclic loading produces a net settlement for each cycle. However, the net settlement decreases as the number of cycles increases and approaches a very small value. The data available do not indicate whether a zero net settlement will result from a sufficently large number of load cycles.

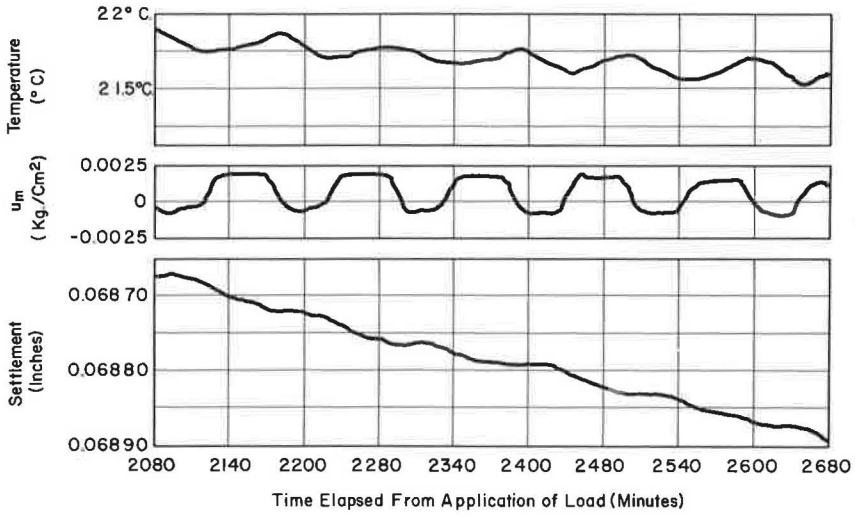

Figure 14. Effect of temperature on pore water pressure at base and settlement during secondary compression.

3. Load cycling reduces the amounts of primary and secondary compression to a small fraction of their initial magnitudes under a given load. However, the cycling does not appear to affect the shape of the time-settlement curve, as expressed by the ratio R_s/R_{100}.

4. The settlement-pressure curve returns to the original virgin curve after load cycling. The load cycling appears to induce a prestress effect since the return to the virgin curve is characterized by the presence of a "quasi-preconsolidation pressure" larger than the actual preconsolidation pressure.

5. The limited data available indicate that the coefficient of secondary settlement, R_s, is independent of the length of drainage path for a given specimen thickness.

6. The flexibility of the pore pressure measuring system becomes significant when the soil is subjected to load cycling, due to the low value of compressibility for the highly precompressed soil. Use of the theoretical expression from Perloff et al. (12) assists in accounting for this effect.

7. Temperature effects are important, even for small temperature variations, when very low pore water pressures are measured during secondary compression.

REFERENCES

1. Buisman, A. S. Results of Long Duration Settlement Tests. Proc. First International Conference on Soil Mechanics and Foundation Eng., Cambridge, Vol. I, p. 103, 1936.
2. Crawford, C. B. Interpretation of the Consolidation Test. Jour. of Soil Mechanics and Foundation Div., ASCE, Vol. 90, No. SM5, Sept. 1964.
3. Girault, P. A Study on the Consolidation of Mexico City Clay. Ph. D. thesis, Purdue Univ., Layfayette, Indiana, 1960.
4. Gray, Hamilton. Progress Report on Research on the Consolidation of Fine-Grained Soils. Proc., First Internat. Conf. on Soil Mechanics and Foundation Eng., Vol. 2, Cambridge, p. 138, 1936.
5. Haefeli, R. and Schaad, W. Time Effects in Connection with Consolidation Tests. Proc. Sec. Intern. Conf. on Soil Mechanics and Foundation Eng., Vol. III, Rotterdam, p. 23, 1948.
6. Hanrahan, E. T. An Investigation of Some Physical Properties of Peat. Geotechnique, Vol. 4, No. 3, p. 108, Sept. 1954.

7. Leonards, G. A. and Altschaeffl, G. A. The Compressibility of Clay. Jour. of Soil Mechanics and Foundation Div., ASCE, Vol. 90, No. SM5, Sept. 1964.
8. Leonards, G. A. and Girault, P. A Study of the One-Dimensional Consolidation Test. Proc., Fifth Internat. Conf. on Soil Mechanics and Foundation Eng., Paris, Vol. I, p. 213, 1961.
9. Leonards, G. A. and Ramiah, B. K. Time Effects in the Consolidation of Clay. Symp. on Time-Rate of Loading in Testing Soils, Spec. Tech. Publ. No. 254, ASTM, 1960.
10. Moran, Proctor, Mueser, and Rutledge. Study of Deep Soil Stabilization by Vertical Sand Drains. Rept. II, Bur. of Yards and Docks, Dept. of Navy, June 1958.
11. Newland, P. L. and Allely, B. H. A Study of the Consolidation Characteristics of a Clay. Geotechnique, Vol. 10, No. 2, p. 62, June 1960.
12. Perloff, W. H., Nair, K., and Smith, J. G. Effect of Measuring System on Pore Water Pressure in the Consolidation Test. Proc., Sixth Internat. Conf. on Soil Mechanics and Foundation Eng., in press, 1965.
13. Palmer, L. and Thompson, J. Report of Consolidation Tests with Peat. Symp. on Consolidation Testing of Soils, Spec. Tech. Publ. No. 126, ASTM, p. 4, June 1951.
14. Ray, J. W. The Effect of the Principal Stress Ratio on Secondary Compression in Cohesive Soils. M. S. thesis, Ohio State Univ., Columbus, Ohio, March 1963.
15. Taylor, D. W. Research on Consolidation of Clays, Dept. of Civil and Sanitary Eng., MIT, Ser. 32, Aug. 1942.
16. Terzaghi, K. Die Berechnung der Durchlassigkeitsziffer des Tones aus dem Verlauf der hydrodynamischen Spannungaerscheinungen. Akademie der Wissenschaften in Wien. Sitzungsberichte. Mathematisch-naturwissenchaftliche Klasse. Pt. IIa, Vol. 132, No. 3-4, pp. 125-138.
17. Wahls, H. E. Primary and Secondary Effects in the Consolidation of Cohesive Soils. Ph. D. thesis, Northwestern Univ., Evanston, Ill., 1961.
18. Wahls, H. E. Analysis of Primary and Secondary Consolidation. Jour. of Soil Mechanics and Foundation Div., ASCE, Vol. 88, No. SM6, Dec. 1962.

Appendix

METHOD FOR DETERMINING AVERAGE EFFECTIVE CONSOLIDATION PRESSURE

To determine the shape of the settlement-pressure curve for a given pressure increment, it is necessary to know the average effective consolidation pressure at a given time, $(\sigma'_c)_t$, defined as

$$(\sigma'_c)_t = \sigma_c - (u_{avg})_t \tag{1}$$

where σ_c is the applied vertical consolidation pressure, and $(u_{avg})_t$ is defined by

$$(u_{avg})_t = \frac{1}{H} \int_{x=0}^{H} u\,(x, t)_t \, dx \tag{2}$$

where x is the depth from the top of a one-dimensional consolidation specimen, H is the thickness, $u\,(x,t)_t$ is the pore water pressure isochrone corresponding to time t.

The expression for $u\,(x,t)$ for a one-dimensional consolidation test in which pore water pressures are measured at the base of the specimen, with a flexible system is given by Perloff et al. (12) as

$$u(x,t) = 2u_o \sum_{n=1}^{\infty} \frac{(A_n + \eta^2/A_n)\sin A_n - \eta}{(A_n^2 + \eta^2 + \eta)\sin A_n} \sin \frac{A_n x}{H} e^{-A_n^2 T} \quad (3)$$

where

u_o = initial uniform pore water pressure for $o < x < H$ (equal to applied pressure increment, $\Delta\sigma$);

$\eta = \frac{AHm_v}{\lambda}$ = stiffness of measuring system relative to that of soil skeleton;

A = specimen area;

H = specimen thickness;

m_v = the coefficient of volume compressibility of the soil;

λ = volumetric compliance of pore water pressure measuring system, i.e., the system volume demand per unit pressure change;

A_n = positive roots of the $A_n \tan A_n = \eta$;

e = base of natural logarithms; and

$T = \frac{c_v t}{H^2}$ = a dimensionless time factor.

Eq. 3 was derived on the basis of the classical hydrodynamic consolidation assumptions about soil properties.

Substituting Eq. 3 into Eq. 2 and integrating gives the theoretical expression for u_{avg}:

$$u_{avg} = 2u_o \sum_{n=1}^{\infty} \frac{(A_n + \eta^2/A_n)\sin A_n - \eta}{A_n(A_n^2 + \eta^2 + \eta)\sin A_n} (1 - \cos A_n) e^{-A_n^2 T} \quad (4)$$

When $\eta = \infty$, Eq. 4 reduces to the Terzaghi (16) equation for a single drained specimen.

The theoretical value of the measured pore water pressure at the base (Perloff et al., 12) is

$$u_{meas} = 2u_o \sum_{n=1}^{\infty} \frac{(A_n + \eta^2/A_n)\sin A_n - \eta}{A_n^2 + \eta^2 + \eta} e^{-A_n^2 T} \quad (5)$$

Solving Eq. 5 for u_o and substituting this into Eq. 4 gives the average pore water pressure in terms of the measured pore water pressure at the base:

$$u_{avg} = u_{meas} \frac{\sum_{n=1}^{\infty} \frac{(A_n + \eta^2/A_n)\sin A_n - \eta}{A_n(A_n^2 + \eta^2 + \eta)\sin A_n} (1 - \cos A_n) e^{-A_n^2 T}}{\sum_{n=1}^{\infty} \frac{(A_n + \eta^2/A_n)\sin A_n - \eta}{A_n^2 + \eta^2 + \eta} e^{-A_n^2 T}} \quad (6)$$

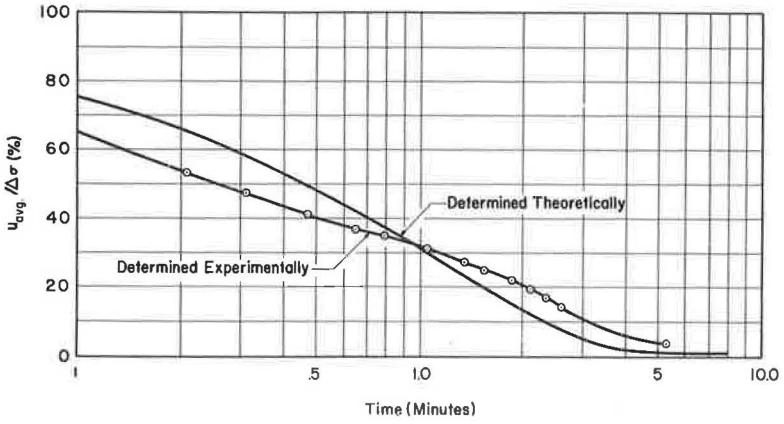

Figure 15. Comparison of average pore water pressure determined theoretically and experimentally.

Thus, if the measured pore water pressure at the base of the specimen is known, the average pore water pressure, and therefore the effective consolidation pressure, can be determined.

If the measured value of u_{meas} were identical to that predicted by Eq. 5, then Eqs. 4 and 6 would lead to identical results. In such a case, it would not be necessary to measure pore water pressures to know σ'_c. However, when the measured and theoretical pore water pressures at the base are not equal, Eqs. 4 and 6 lead to very different results. This is illustrated in Figure 15, which shows the relationship between u_{avg} and time, as predicted by Eq. 4, and as predicted by Eq. 5 using the measured pore water pressure, for the last pressure increment applied to specimen 4 (Fig. 6). The relationship determined from the measured pressures is not the same as that from purely theoretical considerations.

The validity of Eq. 6 depends on the assumption that the relationship between u_{avg} and u_{meas} will be the same at a given time factor, even if the magnitude of u_{meas} is different from that predicted by theory. This assumption is probably reasonable, at least for time factors greater than 0.1 (t = 0.26 min for this increment), because the ratio of the two series in Eq. 6 changes very little as the time factor changes, when $T > 0.1$.

Shrink-Swell Potential of Soils*

GEORGE W. RING, III, Highway Research Engineer, U. S. Bureau of Public Roads

ABRIDGMENT

•THIS IS a report on a laboratory method for determining the shrink-swell potential of soils. In a recent study by the Bureau of Public Roads, a new test procedure has been developed. The purpose of the study was to develop a rapid, reliable method for measuring the potential volume change of soils subjected to alternate wetting and drying.

The results of most test procedures for measuring volume change characteristics of soils are affected by the molding moisture and density condition of the test specimen. For example, dense dry soils swell more than loose wet soils when soaked, while loose wet soils shrink more than dense dry soils when dried. Thus, tests measuring either shrinking or swelling alone are not suitable for determining a soil's shrink-swell potential since the test results are dependent on the initial moisture and density condition.

In an attempt to find a suitable method for determining shrink-swell potential, 2 other types of tests were examined: (a) the Georgia volume-change test, and (b) a rapid cyclic wetting and drying procedure based on Porter's work in Texas.

Tests were first made by the Georgia method. This method for determining volume change measures both swell and shrinkage. Briefly, the procedure consists of compacting two identical specimens, then one is soaked while the other is dried. The test value is determined from the combined volume change of the two specimens. In some of the Public Roads tests by the Georgia method it was noticed that some medium to low plasticity soils exhibited high swell characteristics when soaked, evidently due to the compaction of the specimen. Also, some high plasticity soils swelled much more during a second soaking than during the normal first soaking period. Both of these occurrences suggested that an approach based on Porter's studies would be more logical.

Consequently, another test procedure was devised to determine whether alternate wetting and drying, as suggested in Porter's studies, would achieve an equilibrium condition of shrinking and swelling regardless of initial moisture and density condition. In this procedure, three 2-in. diameter specimens of soil were molded to cover a wide range of initial moisture and density conditions. After molding, the three specimens were subjected to 4 cycles of alternate wetting and drying under a ¼-psi surcharge. Figure 1 shows the molds, surcharges and dial indicator for measuring changes in height.

Using the cyclic wetting and drying procedure, tests were made on 12 soils having a wide range of shrink-swell potential. They ranged from a silt having a PI of 4 (low shrink-swell potential) to a bentonite having a PI above 300 (very high shrink-swell potential). Wet-dry cyclic changes in height for two of the soils having quite different volume-change characteristics are shown in the next two figures.

Figure 2 shows the changes in height for Cecil soil which has a low shrink-swell potential. During the first soaking, the height change of the specimen compacted air dry was much more than occurred in the specimen which was compacted at optimum moisture content. However, after drying, the height change of these two specimens during the second soaking is more nearly the same. After 2 more cycles, the height change is approximately equal for all three specimens.

Figure 3 shows the changes in height for Iredell soil, which has a high shrink-swell potential. As occurred in the Cecil soil, the greatest differences in height changes

*The complete text of this article (including references) may be found in Public Roads Magazine, Vol. 33, No. 6, Feb. 1965.

Paper sponsored by Committee on Soil and Rock Properties.

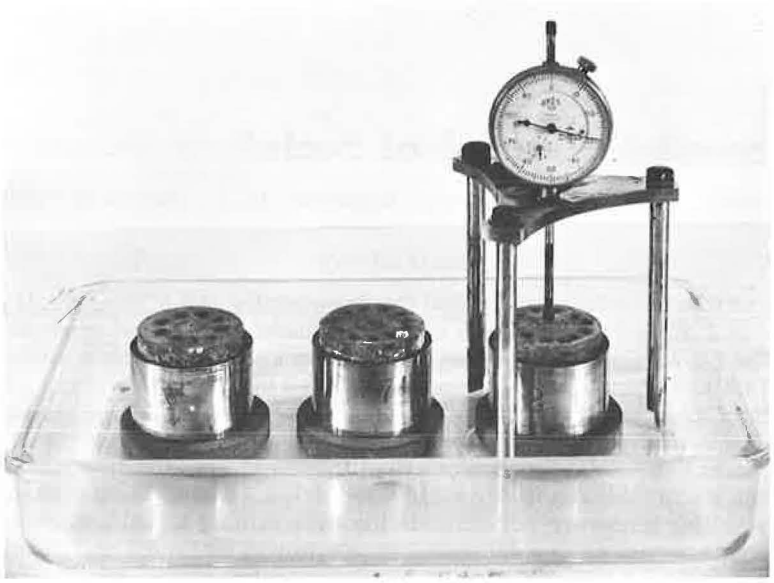

Figure 1. Apparatus for cyclic wetting and drying test.

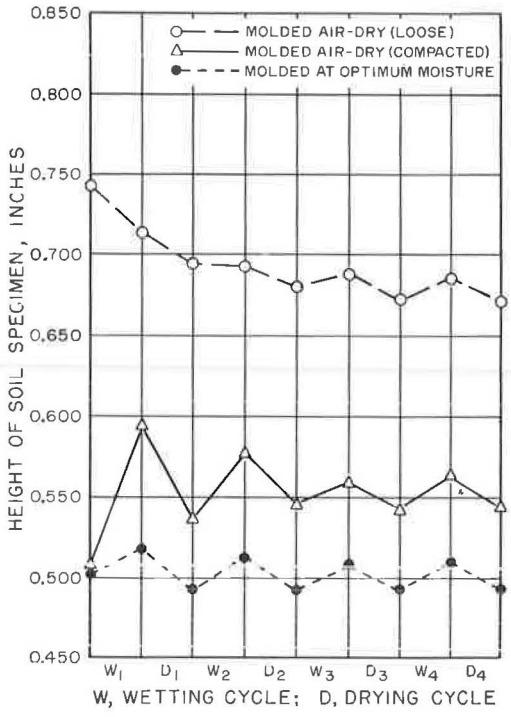

Figure 2. Height change of 3 specimens of Cecil soil when alternately wetted and dried under a 0.25-psi surcharge.

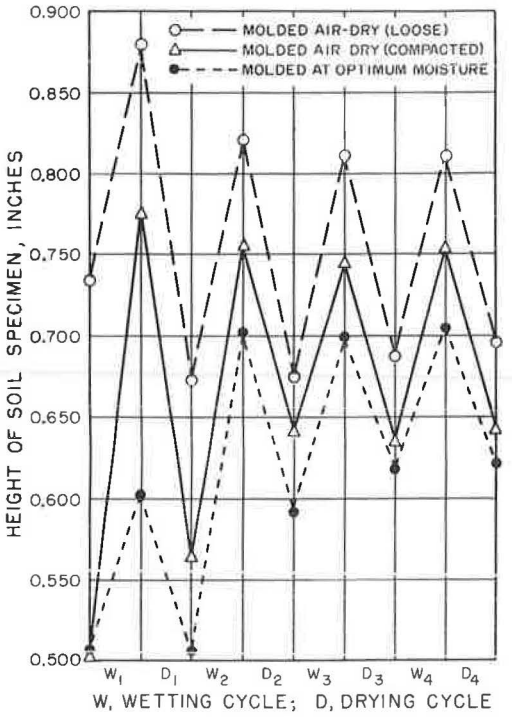

Figure 3. Height change of 3 specimens of Iredell clay when alternately wetted and dried under a 0.25-psi surcharge.

between the 3 specimens occurred during the first soaking. However, for both soils, the height change of all specimens was essentially consistant after several cycles of wetting and drying. At this point, the effects of the initial moisture and density condition appear to have been minimized and an equilibrium shrink-swell condition achieved

by this procedure. The shrink-swell potential for each soil was then taken as the volume change which occurred during the drying in the 4th cycle. The volume of the specimens before drying was calculated from their measured height and diameter, while the volume of the specimens after drying was measured by mercury displacement.

Up to this point, the study led to a method for determining shrink-swell potential uninhibited by molding moisture and density. However, this cyclic wetting and drying method requires one or more weeks to complete a test. In an effort to shorten the time required to obtain an estimate of shrink-swell potential, it was hoped that shrink-swell potential could be related to some other test requiring less testing time. For this reason, in the second part of the study, the same 12 soils were tested by 8 other volume change or swell pressure tests and the results of the tests compared to the shrink-swell potential.

The 8 other tests were plasticity index, shrinkage limit, AASHO T 190 (expansion pressure), CBR volume change, AASHO T 116 (volume change of soils), the Georgia volume change method, total surface area and linear shrinkage.

Summarizing this second part of the study: the results of the 8 other tests were related to shrink-swell potential with varying degrees of success. Table 1 indicates the general quality of the relationships and presents possible reasons as to why certain soils did not readily conform. Four of the tests, PI, Georgia volume change, surface area and linear shrinkage, appear to be closely related to shrink-swell potential. The Georgia method requires the longest testing time (2 days). Surface area measurements require the next longest time (from 1 to 2 days). The PI and linear shrinkage tests both require from 16 to 24 hours.

Based on the good correlation with shrink-swell potential (Fig. 4) and ease of testing, linear shrinkage was selected as the best substitute for the slower cyclic wetting and drying method.

In conclusion, most previously developed test methods for measuring shrinking and swelling characteristics of soils are influenced by the molded moisture and density of the test specimen.

The objective of this laboratory study, to develop a method to evalute a soils' shrink-swell potential independent of its molding moisture and density, appears to have been reasonably well achieved with the development of a new test method employing cyclic wetting and drying.

Although from 1 to 100 weeks are required to complete a shrink-swell potential test, comparisons of the results obtained by this test to 8 "standard" tests for a wide range of soil types indicate that the linear shrinkage test has real potential as a substitute for the very time-consuming cyclic wetting and drying method.

The relationship of linear shrinkage to shrink-swell potential was very good for the linear shrinkage test method described in the Appendix. However, further investigations, not reported here, were devoted specifically to factors influencing the linear shrinkage test. The primary purpose of these investigations was to find a modified procedure that would provide an even better correlation. Results obtained by an alternate procedure, devised as a result of the supplementary studies, did not correlate as well with shrink-swell potential as those obtained by the test method herein described. The study, however, did show the variables and their quantitative effect on linear shrinkage test results. A limited supply of an informal report on the supplementary study is available. Interested researchers may obtain copies without cost by addressing requests to the Bureau of Public Roads, Washington, D. C., 20235, attention: Materials Division, Office of Research and Development.

APPENDIX

SUGGESTED TEST METHOD FOR DETERMINING THE LINEAR SHRINKAGE OF SOILS

Definition

1. The linear shrinkage of a soil is that change in length of a bar of soil as determined in accordance with the following procedure.

TABLE 1

RELATIONSHIPS OF STANDARD TEST RESULTS TO SHRINK-SWELL POTENTIAL

Test Method or Measurement	Quality of Relationship to Shrink-Swell Potential	Remarks
Plasticity index	Good	May overestimate shrink-swell potential of soils containing iron oxides and inactive clays.
Shrinkage limit	Fair	Underestimates shrink-swell potential of bentonitic soils.
AASHO: T-190	Poor	Molding moisture and density conditions not suitable for prediction of shrink-swell potential.
CBR	Fair	Relationship with shrink-swell potential slightly improved for specimens molded to AASHO: T-180.
AASHO: T-116	Fair	May overestimate the shrink-swell potential of soils sensitive to method of compaction.
Georgia volume change test	Good	May overestimate shrink-swell potential of micaceous soils; method not suitable for bentonite soils.
Surface area	Good	May overestimate the shrink-swell potential of high-activity clays mixed with sands.
Linear shrinkage	Good	Test fairly rapid and easy to perform.

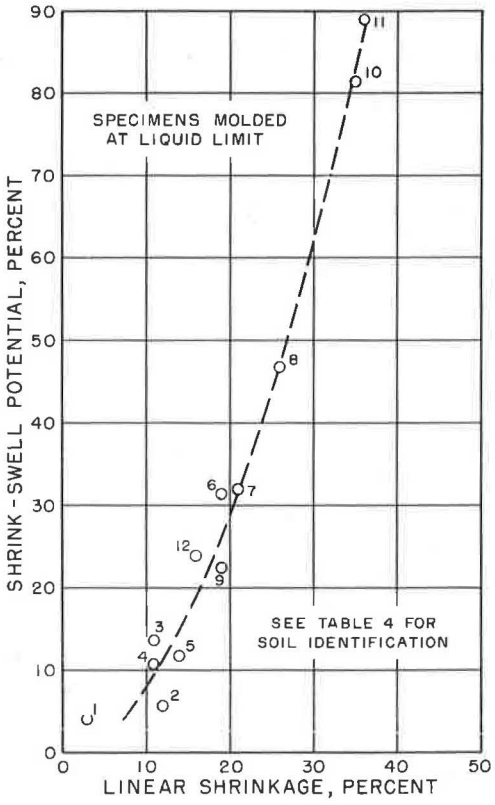

Figure 4. Relation of linear shrinkage to shrink-swell potential.

Apparatus

2. (a) Linear shrinkage mold - A Teflon mold 20 cm long and having a semi-circular cross-section of 2.54-cm diameter
   (b) Commercial petroleum jelly
   (c) Distilled water
   (d) Evaporating dish, about 4½ in. in diameter
   (e) Balance, 500-gm capacity, sensitive to 0.1 gm
   (f) Spatula, having a blade about 3 in. in length and about ¾ in. in width
   (g) Drying oven, 70 C ± 5 C
   (h) Scale, length 30 cm graduated to ½ mm

Sample

3. A sample of air dry soil weighing about 150 gm shall be taken from the thoroughly mixed portion of the material passing the No. 40 (420-micron) sieve.

Procedure

4. (a) The soil sample shall be placed in the evaporating dish and thoroughly mixed with 45 to 60 cc of distilled water by alternately and repeatedly stirring, kneading and chopping with a spatula. Further additions of water shall be made in increments of 3 to 8 cc until the soil is at or slightly above its liquid limit (see AASHO T 89-60). Each increment of water shall be thoroughly mixed with the soil as previously described before another increment of water is added.

(b) The mixture shall be placed in a linear shrinkage mold which has been previously lubricated with 0.30-g petroleum jelly. After firmly pressing the mixture into the mold with the spatula, excess material shall be removed by trimming with the straight edge of the spatula.

(c) The mold containing the mixture shall be placed in an oven at 70 C ± 5 C for 16 hours or until constant weight has been obtained.

Note 1: When the oven must be set at 100 C for other soil tests, linear shrinkage specimens may be dried at this temperature. However, the higher temperature will result in more cracking of the specimen and slightly lower test values.

(d) The soil specimen shall be removed from the oven, allowed to cool and then the length of both the top and bottom measured.

Note 2: For broken specimens, the lengths of the individual pieces should be marked and accumulated on a strip of paper; the total length can be determined directly by measuring the end points on the strip.

Calculation

5. The linear shrinkage of the specimen shall be expressed as follows:
Linear shrinkage (in percent) =

$$\frac{\text{Mold length} - \frac{\text{Top + bottom length of dried specimen}}{2}}{\text{mold length}} \times 100$$

A Method of Determining Swell Potential of An Expansive Clay

W. D. BUDGE, Assistant Professor, Department of Civil Engineering, Brigham Young University; and
E. SAMPSON, JR., and R. L. SCHUSTER,
Associate Professors, Department of Civil Engineering, University of Colorado

ABRIDGMENT

•THE SUBGRADE volume change occurring when highway pavements are placed in cut sections is of particular concern in this study. This condition appears to be ideal for swell of subgrade soil since overburden removel reduces the confining pressure in the subgrade while the relatively light pavement structure provides an impermeable ground cover which induces an accumulation of water under the pavement. Such an accumulation probably results from both the interference of normal moisture evaporation and the ingress of surface water made possible by the excavation. This combination of pressure release and moisture increase causes an effective stress decrease in the soil and can cause pavement heave which may be of the order of several inches. When this heave is accompanied by differential movements, the structure will crack.

This study is concerned with the use of the one-dimensional consolidometer test as a method for determining the swell characteristics of an expansive subgrade soil and for predicting its swell potential. Although the method devised is applicable to any expansive soil, it was specifically applied to a stiff, fissured clay shale which serves as subgrade for Interstate 70 northwest of Limon, Colorado. Since completion of this part of Interstate 70 in 1959, the expansive characteristics of this subgrade soil, which is a part of the Laramie formation of eastern Colorado, have resulted in considerable heaving and faulting of the concrete pavement. This distress has been confined to cut sections and pavement heave in these sections has been as great as 1.0 ft in the five years since construction.

It was necessary to design new sampling equipment to obtain satisfactory consolidometer-test samples in this hard, fissured material. The sampler designed contains a series of liners, which enable the test specimens to remain confined in linear rings from time of field sampling until the consolidometer test is completed in the laboratory. Each individual liner ring has the same height as the diametrically enlarged consolidometer ring into which it is fitted. Complete lateral confinement is thus maintained on the specimens during all phases of the sampling and testing procedure; this prevents stress relief accompanied by premature expansion during transfer of the sample into the consolidometer.

A relatively rapid method of determining the expansion characteristics of a soil was developed in which the sample is loaded and unloaded in single increments. This method provides reliable information both for identification and volume change prediction of high volume change soils. The swell curve obtained in this consolidometer test procedure yields not only the swell index as an indicator of swell potential, but is utilized, together with the soil stress changes resulting from overburden removal in construction of the cut, to estimate the portion of surface heave likely to result from this weight removal. The portion of total heave resulting from moisture increase due to pavement cover and/or excavation is obtained in a similar swell test in which the soil is given free access to water while under full overburden pressure. These two laboratory volume changes resulting from pressure release and soil moisture increase are used

Paper sponsored by Committee on Soil and Rock Properties.

to estimate total surface heave. Such estimation enables the engineer to consider the implications of this movement on the proposed structure, and possibly may provide insight concerning the best means of preventing such movement.

The validity of this method of surface heave prediction can only be established with certainty by comparing a predicted quantity of heave with actual pavement heave at a site where heave prediction is made before highway construction. Such verification has not yet been attempted, since no new Colorado highways on swelling soils are at the proper stage of construction. However, an excellent field check was obtained at the site on Interstate 70 by sampling the highly expansive clay shale below existing pavement level at a point outside the cut slope but close enough to the cut so that soil with the same characteristics was dealt with. The potential heave of the soil lying below cut grade as determined by this method was about 0.6 ft, a value very close to the average measured heave of 0.65 ft which the pavement had undergone at that point in the five years since construction.

By means of this method it is possible to estimate the potential heave of increments of soil at any sampling depth. As expected, it was shown in this study that layers of soil immediately beneath the pavement contribute more to heave of the pavement than increments at greater depth. Of the 0.6 ft total potential heave estimated for this site, about 0.24 ft of swell was shown by the consolidometer test method to have derived from the uppermost 10 ft below cut grade; the second 10 ft of soil contributed about 0.13 ft of swell; the third 10 ft contributed about 0.09 ft of swell, etc.

Deformation and Flow Properties of Clay Soils From the Viewpoint of Modern Material Science

MEHMET A. SHERIF, Assistant Professor of Civil Engineering, University of Washington, Seattle

•PERHAPS the most important single contribution to the understanding of shear strength in clay was made by C. A. Coulomb (5). In an essay dated 1776, Coulomb defined the shear strength of soil as:

$$\tau = C + \sigma_n \tan \phi \qquad (1)$$

(Coulomb considered C & ϕ as constants for a given soil.)

Further research by Hvorslev (10) and Terzahgi have led to the following modification of the Coulomb formula:

$$\tau = C' + \sigma_n' \tan \phi' \qquad (2)$$

This formula, known as the Hvorslev-Terzaghi failure criterion, is the one most widely accepted by the profession at this time. C' is known as true cohesion which depends on the overconsolidation pressure, σ_n is the effective normal stress, and ϕ is the effective angle of internal friction and is considered constant for a given soil. Furthermore, application of Eq. 2 necessitates the measurement of pore pressures generated during the shearing process.

Experiments similar to those of Hvorslev were reported by Hogentogler. Winterkorn's analysis (19) of Hogentogler's data reveals that both cohesion and angle of friction increase with increasing pressure to a certain limit, and continue as constants thereafter (Fig. 1). Such interpretation represents a logical evaluation of the experimental data and is in harmony with the colloidal and physico-chemical factors involved. If two clay plates surrounded by chains of ions and dipoles approach one another, their interaction increases, as will their cohesion and friction as the particles come closer. There is a point, however, at which the respective parts are so strongly held that they resist greater thinning (Fig. 2). When this stage is reached, the entire system is in a solid state and any increase in shear strength thereafter depends on the normal stress alone.

The systematic investigation of the fundamentals of shear strength of cohesive soils begun by Hvorslev (10) in Vienna was continued by L. Rendulic (13). The latter performed experiments on Vienna clays and devised a clever method for comprehensive graphical representation of the relationships between void ratio (water content) and stress conditions in triaxial testing. Rendulic represented σ_1 by σ_a (axial stress) and σ_2 and σ_3 by their resultant $\sigma_r \sqrt{2}$ on the $\sigma_a = 0$ plane. The plane formed by σ_a and $\sigma_r \sqrt{2}$ is shown in Figure 3a.

The line OH corresponds to hydrostatic conditions of loading and, therefore, no failure will occur along this line. Shear stresses will be induced in the sample if $\sigma_r \sqrt{2}$ is held constant while σ_a is allowed to increase. The deviation of the loading conditions from the hydrostatic state continues increasing until a failure is reached (line OC represents the failure envelope).

Paper sponsored by Committee on Physico-Chemical Phenomena in Soils

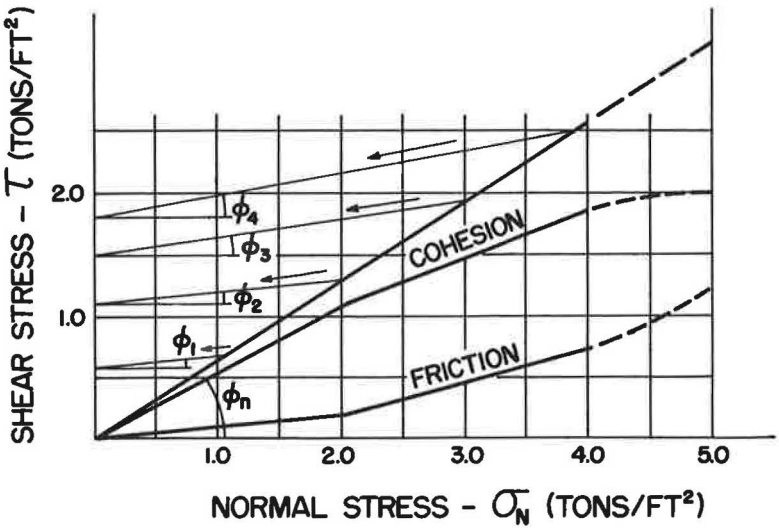

Figure 1. Behavior of cohesion and angle of friction under increasing pressure.

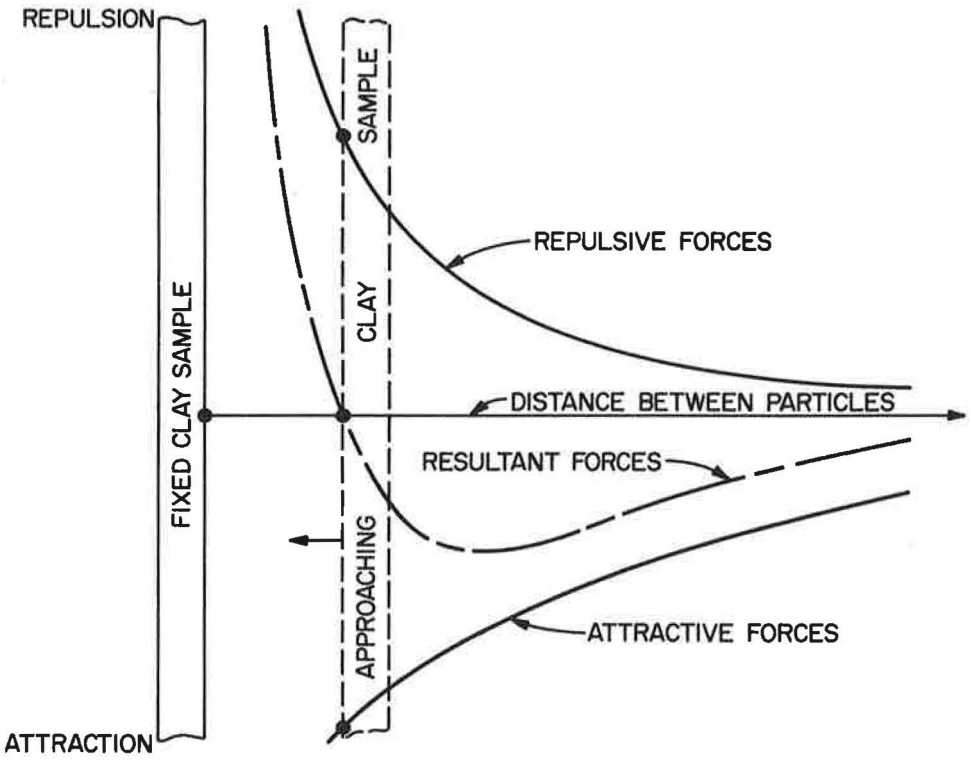

Figure 2. Variation of internal attractive and repulsive forces as a function of distance between clay particles.

To illustrate certain properties and ideas associated with the diagram in Figure 3a, consider the four samples in Figure 3b which are consolidated under hydrostatic pressures of σ_{ac_1}, σ_{ac_2}, σ_{ac_3} and σ_{ac_4}. If these samples are subjected to shearing

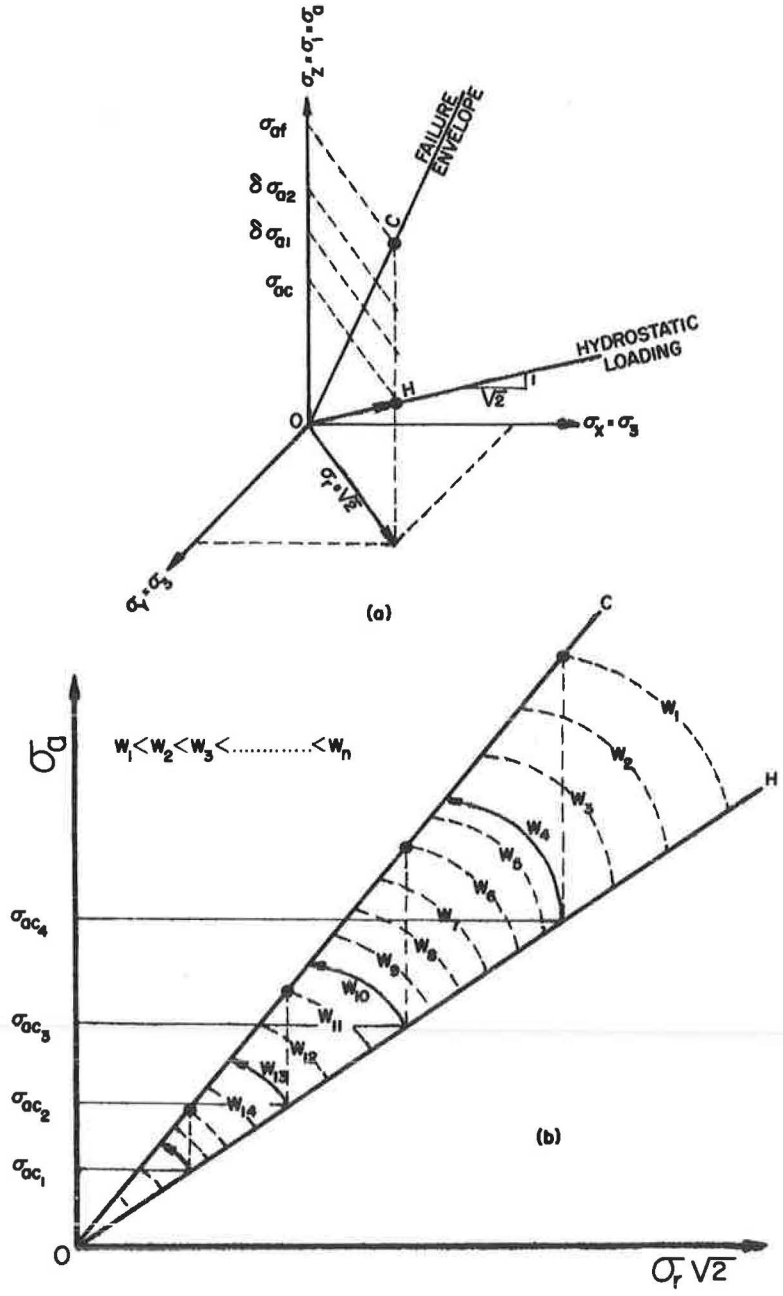

Figure 3. (a) Relationships between void ratio (water content) and stress conditions in triaxial testing; (b) four samples consolidated under hydrostatic pressures.

stresses under drained conditions until failure is reached, the path traced by the effective stress increments will be parallel to the σ_a axis. (These traces are shown by vertical dotted lines in Fig. 3b.) If the volume change under each load increment is measured, the moisture content corresponding to each of these load increments will be known from the water content at failure. Hence, the contours of equal moisture content lines can be drawn, as shown by the light dotted lines.

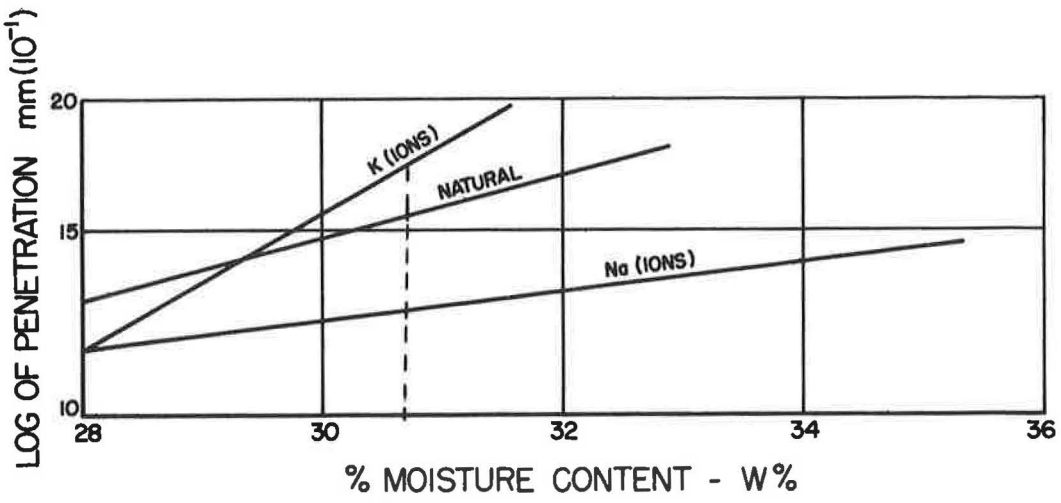

Figure 4. Exponential relationship between shear strength and moisture content.

If these samples were sheared in undrained tests with pore pressure measurements taken, the trace of the effective stresses would follow the path indicated in Figure 3b with solid lines and arrows. (Since no volume change is allowed during such tests, the effective stress path is also, by definition, the constant moisture content contour.) According to Rendulic, these lines have the same general configuration as the contours representing the constant moisture contents.

One of the most important conclusions to be derived from Rendulic's results is the existence of a unique relationship between the effective stresses and moisture contents at all levels. Viewed in the light of Terzaghi's fundamental concept, which states that the strength and deformation characteristics of soils are governed by the effective stresses, this conclusion based on Rendulic's experiments provides a logical connection between the shear strength of the soil and its moisture content at failure.

Experiments performed by Winterkorn on Putnam clays have shown an exponential relationship between the shear strength and moisture content (Fig. 4). This figure also shows the effect of the ion in the system on the shear strength of the soil.

Further investigations by Rutledge and Henkel confirmed Winterkorn's findings and also indicated that the failure envelope defined in terms of moisture content and log $(\sigma_1 - \sigma_3)$ is parallel to the standard e log σ consolidation curve. In recognition of their contribution, the author thought it appropriate to designate this theory as the Winterkorn-Rutledge-Henkel failure criterion, as expressed in the following:

$$\tau_f = \tau_i \, e^{\beta (w_i - w_f)} \tag{3}$$

where

w_i, w_f = initial and final moisture contents;
τ_i, τ_f = shear strengths corresponding to moisture contents w_i and w_f, respectively; and
β = material constant.

This representation (Eq. 3) of the shear behavior has definite advantages over the one expressed by Eq. 2 because it eliminates the measurement of pore pressures generated during the shear. Also, in defining the strength in terms of moisture content, it considers the strength as related to volumetric effects, thus representing the

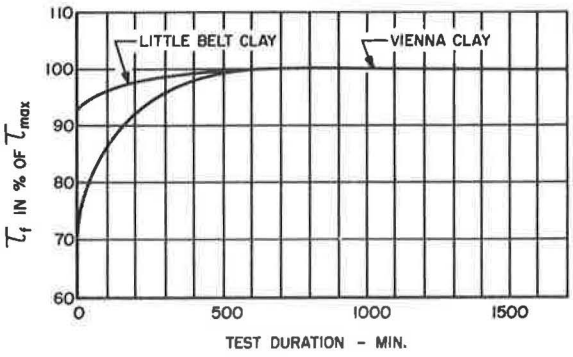

Figure 5. Relationship of increase in shear strength to increase in shear test duration.

interrelationship between the internal secondary bonds, defined as a function of atomic distances in the soil system, and the overall strength of the soil.

Notwithstanding its superiority over the Hvorslev-Terzaghi equation, the Winterkorn-Rutledge-Henkel failure criterion must be supplemented by consideration of time effects to define completely the shear behavior of saturated cohesive soils. Such consideration should ultimately relate experimentally observed increases or decreases in shear strength with time to pertinent changes in microstructure.

The author has investigated moisture content-time effects on artificially prepared saturated remolded New Jersey Grantham clay and on Tennessee C & C clay. Experimental results indicate a possible new direction in the knowledge of the shear response of soils. A survey of earlier researchers' conclusions and a discussion of author's findings follow.

PREVIOUS TIME EFFECT STUDIES ON SHEAR STRENGTH

Hvorslev was among the first investigators of time effects on the shear strength of soils. He performed a series of direct shear tests on saturated remolded Vienna and Little Belt clays. Tests on normally consolidated samples of both clays showed an increase in shear strength with the increase in shear test duration (Fig. 5). This discovery was not astonishing, however, because Hvorslev allowed drainage during the shear. Accordingly, the soil requiring the longest shearing time had the lowest moisture content at failure and, hence, the greater shear strength. Since the effect of variations in time and moisture content were not separated in these experiments, no real conclusion can be derived from Hvorslev's results.

Casagrande and Wilson (4) examined the shear behavior of undisturbed clays and clay shales at natural moisture contents somewhere between the plastic limit and the liquid limit. All tests were conducted under undrained conditions, with moisture contents kept constant throughout the experiments. One of the clays showed a continuous reduction in shear strength with increasing time duration of shear test, whereas other clays showed an increase in shear strength with increasing time, after initial sudden decrease (Fig. 6).

These two investigators have attributed the difference in the behavior of the clays to their degree of saturation. Though the degree of saturation may be an important factor, other material behavior aspects can also be responsible for this finding.

Goldstein (8) conducted studies on remolded as well as on undisturbed clay samples at liquid consistency above the plastic limit. He established a linear relationship between the reduction of strength and the logarithm of time (Fig. 7). His equation defining this soil behavior is:

$$q_t = q' \log\left(\frac{t_o}{t}\right) \qquad (4)$$

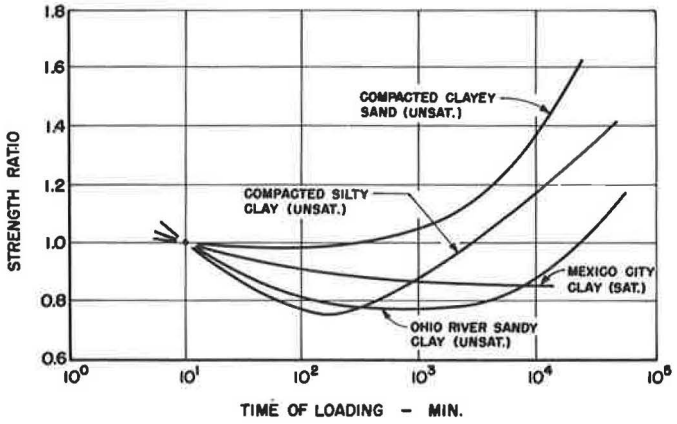

Figure 6. Relationship of shear behavior of undisturbed clays and clay shale to time duration of shear test.

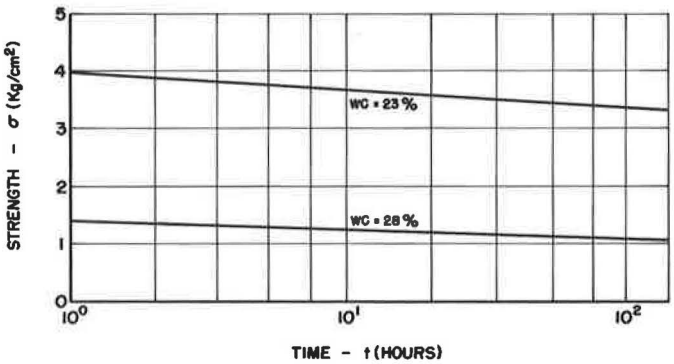

Figure 7. Relationship between reduction of strength and logarithm of time.

where

q_t = strength at time t;
q' = decrease in strength for a logarithmic cycle of time; and
t_o = reference time.

In their experiments on undisturbed Norwegian clays at moisture contents well above the plastic limit, Bjerrum, Simons and Toblaa (3) also found a reduction in shear strength with increasing time to failure (Fig. 8).

In view of the differences in the experimental findings of these researchers and because of the many discrepancies in other hypotheses regarding the time effects on the shear strength of saturated cohesive soils, further investigation along this line seemed in order. Since most of the arguments presented in defining the shear behavior of Grantham clay and C & C Tennessee clay make use of the concepts of modern material science, it is deemed essential at this point to discuss some of the properties of clays.

ENGINEERING PROPERTIES OF CLAYS

Consideration of the theory of collameritic systems (19) provides an understanding of the interrelationships and similarities between the behavior of clays and other engineering materials. According to this theory, there are many analogies between the physical behavior of saturated cohesive soils and that of metals. Figures 9 and 10

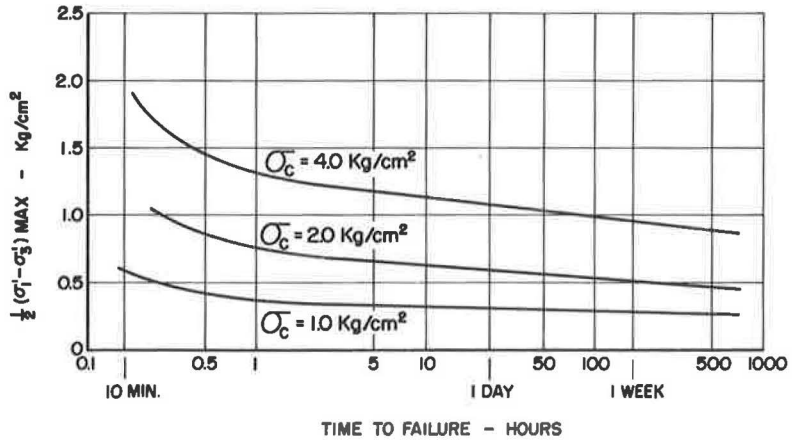

Figure 8. Relationship between shear strength and time to failure.

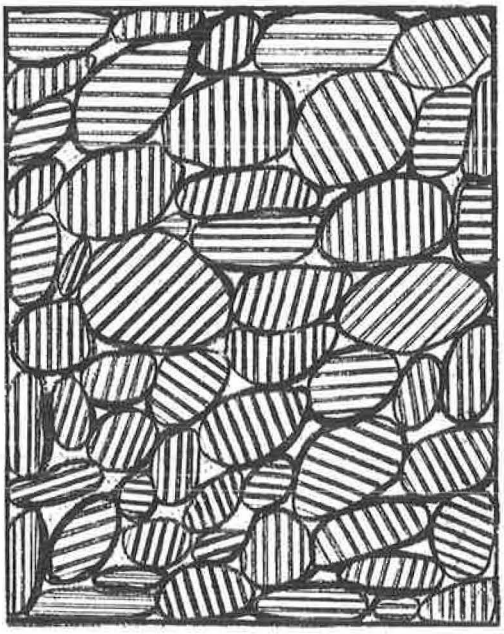

Figure 9. Internal structure of clay sample.

show a clay sample cross-section. The grains, or bundles, are a series of plate-like clay particles held together in a parallel arrangement as a result of secondary aggregation. The individual bundles, in turn, are bound together by secondary bonds.

These figures show a remarkable similarity between the internal structure of a piece of metal and that of a clay sample:

1. The pure crystals in metals are similar to the secondary aggregated grains in clays;
2. The crystalline planes through which plastic deformations take place in metals are similar to the planes between parallel clay plates along which individual plates can deform plastically;
3. The pure crystals in metals are held together by lower melting impurities containing phases that are always present at their surfaces in the same way as secondary aggregated bundles are held together with H-bonds and Van Der Waals' forces, acting in the adsorbed or otherwise adherent aqueous phases; and
4. The strength of impurities in metals decreases with rising temperatures in the same way the ionic and Van Der Waals' attractive forces in clays decrease with increasing moisture content.

The effect of temperature on metals is analogous to the effect of moisture content in clays. Since metals exhibit a distinct stress-strain relationship at different temperatures, it is logical that clays behave differently at different moisture content levels.

All saturated clays with moisture contents between the theoretical shrinkage limit and the theoretical liquid limit possess viscous, elastic, and plastic characteristics.

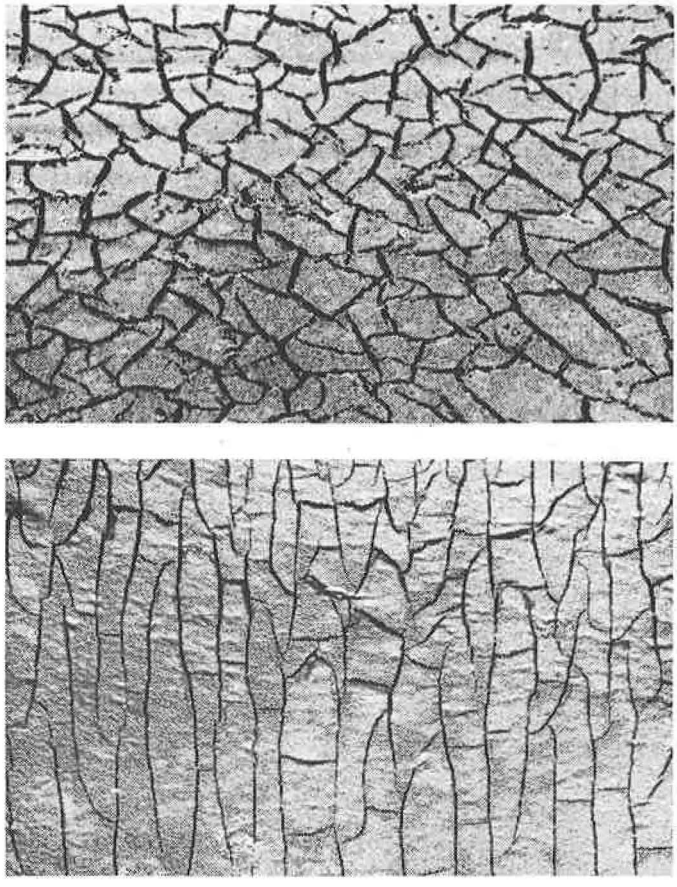

Figure 10. Clay sample cross-section: (a) horizontal section through frozen Ca-modification of a sandy-clayey loam; and (b) vertical section through frozen Ca-modification of a sandy-clayey loam.

Elastic Characteristics

When clay is subjected to stress, elastic deformation occurs. Elastic deformation in saturated clay is basically caused by the elongation or contraction of the clay plates and of the water found in various states of orientation and constraint, in the direction of applied stress. The clay particles are, themselves, anisotropic. The plates resume their former shapes on the removal of such stress.

Plastic Characteristics

True plasticity is a property of crystalline substances. Atoms in a crystal are arranged in various symmetric patterns and form two-dimensional planar lattices inclined toward each other at various angles, depending on the crystallographic symmetry. Lattice planes with the greatest interplanar distances are the most weakly bonded to their neighboring planes. Due to the mechanism of loading, shear stresses are greater in one direction than in others, and plastic flow occurs more easily in planes closely aligned with the direction of the maximum shear forces. Any movement along such planes involves the simultaneous displacement of all the atoms in this plane. Hence, a definite yield value exists which must be exceeded before a plastic flow can be initiated.

Clay-water systems possess secondary plasticity. The platelike clay particles that are lubricated and bonded by the liquid play a role similar to that of the lattice planes in crystals. In clay-water systems, aggregated and oriented clay platelets whose

surfaces are lubricated with adsorbed water, represent the individual gliding plane systems. In these bundles, plasticity is one- or two-dimensional; a large number of such bundles, making up the gross system and oriented in all possible directions, may result in an overall three-dimensional plasticity similar to that observed in normal structural metals (19).

Viscous Characteristics

Clay soils possess high viscosity due to their hydrophilic properties; in addition, they possess the properties of hydrophobic colloids because of their sensitivity to electrolytes. Although the viscosity of the clay-water system depends almost entirely on the volume relationship between the liquid and the solid phases, as inferred from the Einstein formula, many investigators have observed that the addition of small amounts of electrolytes produces change in their viscosity. Whenever the induced electrolyte affects the magnitude of the ζ potential, it likewise affects the viscosity of the system in direct proportion. Changes of considerable magnitude in viscosity result from structural changes, especially those involving dispersion or flocculation.

EXPERIMENTAL INVESTIGATION

Type and Property of Materials

Tests were performed on two types of clays, New Jersey Grantham clay and Tennessee C & C clay. Their physical properties are summarized in Table 1.

Types of Tests Performed

The laboratory investigation included four groups of tests on Grantham clay and one group on C & C Tennessee clay, as indicated in Table 2.

BEHAVIOR OF SATURATED REMOLDED GRANTHAM CLAY AS A FUNCTION OF MOISTURE CONTENT AND TIME

Analysis of the stress-strain diagrams obtained at different rates of shear indicates an interesting relationship between the behavior and shape of these diagrams and the moisture contents of the clay samples examined.

In the case of Grantham clay, there seems to be a transition zone with boundary values defined in terms of moisture content at 44 percent < w < 46 percent (close to plastic limit), above and below which two distinct types of behavior are observed.

The shapes of stress-strain diagrams obtained from samples at moisture contents below the plastic limit indicate that the material clay undergoes pseudo-elastic, followed by elasto-viscous, deformations during the initial stages of shear up to a certain stress level, beyond which plastic deformations occur, as shown by the peak stresses in Figures 11 and 12.

To understand further and define the behavior of Grantham clay at moisture contents below the plastic limit, a series of seven samples were consolidated under a given constant hydrostatic stress for a week. Two of the samples were than sheared in undrained tests. On the other five samples, constant stresses corresponding to 95, 90, 85, 80 and 75 percent of the average failure strength obtained from the two previous samples were applied and the soils were allowed to creep (Fig. 13).

These curves show that all deformations ceased a short while after the initiation of creep tests. When the creep samples were sheared after the durations of time indicated on the curves, their strength increased over its initial short-term magnitude (Table 3), indicating the presence of the work-hardening phenomenon. On the basis of these experimental findings, Grantham clay at moisture contents below the plastic limit is defined as work-hardening, viscoelastic-plastic material.

At moisture contents above the plastic limit, however, the stress-strain diagrams demonstrate that after certain stress levels are attained, excessive deformations occur, and the behavior of the clay beyond these levels depends on the rate of shear

(Figs. 14, 15 and 16). This behavior would indicate that the clay bundles resist the stresses pseudo-elastically until a certain stress level is reached, beyond which the internal bonds between the individual aggregated bundles are broken and the system thereafter enters the flow state. It is apparent that this is a viscoelastic behavior.

To determine the type of viscoelasticity possessed by the clay, a series of creep tests under constant stresses were performed (Fig. 17). The fact that the creep test results show that the soil deformed at a constant rate of flow beyond the initial stage indicates liquid viscoelasticity.

The liquid viscoelastic material is characterized by a constant rate of flow under constant creep stresses, indicating the existence of statistical equilibrium between the number of bonds broken in the process of flow and the number of bonds formed during the same process. Thus, the liquid viscoelastic material's response under a given state of stress would be independent of the stress history (or stress path) of the material and would only be a function of the magnitude of applied stresses. In Figure 18, $\alpha_1 = \alpha_2'$, $\alpha_2 = \alpha_3'$ and $\alpha_4 = \alpha_5'$, regardless of the stress path.

To emphasize time effects in determining the strength of liquid viscoelastic soils, consider a series of five samples consolidated under the same hydrostatic pressure σ_3 and allowed to creep under constant stresses corresponding to 90, 80, 75, 65 and 55 percent of the initial short-term failure strength, until the tertiary portion of the creep deformation is attained (Fig. 19). Since liquid viscoelastic materials are non-work-hardening, each of the previous samples would reach a level of strain e (t), at which excessive deformations occur.

Defining the lower limit of these tertiary strains as the failure strain, we demonstrate the dependence of shear strength of liquid viscoelastic materials on the duration of the constant stress. The strength of liquid viscoelastic clay decreases due to continuous creep flow. Therefore, to define the strength to be used in actual design problems, we must seek a maximum stress level that does not cause continuous deformation, thus effecting continuous reduction in shear strength. Such a stress level exists for all real materials and is known as the creep limit. Its obtained value corresponds to the intercept of the stress vs rate of constant creep strain curve on the stress ordinate. Such a curve can be constructed from a series of creep tests on soils at constant moisture contents, deforming under various stresses.

The creep limits for liquid viscoelastic Grantham clay at moisture contents of 49.43 and 51.4 are 38 and 29 percent, respectively, of their short-term strength. (The short-term strength for both samples is defined at 20 percent strain.)

When the shear strength of Grantham clay is defined at peak stresses for samples with moisture contents below the plastic limit and at 20 percent strain for samples with moisture contents above the plastic limit, the diagrams shown in Figure 20 (for undrained tests) and in Figure 21 (for unconfined tests) are obtained. The fact that the failure strength is not decreased by decreasing rate of shear for soils at moisture contents below the plastic limit indicates that the strength of such soils can be defined at peak stresses, and the Winterkorn-Rutledge-Henkel failure criterion adequately defines the failure design strength envelope.

The same criterion does not apply, however, to Grantham clay with moisture contents above the plastic limit because the strength of the soil decreases with decreasing rate of shear. Hence, the w percent vs log $(\sigma_1 - \sigma_3)$ curves, which lie above the plastic limit in Figures 20 and 21, do not represent the design strength of the soil but merely indicate the strength corresponding to a certain duration of time.

Therefore, to represent a complete design failure strength envelope, the percentage moisture content must be plotted against the log $(\sigma_1 - \sigma_3)$ defined at peak stresses (for samples at moisture contents below the plastic limit), and against the log $(\sigma_1 - \sigma_3)$ defined at creep limit (for soils above the plastic limit). Such an experimental envelope obtained on Grantham clay is shown in Figure 22.

In view of these experimental findings, the mechanical model shown in Figure 23 would represent the flow and deformation characteristics of the Grantham clay at moisture contents below the plastic limit. The equation defining the mathematical

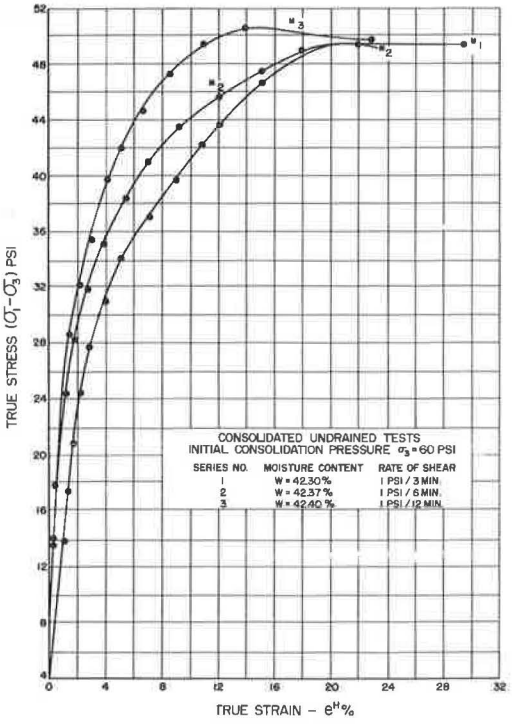

Figure 11. Effect of moisture content, at different rates of shear, on stress-strain behavior of Grantham clay.

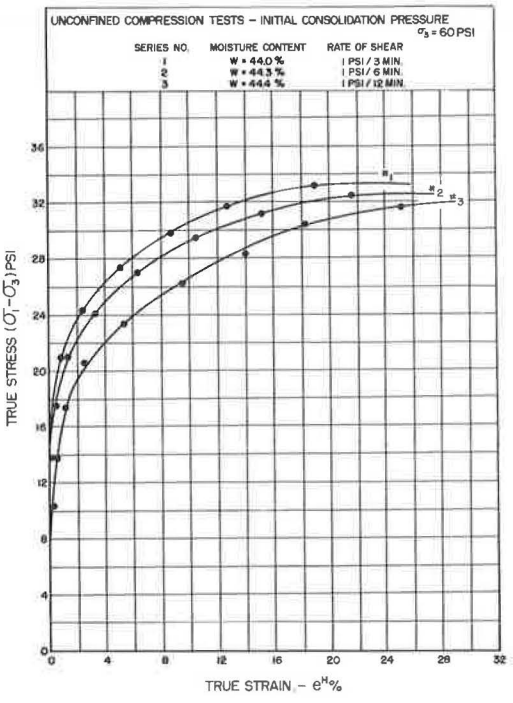

Figure 12. Effect of moisture content, at different rates of shear, on stress-strain behavior of Grantham clay.

TABLE 1

PROPERTIES OF CLAYS INVESTIGATED

Type of Clay	L. L. (%)	P. L. (%)	S. L. (%)	Specific Gravity	Degree of Saturation (%)	Color	Molding Moisture Content (%)
Grantham	68	44	19	2.6	99	white	56
Tennessee	68	35.4	-	2.5	100	white	47

TABLE 2

CLAY GROUPS INVESTIGATED

Grantham				C & C Tennessee
Group I[a]	Group II[a]	Group III	Group IV	
Consolidated undrained tests at different rates of shear: 1 psi[b]/3 min 1 psi/6 min 1 psi/12 min	Consolidated undrained but unconfined tests sheared at same rates as Group I	Creep tests on samples at moisture contents above the plastic limit	Creep tests on samples at moisture contents below the plastic limit	Consolidated undrained tests at different rates of shear: 0.5 psi/1 min 0.5 psi/5 min 0.5 psi/30 min

[a]All data obtained from stress-controlled tests.

[b]1 psi on loader corresponds to 25 lb on soil sample. (The samples were 6.5 in. high and 2.8 in. in diameter.)

TABLE 3

CREEP SAMPLES[a]

Measurement	Sample No.			
	I	II	III	IV
Constant creep stress (psi)	57	54	50	47
Duration of stress (hr)	533	556	552	586
Shear strength (σ_1 - σ_3) psi	-	71.2	70	69.8
Moisture content (w%)	-	40.67	40.65	40.7

[a]Initial shear strength (σ_1 - σ_3) = 64 psi; w initial = 40.7 percent.

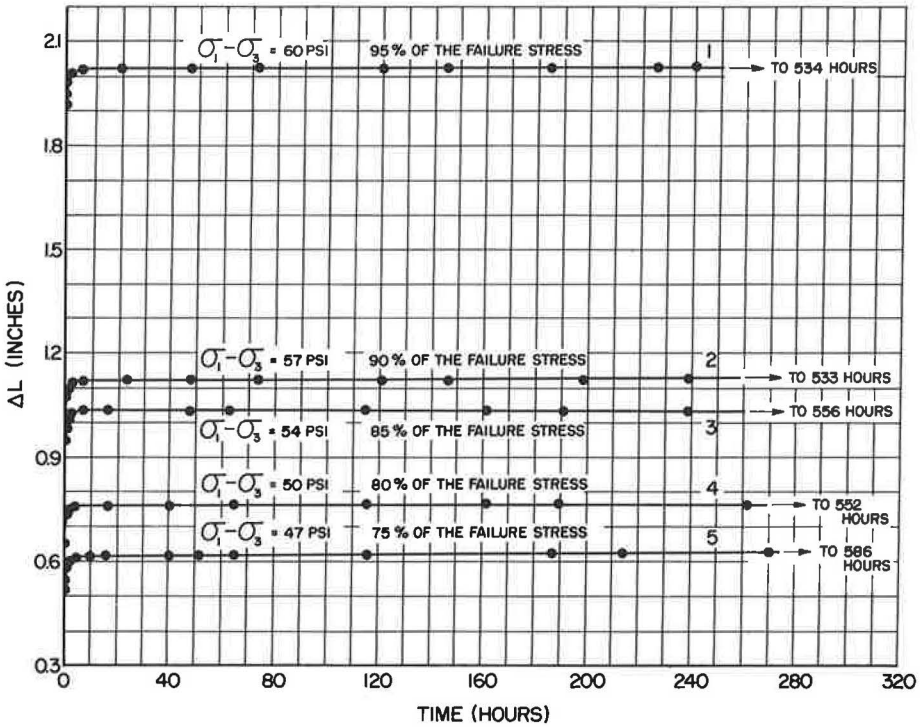

Figure 13. Creep tests, series A, showing behavior of Grantham clay with moisture contents below the plastic limit.

Figure 14. Behavior of clay with moisture contents above the plastic limit.

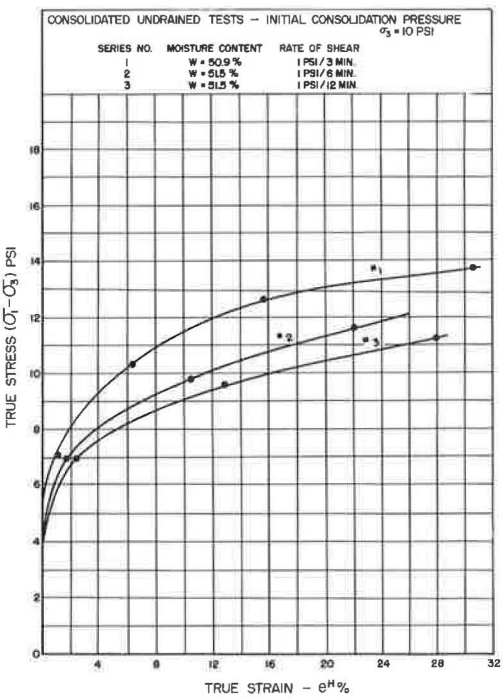

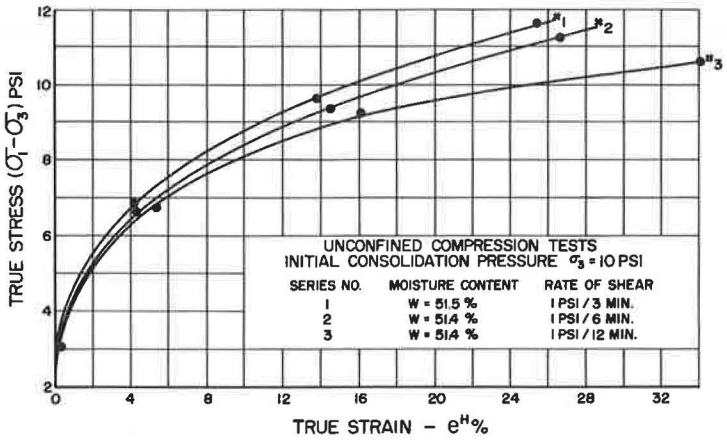

Figure 15. Behavior of clay with moisture contents above the plastic limit.

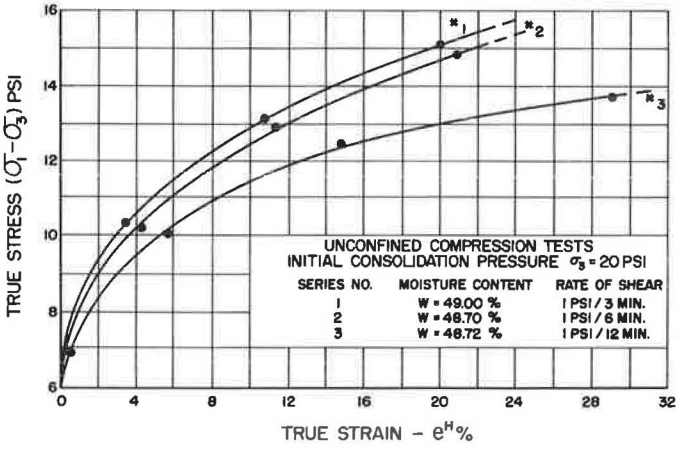

Figure 16. Behavior of clay with moisture contents above the plastic limit.

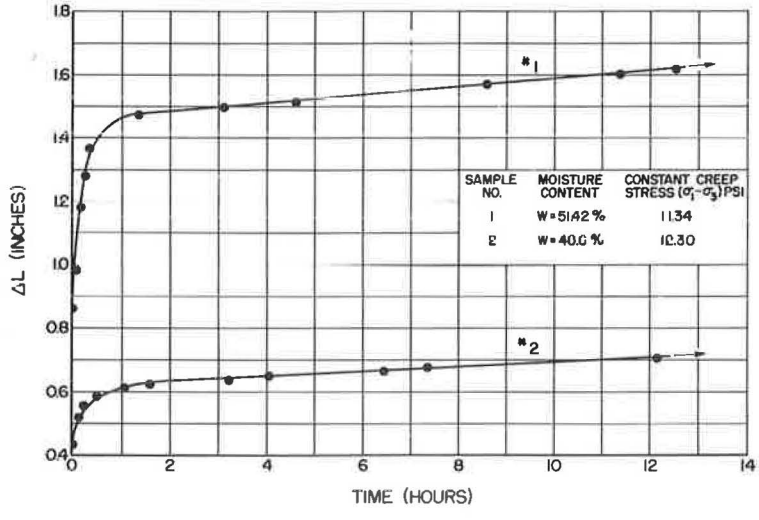

Figure 17. Creep tests, series B, to determine type of viscoelasticity possessed by clay.

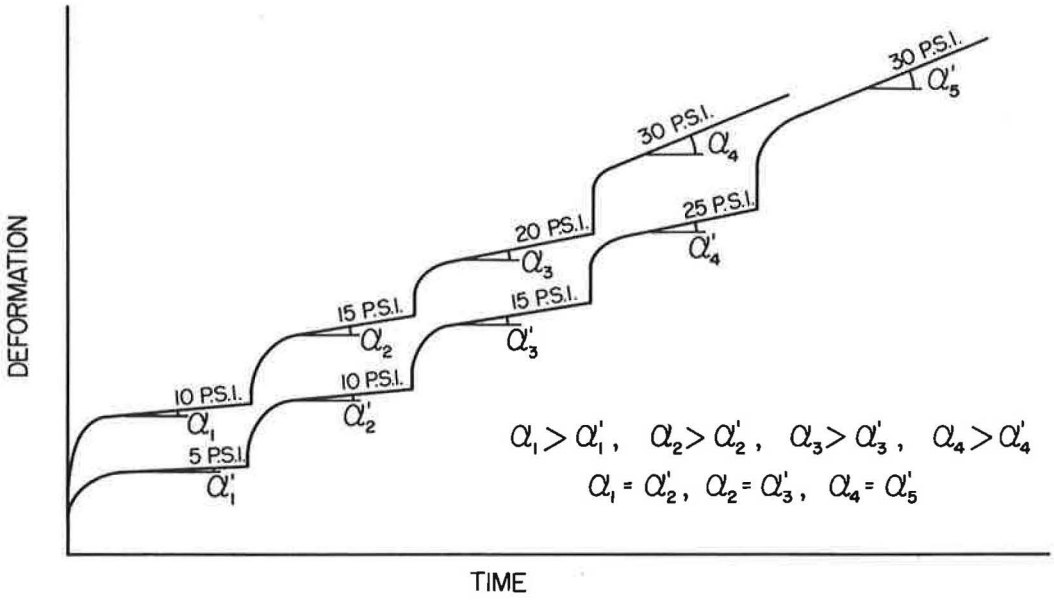

Figure 18. Creep flow of liquid viscoelastic material.

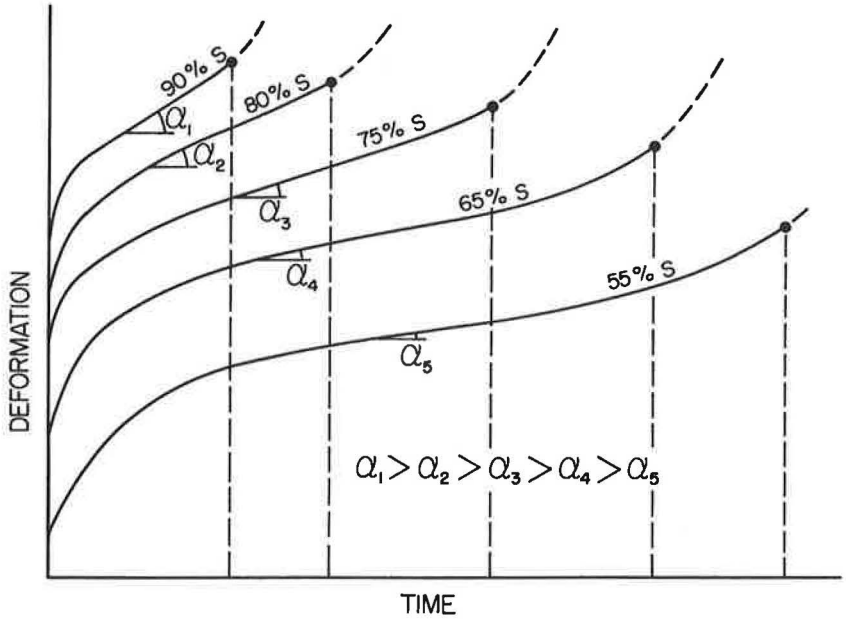

Figure 19. Creep flow of liquid viscoelastic soil.

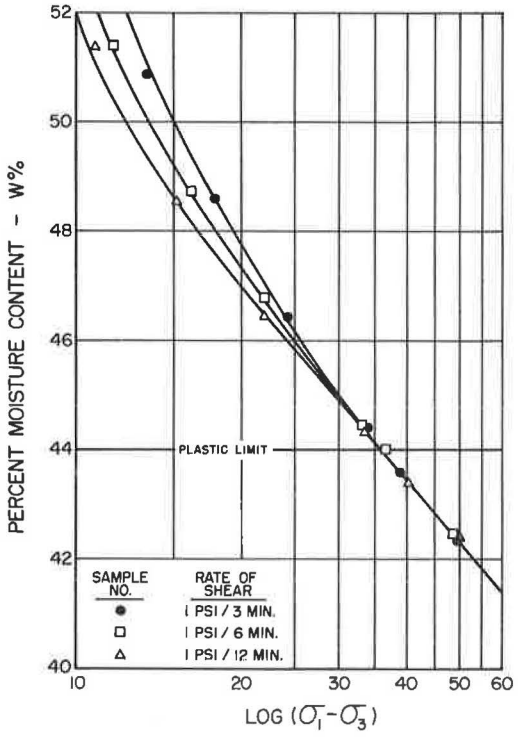

Figure 20. Consolidated undrained tests on Grantham clay.

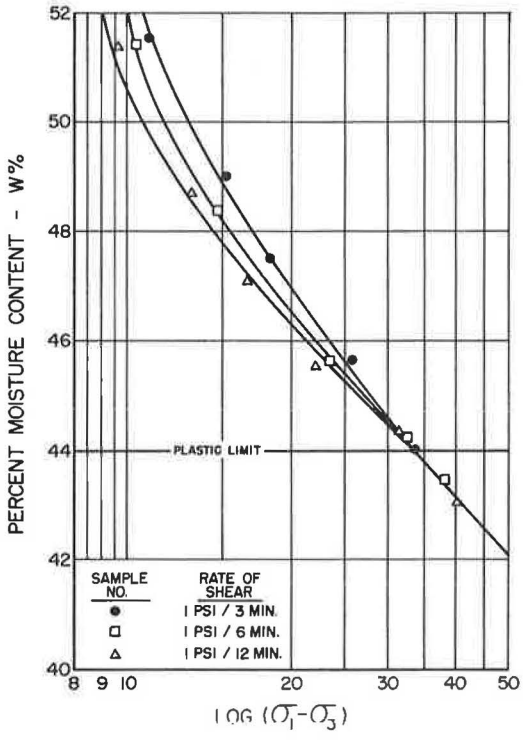

Figure 21. Unconfined compression tests on Grantham clay.

behavior of the soil can, in turn, be obtained from the aforementioned representative mechanical model:

$$\sigma - \theta(\dot{e})^{-1} = G_2 e - \frac{G_2}{G_1}\sigma + \eta\dot{e} - \frac{\eta_2}{G_2}\dot{\sigma} \qquad \text{(for } \sigma < N.f\text{)} \tag{5}$$

where

$\sigma, \dot{\sigma}$ = stress, rate of stress;
$e, \dot{e}$ = strain, rate of strain;
G_1, G_2 = shear moduli of elasticity for Hookian element, for Kelvin body;
η = coefficient of viscosity;
N.f = plastic or yield limit; and
$\theta(\dot{e})^{-1}$ = work-hardening parameter.

The model shown in Figure 24, would define the rheological behavior of the Grantham clay at moisture contents above the plastic limit. The St. Venant element between the Newtonian dashpot and the Kelvin body corresponds to the creep limit, indicating the existence of a certain energy barrier that must be exceeded before any constant rate of flow can be initiated. The rheological equations representing the shear behavior of the soil can be obtained from the above model, depending on the level of stress:

$$\dot{e} + \frac{\eta_2}{G_2}\ddot{e} = \frac{\sigma}{\eta_1} + \dot{\sigma}\,\frac{\eta_1 G_2 + \eta_2 G_1 + \eta_1 G_1}{\eta_1 G_1 G_2} + \ddot{\sigma}\,\frac{\eta_2}{G_1 G_2} \qquad \text{(for } \sigma > \sigma_y\text{) and} \tag{6}$$

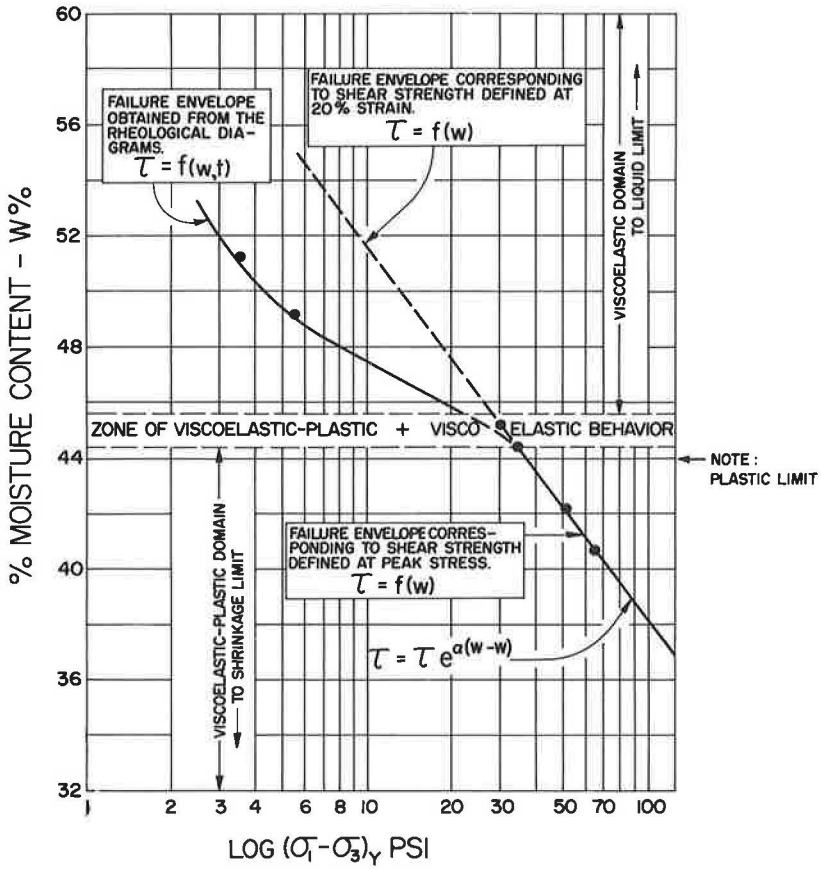

Figure 22. Shear behavior of Grantham clay.

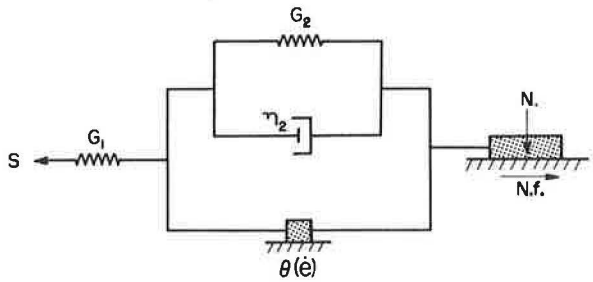

Figure 23. Rheological model representing the behavior of the clay below transition zone (below plastic limit).

$$\sigma = G_2 e + \frac{G_2}{G_1}\sigma + \eta_2 \dot{e} - \frac{\eta_2}{G_1}\dot{\sigma} \qquad (\text{for } \sigma < \sigma_y) \tag{7}$$

To gain further insight into the time effects in shear strength, additional experiments were conducted on saturated remolded C & C clay.

SHEAR BEHAVIOR OF C & C TENNESSEE CLAY AS A FUNCTION OF MOISTURE CONTENT AND TIME

The physical properties of C & C clay and the types of experiments conducted on this soil are summarized in Tables 1 and 2, respectively.

The results obtained from 31 shear tests are shown in Figure 25. Analysis of shear strength, time and moisture content relationships reveals two interesting features: (a) the shear strength of C & C clay is time-independent at moisture contents below the plastic limit; and (b) the shear behavior of the clay is time-dependent at moisture contents above the plastic limit.

The fact that the failure envelope of series C is to the right of the failure envelope of series B (Fig. 25) indicates that C & C Tennessee clay exhibits work-hardening viscoelastic behavior. Work-hardening, in general, can be considered functionally related inversely to the rate of shear. Therefore, at relatively higher rates of shear, its effect would not be very pronounced. (This is particularly obvious from the experimental results indicating an increase in the resistance of wires during the drawing process when the material is allowed to relax slightly.) Therefore, the reduction in shear strength due to creep is greater than the gain in shear strength due to work-hardening for test series B as compared to test series C.

The complete cessation of creep deformation under constant stresses after a certain period of time (Figs. 26 and 27), and the increase in shear strength of samples after creep (Table 4), further verify the existence of work-hardening.

Since the shear strength of the C & C clay does not decrease indefinitely with increasing time to failure, the design shear strength of work-hardening viscoelastic soil can be defined, without reservation, at 20 percent strain.

In conclusion, the shear strength of viscoelastic plastic and work-hardening viscoelastic soils can be defined at the peak stress and at 20 percent strain, respectively. The strength of liquid-viscoelastic soils, however, should be defined at the creep limit.

APPLICATION OF THEORY TO UNDISTURBED SOILS

To determine the usefulness of the theory advanced in this paper to practicing civil engineers, it was decided to conduct a series of experiments on undisturbed soils.

Three 2- by 2- by 2-ft block samples of over-consolidated Seattle clays were obtained at various depths below the ground surface.

Table 5 indicates some of the basic engineering properties and Figure 28 shows grain size distribution for these clays.

A series of samples 6.5 ft high and 2.8 ft in diameter were prepared from each block and were consolidated under 90 psi and sheared in a stress controlled loader at the rate of 25 lb/3 min in an undrained condition. The results obtained from these tests are given in Table 6.

The rest of the samples were dressed in two rubber membranes and consolidated under 90 psi for the same amount of time as the previous samples. On completion of the consolidation process, the water outlets were closed and the samples were subjected to constant creep stresses corresponding to a certain precentage of the short-term strength.

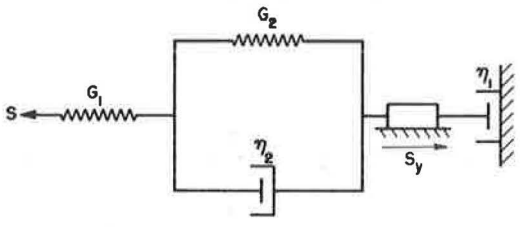

Figure 24. Rheological model representing the behavior of the Grantham clay above transition zone (above plastic limit).

Figures 29, 30, 31, 32, 33 and 34 show the test samples failing under creep stresses much less than their initial short-term strength. The constant creep stress vs constant creep flow curves for the block samples I, II and III are shown in Figures 35, 36 and 37, respectively. From these respective curves the creep limits are found to be 50, 53 and 57 percent of the short-term strength of the soils. To ascertain that the creep limits obtained from plots such as shown in Figures 35, 36 and 37 actually correspond to the value of the maximum creep stress that does not cause continuous creep flow, a sample

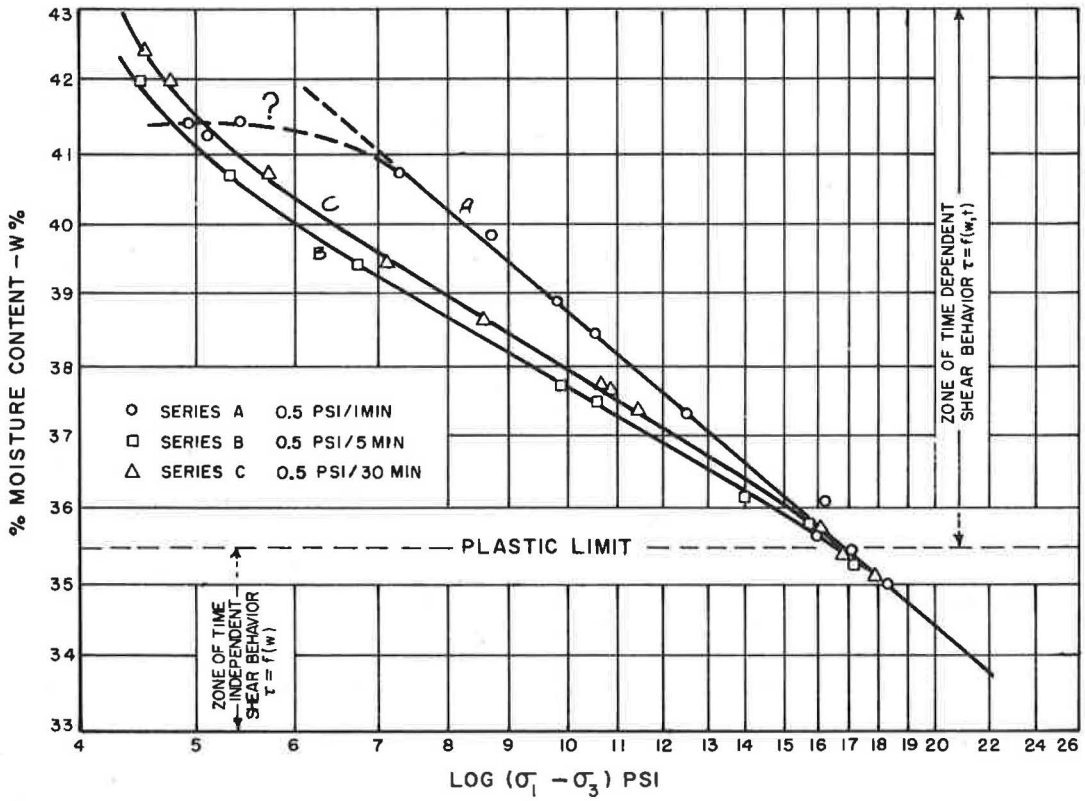

Figure 25. Shear behavior of C & C Tennessee clay.

TABLE 4

CREEP TEST

Sample No.	Moisture Content (%)	Constant Creep Stress (psi)	Initial[a] Shear Strength (psi)	Shear Strength After Creep (psi)
1	39.0	5.76	9.6	11.2
2	41.2	4.82	7.0	7.7

[a]Rate of shear = 0.5 psi/min.

TABLE 5

BASIC PROPERTIES OF SEATTLE CLAYS

Block Sample No.	Location (Sta.)	Depth (ft)[a]	L. L.	P. L.	S. G. (%)	Natural Moist. Cont. (%)
1	2209 + 20	36	44.4	28.0	2.76	29.0
2	2210 + 50	40	34.0	25.0	2.74	24.4
3	2195 + 70[b]	6	47.7	22.0	2.70	24.76

[a]Distance below surface level at which samples were obtained.
[b]Near tunnel.

TABLE 6

TEST RESULTS

Block No.	Sample No.	Natural Moist. Cont. (w%)	Failure Deviator Stress $(\sigma_1 - \sigma_3)_f$	Avg. Strength $(\sigma_1 - \sigma_3)$ (psi)
1	1	29.0	200.0	198.0
	2		197.5	
	3		198.2	
2	1	24.4	221.0	219.0
	2		217.0	
	3		218.0	
	1	24.7	147.0	148.0
	2		146.0	
	3		151.0	

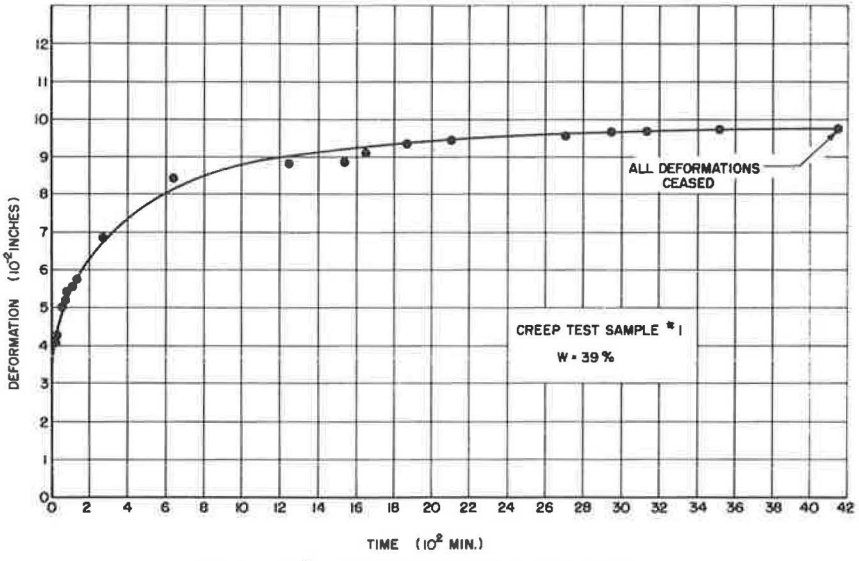

Figure 26. Creep test on C & C clay.

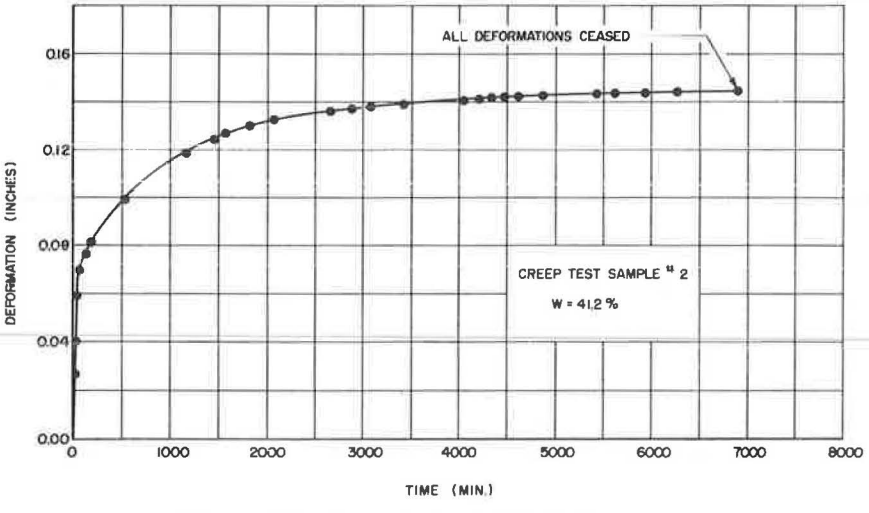

Figure 27. Creep test on C & C clay.

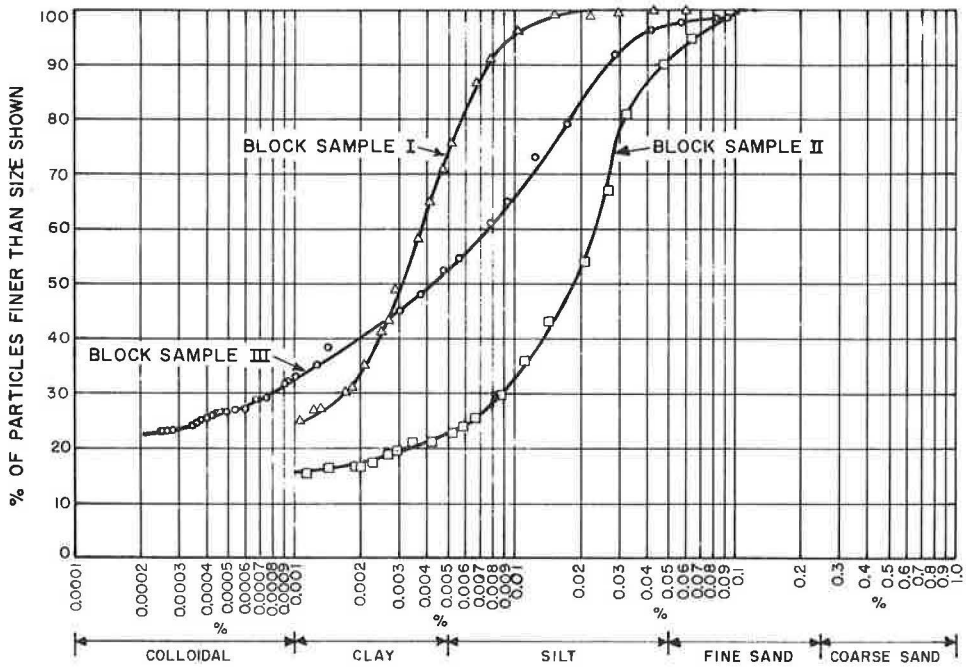

Figure 28. Grain-size distribution.

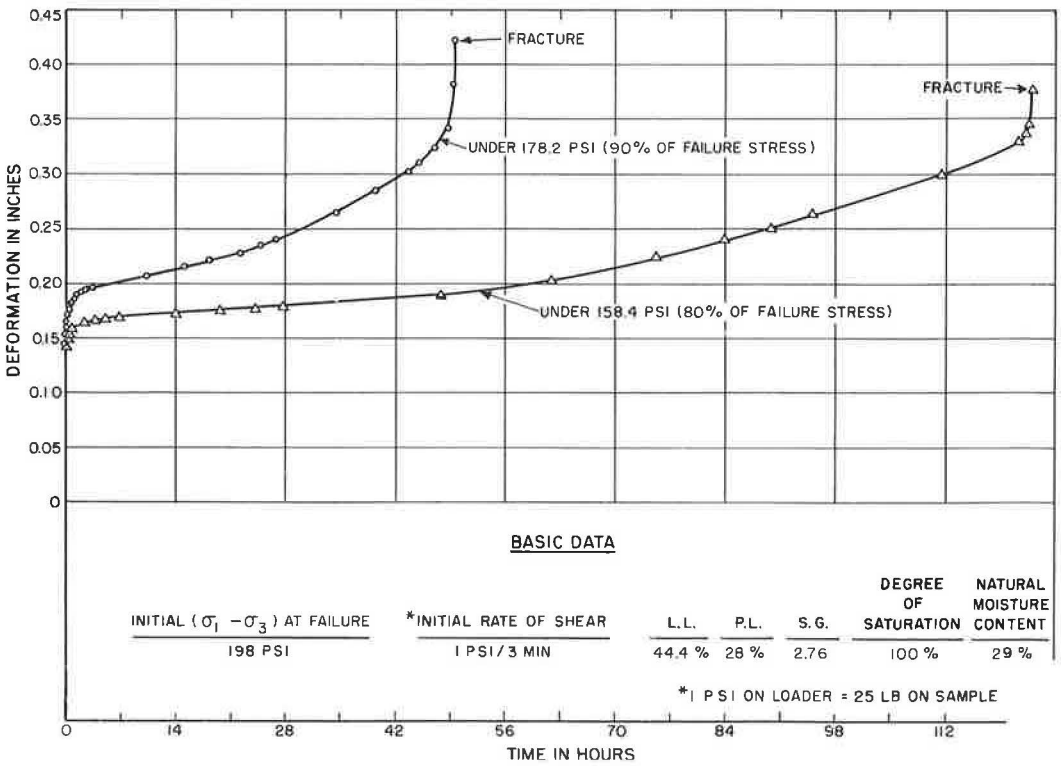

Figure 29. Creep series No. I on over-consolidated Seattle clays.

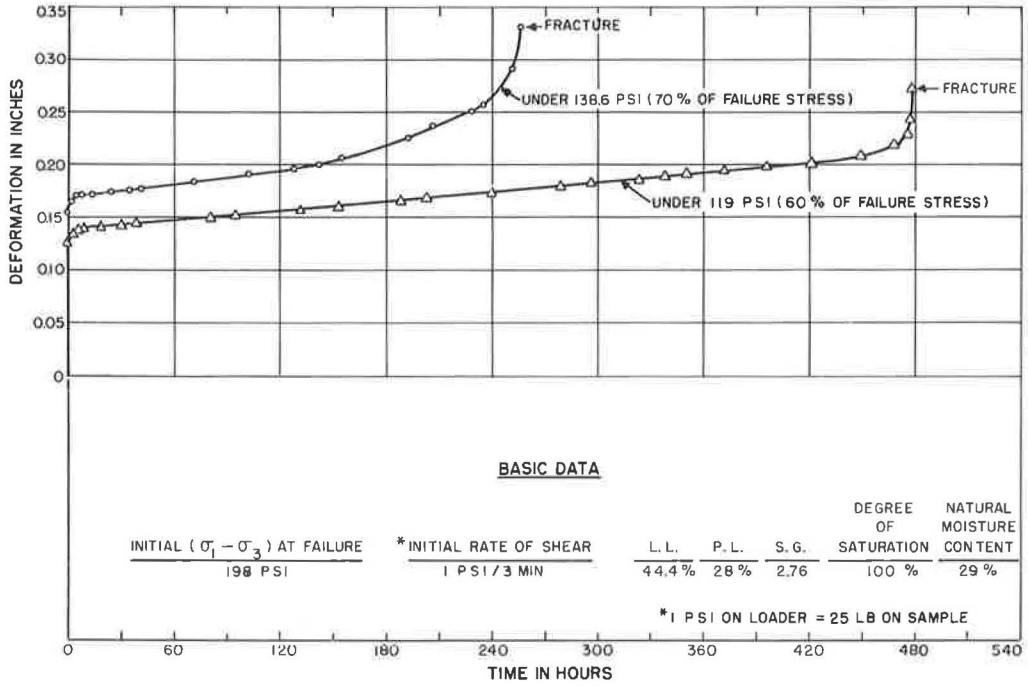

Figure 30. Creep series No. I on over-consolidated Seattle clays.

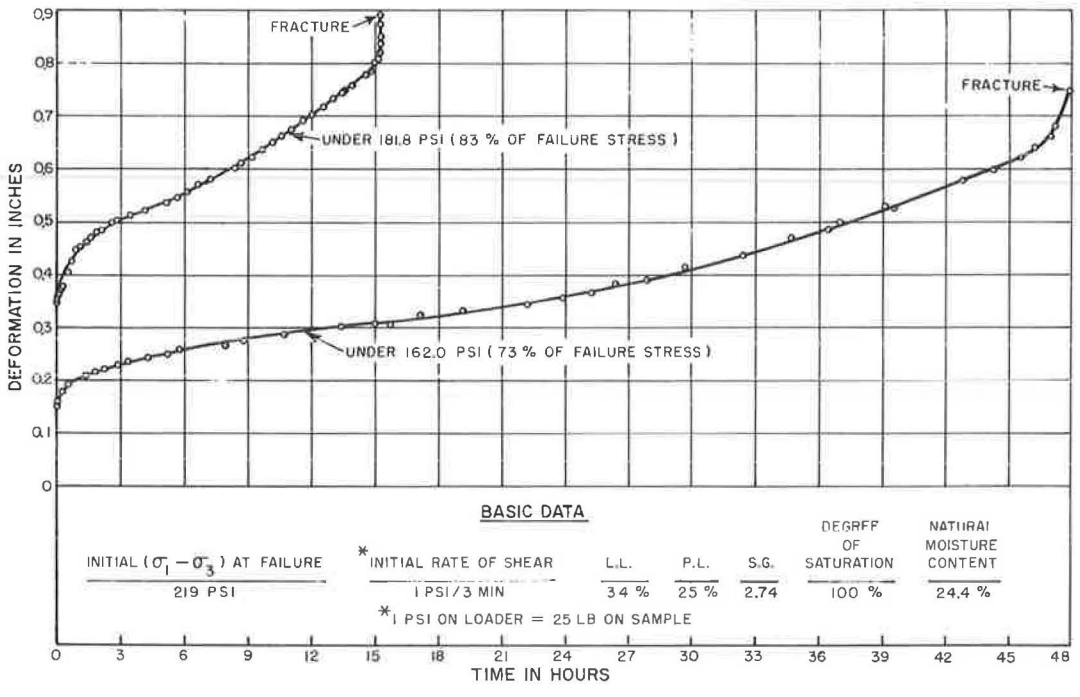

Figure 31. Creep series No. II on over-consolidated Seattle clays.

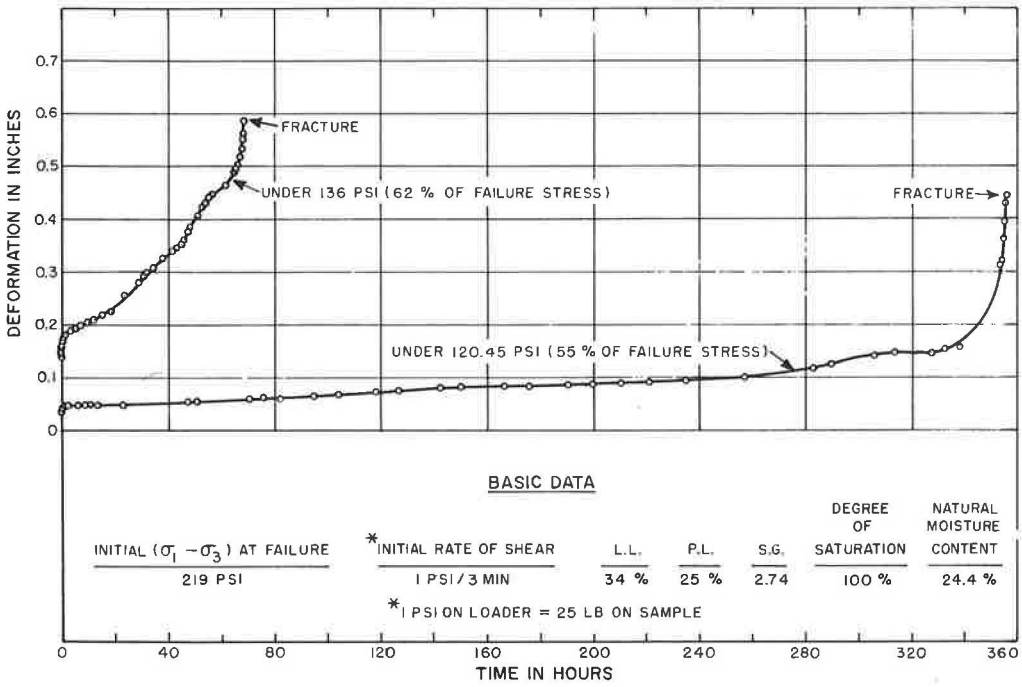

Figure 32. Creep series No. II on over-consolidated Seattle clays.

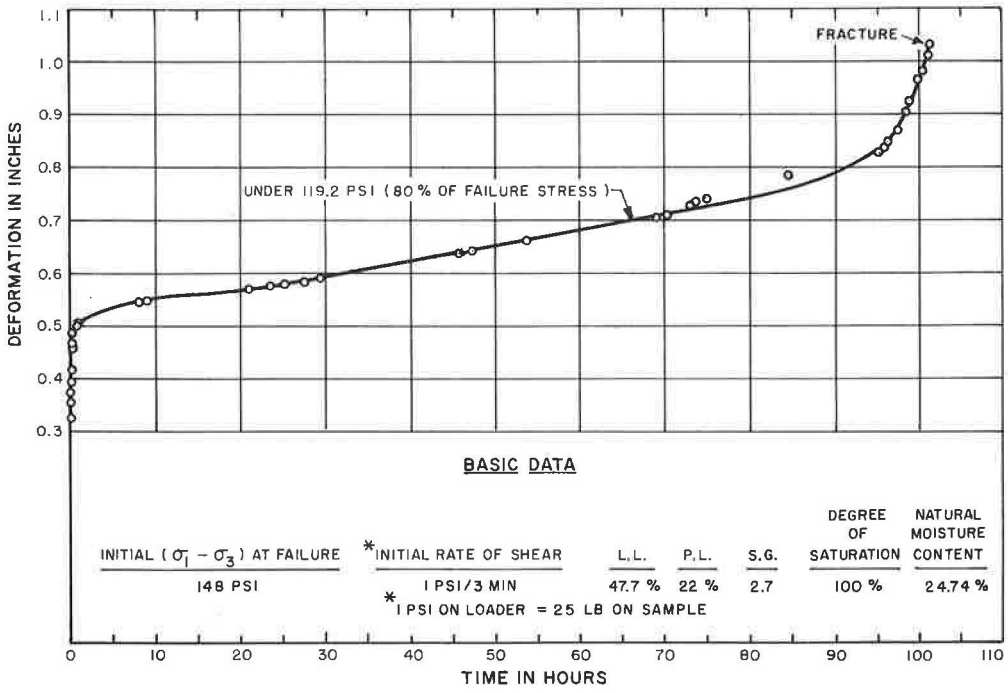

Figure 33. Creep series No. III on over-consolidated Seattle clays.

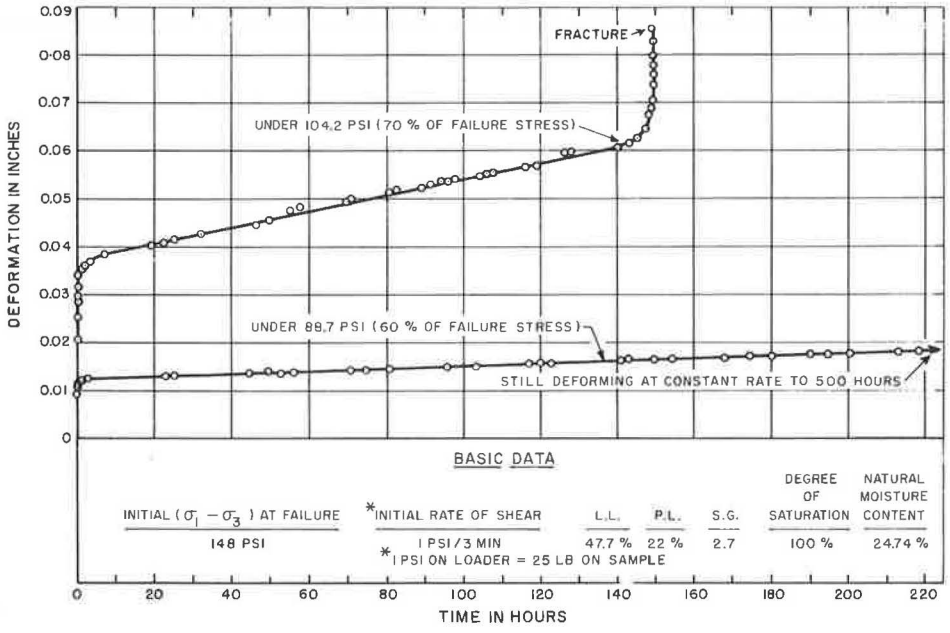

Figure 34. Creep series No. III on over-consolidated Seattle clays.

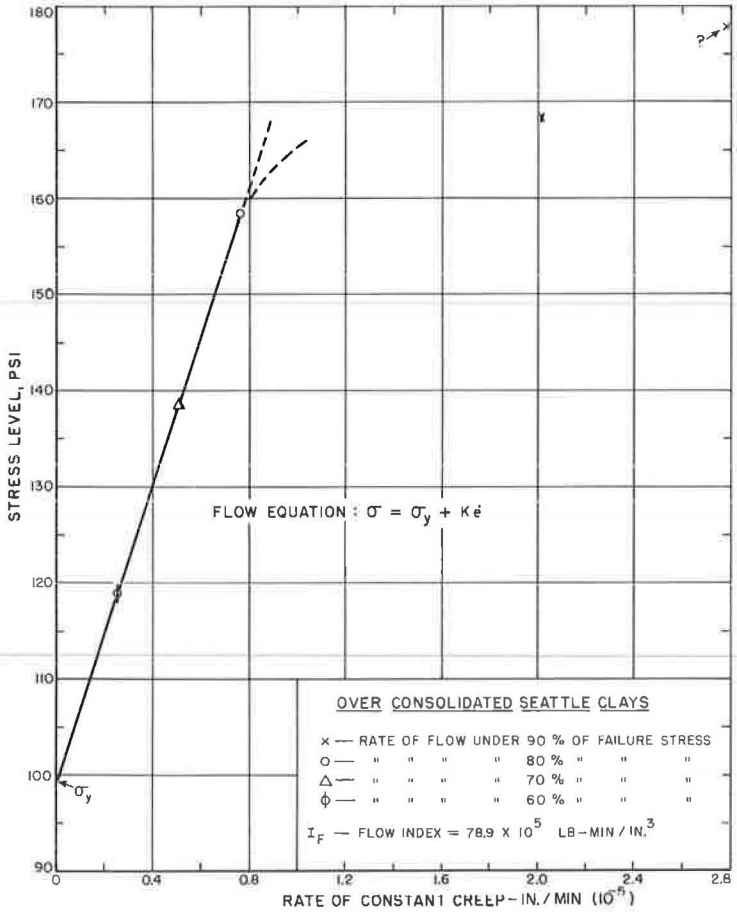

Figure 35. Stress vs rate of constant creep strain (from creep series No. I).

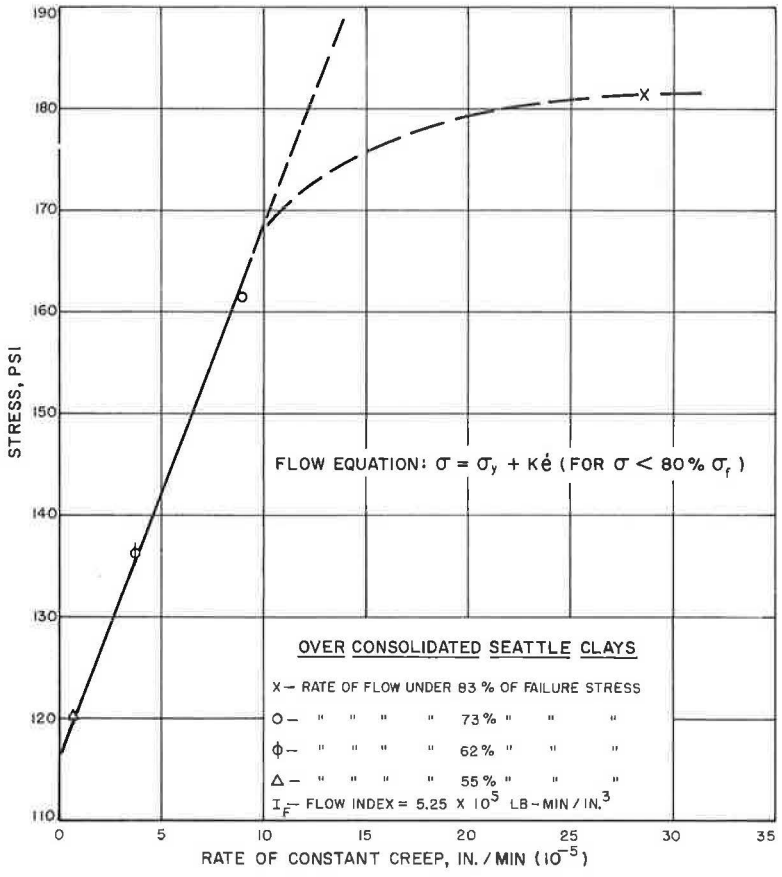

Figure 36. Stress vs rate of constant creep strain (from creep series No. II).

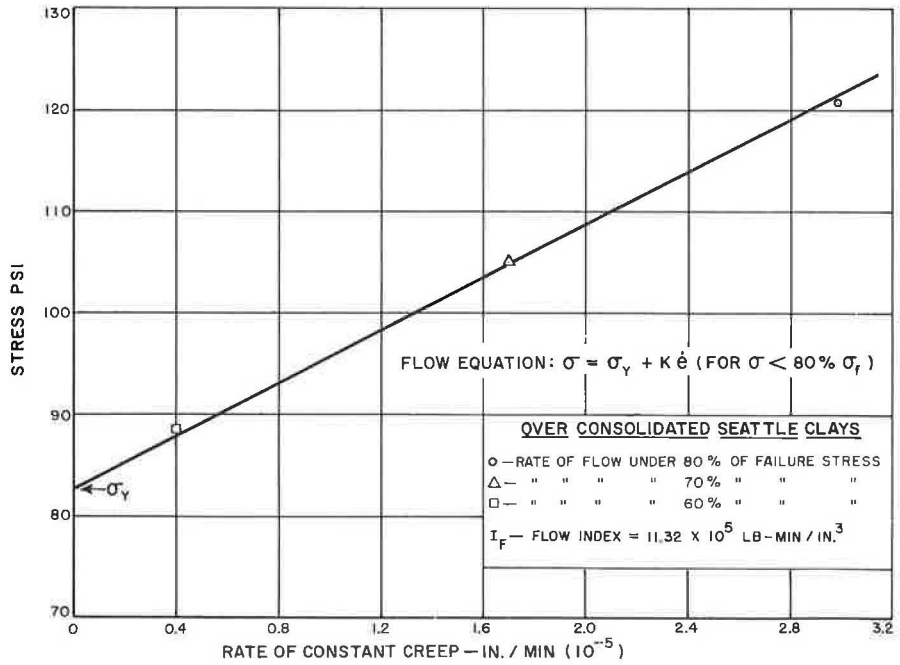

Figure 37. Stress vs rate of constant creep strain (from creep series No. III).

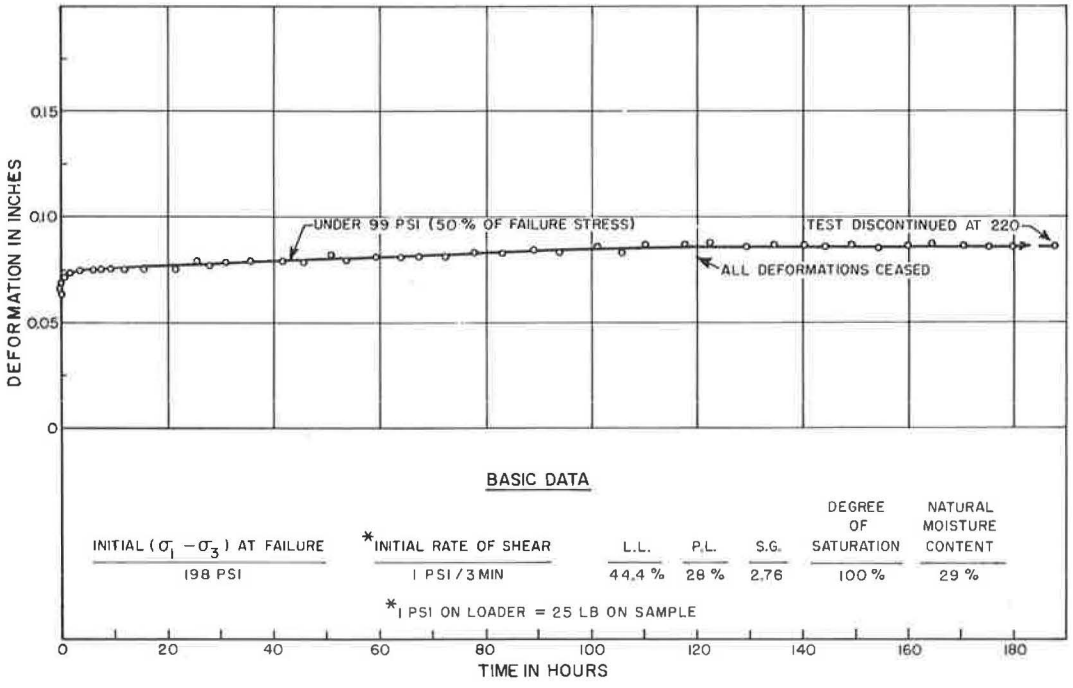

Figure 38. Creep series No. I on over-consolidated Seattle clays.

from block sample I was subjected to a constant creep stress corresponding to 50 percent of its short-term strength (creep limit) and allowed to creep. Figure 38 shows that all deformation stopped after 115 hr thus indicating the validity of the author's proposed method in determining the magnitude of creep limits. Experiments on two other types of soils not included in this report also confirm these findings.

On the completion of creep, the soil sample was sheared in an undrained test and a value of 5 percent reduction in its shear strength was observed.

In conclusion, it could be stated that the proposed theory is applicable to disturbed and undisturbed soils, and should find an immediate practical application in soil mechanics, especially in problems dealing with slope stability and lateral earth pressures against retaining structures.

REFERENCES

1. Baver, L. D. Soil Physics. John Wiley & Sons, 1940. 370 pp.
2. Baver, L. D. The Effect of the Amount and Nature of Exchangeable Cations on the Structure of a Colloidal Clay. Agricultural Exper. Sta. Res. Bull., No. 129, Univ. of Missouri, 1929. 48 pp.
3. Bjerrum, L., Simons, N. and Torblaa, I. The Effect of Time on the Shear Strength of a Soft Marine Clay. Brussels Conference on Earth Pressure Problems, Vol. I. 1958.
4. Casagrande, A., and Wilson, S. D. Effects of Rate of Loading on the Strength of Clays and Shales at Constant Water Content. Geotechnique, Vol. 2, 1950.
5. Coulomb, C. A. Essai sur une Application des Regles de Maximis et Minimis a Quelques Problemes de Statique Relatifs a l'Architecture. Mem. Div. Sav., Academie des Sciences, Paris, 1776.
6. Czeratzki, W., and Frese, H. The Importance of Water in the Formation of Soil Structure. Highway Research Board Spec. Rept., No. 40, pp. 200-211, 1958.
7. Deryagin, B. V. The Force Between Molecules. Scientific American, Vol. 203, No. 1, 1960.

8. Goldstein, M. Long Term Strength of Clays and Depth Creep of Slopes. Proc. of Fourth Internat. Conf. on Soil Mechanics and Foundation Eng., Vol. 2, 1957.
9. Menkel, J. D. Correlation Between Deformation, Pore Water Pressure and Strength Characteristics of Saturated Clays. Ph.D. thesis in Eng., Imperial College of Sci. and Tech., London, 1958.
10. Hvorslev, M. J. Physical Components of the Shear Strength of Saturated Clays. A. S. C. E. Proc., Res. Conf. on the Shear Strength of Cohesive Soils, Boulder, Colorado, 1960.
11. L'Hermite, M. R. Considerations sur la Viscosite, la Plasticite et le Frottement Interne. Annales de l'Institute Technique du Batiment et des Travaux Publics, No. 8, Paris, Feb. 1948. 6 pp.
12. Reiner, M. Twelve Lectures on Theoretical Rheology, Amsterdam, North Holland Publishing Co., 1949.
13. Rendulic, L. Ein Grundgesetz der Tonmechanik und sein experimentaller Beweis. Bauingenieur, Vol. 8, Berlin. 459 pp.
14. Rutledge, P. C. Review of the Cooperative Triaxial Research Program of the War Department, Corps of Engineers. Soil Mechanics Fact Finding Survey, Progress Rept.: Triaxial Shear Research and Pressure Distribution Studies on Soil. U. S. Waterways Exper. Sta., Vicksburg, Miss., pp. 1-182, 1947.
15. Skempton, A. W., and Bishop, A. W. The Gain in Stability Due to Pore Pressure Dissipation in a Soft Clay Foundation. Cinquieme Congres de Grands Barrages, Paris, 1955.
16. Tschebotarioff, G. P. Soil Mechanics, Foundations and Earth Structures. New York, McGraw-Hill, 1951, 655 pp.
17. Verwey, E. J. W., and Overbeek, J. Th. G. Theory of the Stability of Lyophobic Colloids. Elsevier Publ. Co., 1948.
18. Winterkorn, H. F. Macromeritic Liquids. Symposium on Dynamic Testing of Soils, ASTM Proc., pp. 77-99, 1953.
19. Winterkorn, H. F. Soil Mechanics. McGraw-Hill Encyclopedia of Science and Technology, Vol. 12, McGraw-Hill, 1960.
20. Winterkorn, H. F., and Moorman, B. B. A Study of Changes in the Physical Properties of Putnam Soil Induced by Ionic Substitution. Highway Research Board Proc., Vol. 21, pp. 415-434, 1941.
21. Long Term Stability of Clay Slopes. Geotechnique, June 1964.
22. Scott, R. F. Principles of Soil Mechanics. Addison Wesley, New York, 1963. 550 pp.
23. Lambe, T. W. Soil Testing for Engineers. New York, John Wiley, 1951. 165 pp.

Rock Noise in Landslides and Slope Failures

RICHARD E. GOODMAN and WILSON BLAKE
Respectively, Assistant Professor and Research Assistant, Department of Mineral Technology, University of California, Berkeley

•WHEN a rock specimen is placed under load in the laboratory, acoustic disturbances, known as subaudible rock noise (SARN) are emitted. With a sensitive pickup on the specimen and a high grain amplifier, these noises can be detected and, in fact, a number of people have studied rock noises in the laboratory (1-13). An application of this phenomenon is the detection of noises from stressed rock around tunnels and mines as a safety measure in underground work. With the support of the California Department of Highways, the authors have investigated the possible application of rock noise monitoring to landslide and slope stability problems, and discuss their findings in this report.

After constructing and field testing a suitable rock noise detector, a number of recently active landslides and highway cut slope failures in Northern California were monitored to determine whether or not slides emit detectable rock noises. A variety of types and conditions of material were represented in the study, including sheared shale, soft sandstone and claystone, serpentine, peridotite, gabbro, metamorphic rocks, disintegrated granite, volcanic flows, interflow zones of volcanic ash and stream sediments, and ancient slide debris. At each rock noise monitoring location, a preliminary subjective estimate of the state of activity of the slide was made. "Stable" denotes cuts thought to have been in a safe condition at all times; "active" denotes cuts in which there were recent slide scarps or other diagnostic forms of micro-relief, groundwater flowing at springs or drains, and/or recent tension cracks at the surface; "inactive" denotes cuts in which there had obviously once been movements and in which movements might recur, but which appeared to be in a safe state at the time of observation.

There was a definite correlation between the estimated state of activity and the rock noise rate in these slide areas (Table 1). Most of the areas of high noise rate experienced later movements whereas none of the quiet areas did.

INSTRUMENTATION AND PROCEDURE

A rock noise detection instrument consists of a geophone or probe, an amplifier, and a means of monitoring the output signals. Figure 1 shows the 4-channel instrument used in this work. A common power supply operating through a decoupling unit drives 4 high-grain (137 db) low-noise amplifiers which increase the voltage output of the four crystal probes to a sufficient level for recording on magnetic tape.

Drill holes should be provided for rock noise work, particularly in soft rocks and soils. Probes should be placed below the water table, if possible, to increase the coupling with the slide mass. Covering of shallow holes is recommended to exclude air noises.

Our first rock noise detector consisted of a single probe on a relatively short cable, an audio amplifier, and earphones. Although small and lightweight, this instrument had severe shortcomings for quantitative work; batteries lasted only about 15 min, and there was no permanent record of noises observed in the field. We built an instrument package allowing a longer (up to 3 hr) period of monitoring, used greater lengths of cable to allow positioning of probes at depth in drill holes, and recorded the output on magnetic tape.

Paper sponsored by Committee on Engineering Geology.

TABLE 1

SUMMARY OF ROCK NOISE DATA FROM SOME OF THE NORTHERN CALIFORNIA SLIDE AREAS UNDER STUDY

Location	Description	Initial Estimate of State of Activity	Rock Noises (per min)	Observed Movement Aug. 1963-Aug. 1964
HWY 101 near Arnold	Slide in sheared shale	?	<1	None
HWY 101 near Laytonville	Slump in fault zone, schist	Active	>10	Cracking and bulging about 10-ft net movement
HWY 101 North Laytonville	Slump in gabbro and schist	Inactive	<1	None
HWY 101 near Cummings	Slab slide in sheared shale	Active	>10	No change
HWY 101 - Sylvandale (north of Redway)	Cut for new highway in toe of old slide	Active	>10	About 30-ft net movement
HWY 101 near Miranda	New cut	Stable	<1	
HWY 299 near Weaverville	Rock slide disintegrated granite	Inactive	0	
HWY 99 near Shiloah	Rock falls in altered peridotite	Inactive	0	
Lands End, San Francisco	Creeping landslide in serpentine and serpentine clay	Active	>10	Continuous movement, about 2 in./mo

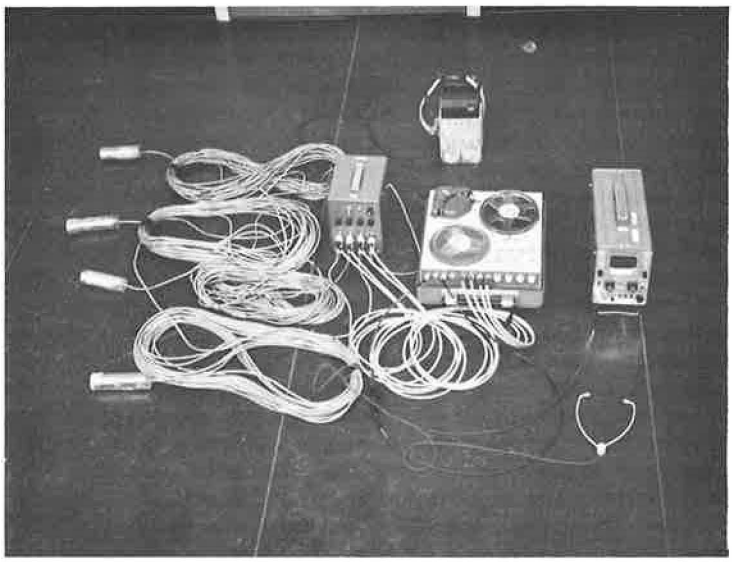

Figure 1. Components of a rock noise detection instrument.

However, a severe limitation was common to both instruments: they consisted of but a single channel.

Single channel rock noise monitoring is satisfactory for monitoring underground work or landslides provided previous work with two or more channels has established

the identity of rock noises and allowed their differentiation from extraneous noise. There are many more sources of extraneous noise near the surface in landslides than there are deep underground in hard rock. Proximity to power lines, radio transmitters, wind and weather, traffic, and construction may make a landslide noisy whether or not there is slide movement. Some of these spurious noises are characteristic and distinct but some resemble true rock noises. Field study with a single channel had demonstrated a correlation between noise rate and slide activity. However, until later work was done with more than one channel, it was not possible to say conclusively whether any given noise event had originated in the slide or was instead some extraneous event such as dripping water or raveling of the sides of drill holes. A small noise near a probe can create intense sounds. To determine a true rock noise event, the investigators reasoned that although the raveling grains or water droplets could excite one probe, they could not possibly have enough energy to send a wave through the earth to a second probe situated more than 10 ft away. Moreover, a true rock noise event, as opposed to a demodulated radio signal, could be expected to travel with the velocity of sound in the medium; therefore, unless its source were equidistant from two probes it would arrive at the separated probes at different times.

To ferret out true SARN events from spurious noises, rock noise was recorded on 4 channels simultaneously, with probe spreads of up to 350-ft radius. Generally, the probe locations were suggested by the availability of drill holes. In the field, during recording, two of the four channels were monitored with earphones on one, and, occasionally, observation of the trace of a portable oscilloscope on a second. In the laboratory, the tape was played back through a 4-trace oscilloscope while listening with earphones on one or another of the channels. When an event appeared to be coincident on two or more channels, a written record was obtained using a high-frequency, direct-writing oscillograph. By playing back the tape at half speed and writing with a paper speed of 50 in./sec, time delays of less than 0.2 milliseconds could be resolved.

CHARACTER OF ROCK NOISE EVENTS AND EXTRANEOUS NOISE

Individual rock noises from landslides and slopes typically consist of high-frequency impulses, ranging from 100 to 1,000 cps, followed by several broadening crossovers. Several events may occur at close intervals creating a train of disturbances that may last for $\frac{1}{10}$ sec or longer. Figure 2 shows a record of a rock noise event. A sudden slippage on a slide during the period of monitoring can create an impulse followed by a damped standing wave if the probe is emplaced in a cased drill hole. Figure 3 shows a record reflecting this type of occurrence.

Earth materials attenuate high-frequency signals in much shorter distances than they attenuate low-frequency signals. Thus, most audio-frequency events are local in origin, originating from within 50 ft of the probe. The attenuation constant of earth materials can be obtained from laboratory experiments on representative samples. However, the frequency range of expectable events cannot be obtained in the laboratory, as the vibration frequency is a system property.

Extraneous noise originating from direct action of wind on the probes sounds like wind and does not complicate rock noise recording. Figure 4a is a record of wind noise. Blowing charges do not cause static because the tubes are shielded. Ground noise generated by blowing trees is of low frequency.

Audio-frequency carrier signals, for example in a telephone line, may create a sustained tone. AC powerlines cause a loud hum which may be filtered out in the laboratory without loss of quality or detail. However, a very strong hum will saturate the amplifier at the gain settings necessary for rock noise recording. A good ground is always necessary.

The crystal probes, even though shielded, will pick up radio signals, especially if monitoring near a radio transmitter. The amplifier, being a nonlinear device, demodulates these signals. There is no confusion with rock noises when the radio message is clear, but when it is garbled or there is static, noises resembling rock noise events may occur. These events may appear on all channels but without measurable delay. At some localities, i.e., in cities at night, the background ratio noise may

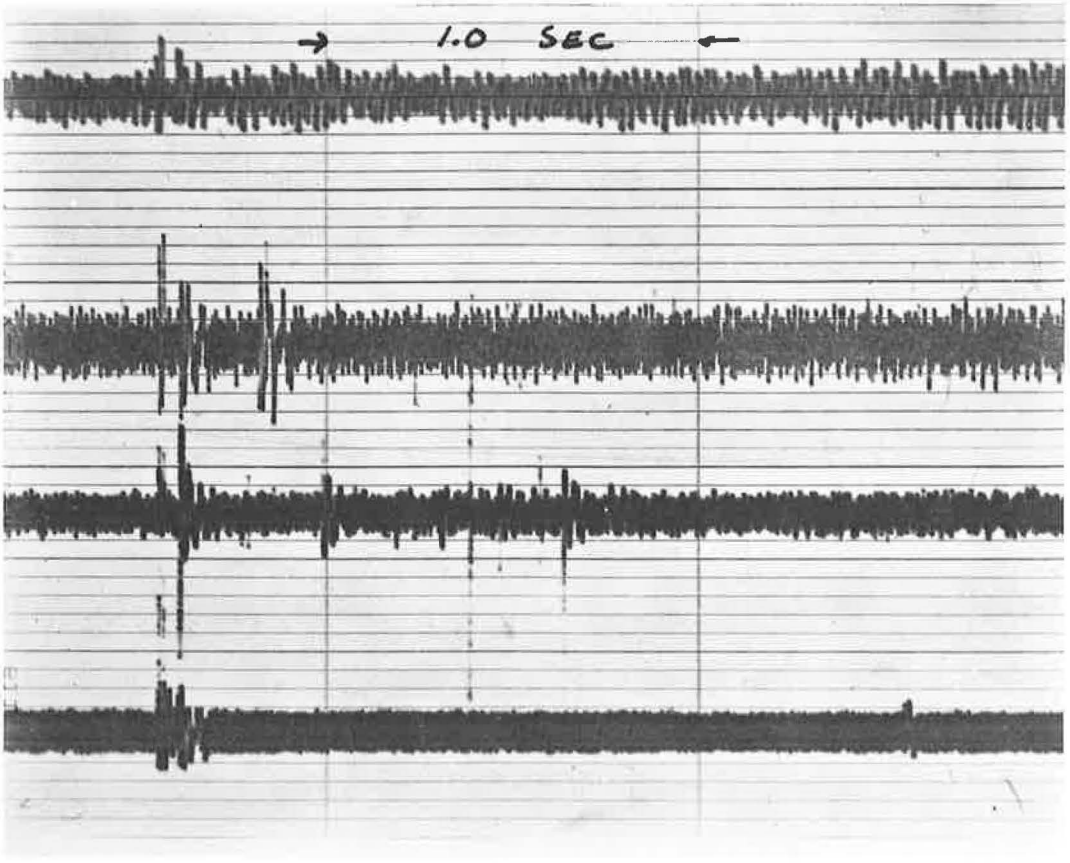

Figure 2. Record of rock noise at Lands End slide.

create a chatter of higher level than rock noise events, effectively blocking the possibility of success in rock noise monitoring.

Talking and traffic noise are recognizable disturbances. Construction activities such as pile driving and percussion drilling do not create difficulties if they are sufficiently distant that the high-frequency portion of their energy input to the ground has been attenuated, i.e., around 500 ft.

Slipping of the probe in the bore hole and raveling of grains onto the probe constitute perhaps the most troublesome sources of extraneous noise in the case of single channel surveys. Even a silt particle causes a sharp snap if it falls onto a probe. Sedimentation on top of a probe positioned below the water table in a drill hole can also cause noise. Intense events lasting $\frac{1}{20}$ sec or longer and appearing only in the channels representing one drill hole were believed to have originated from one of these sources (Fig. 4b). In covered boreholes in hard rock, raveling does not occur.

LOCATION OF ORIGIN OF ROCK NOISE EVENTS

The 4-channel rock noise survey procedure was used because it allowed greater coverage of the slide volume in shorter time, and because receipt of a signal on all four channels makes it theoretically possible to compute the position of the focus of the signal, assuming the medium to be homogeneous.

Let the geophones be positioned at coordinates $P_1 (X_1, Y_1, Z_1)$, $P_2 (X_2, Y_2, Z_2)$, $P_3 (X_3, Y_3, Z_3)$, and $P_4 (X_4, Y_4, Z_4)$, as shown in Figure 5. The wave created by a

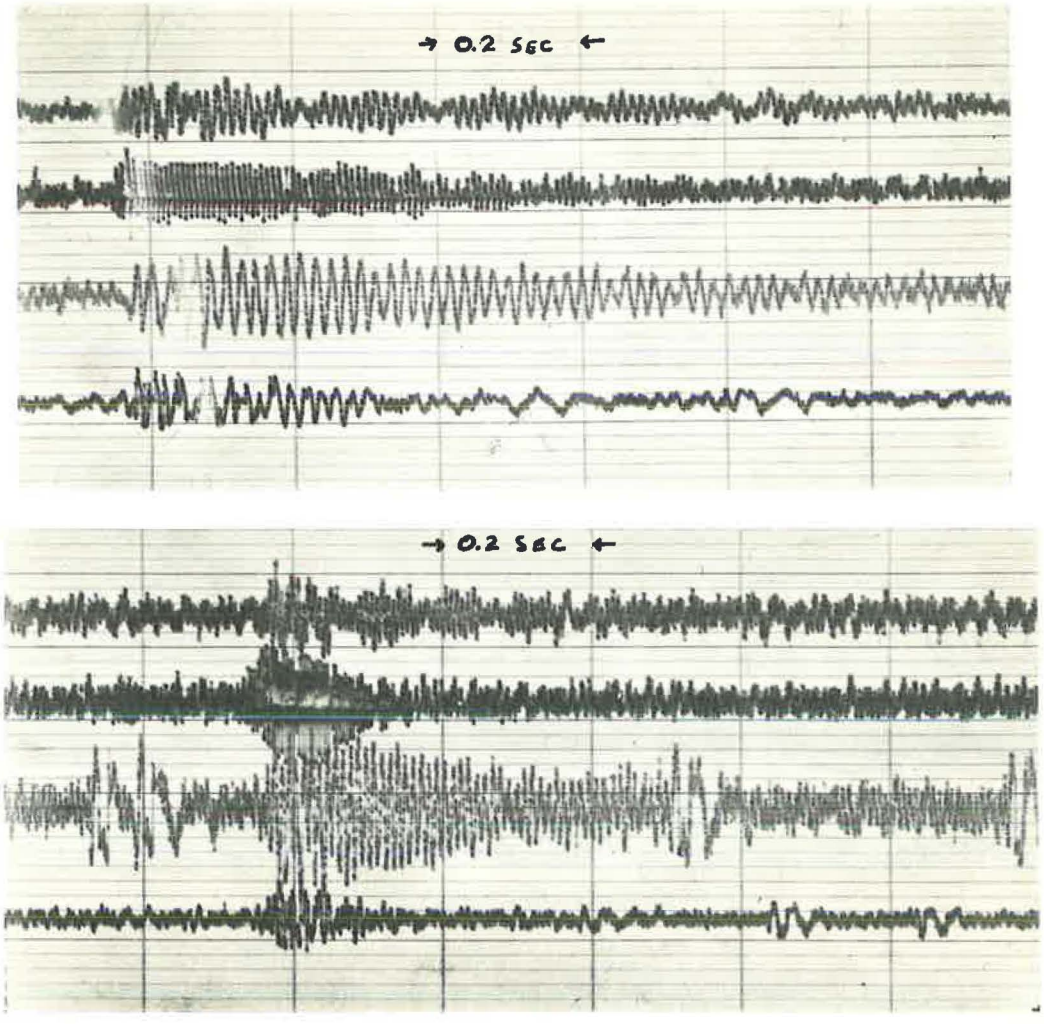

Figure 3. Rock noise records showing sudden slippage on slide.

disturbance at P_o (X_o, Y_o, Z_o) strikes P_1 at time t_1, P_2 at time t_2, P_3 at time t_3, and P_4 at time t_4.

L_1 is the unknown distance from P_o to P_1, and L_{1j} are the differences in focal distances from P_1 and P_j, as shown in Figure 5. If c is the wave velocity in the medium

$$c\,\Delta t_{1j} = L_{1j}$$

$$= \sqrt{(X_j - X_o)^2 + (Y_j - Y_o)^2 + (Z_j - Z_o)^2} - \sqrt{(X_1 - X_o)^2 + (Y_1 - Y_o)^2 + (Z_1 - Z_o)^2}$$

$$j = 2, 3, 4$$

where Δt_{1j} are the 3 differences in arrival time (delay times) between probe positions 1 and 2, 3, and 4.

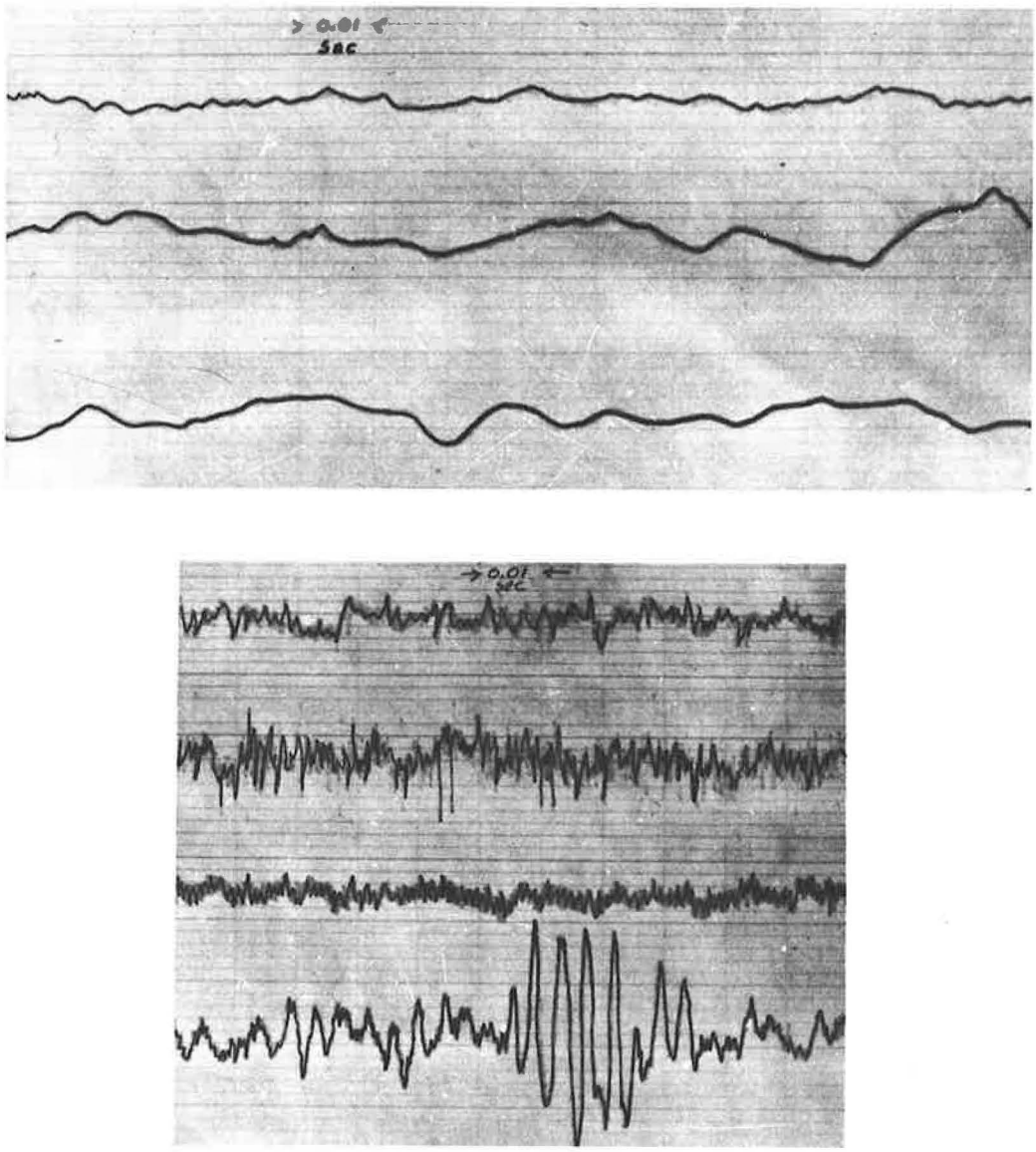

Figure 4. Oscillograph records: (a) wind noise; (b) noise from raveling grains in a borehole.

After simplification and manipulation, these three equations in three unknowns (X_o, Y_o, Z_o) have been solved by iteration on a digital computer.

To check the validity of this method of calculation and the ability of the instrumentation and interpretation techniques to resolve the focus coordinates from actual data, a laboratory experiment was performed. A circular tank 3 ft in diameter and 2 ft high was filled with run of crusher stone and mixed with water to a uniform and essentially homogeneous consistency. Four geophones were placed in the soil and an energy impulse was generated at a known coordinate. The wave velocity was determined from knowledge of the shock time and the first arrival time at any given probe. Figure 6 shows a typical determination of focus coordinates.

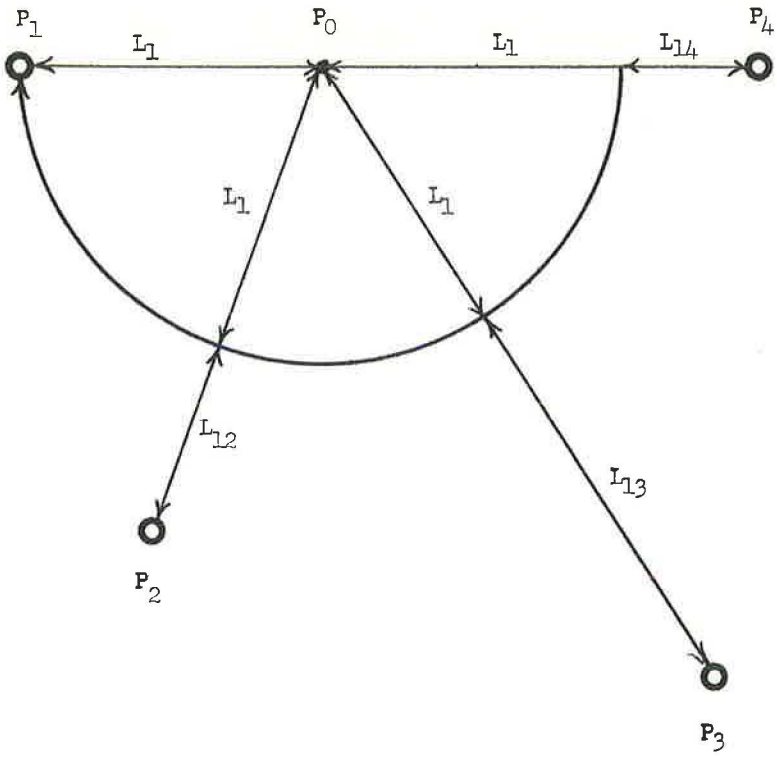

Figure 5. Geometry of delay time analysis.

The first arrival determination was as follows:

t_0 = 2/18 cm × 5 msec/cm = 0.555 msec
t_1 = 3.4/18 cm × 5 msec/cm = 0.943 msec
t_2 = 3.75/18 cm × 5 msec/cm = 1.041 msec
t_3 = 6.9/18 cm × 5 msec/cm = 1.930 msec

The velocity calculations were the following:

6 in./0.555 msec = 10,810 ips
10.1 in./0.943 msec = 10,710 ips
11.25 in./1.041 msec = 10,800 ips
20.9 in./1.930 msec = 10,830 ips

The calculated impulse coordinates (8.852, 0.974, 5.046) were within $\frac{1}{10}$ in. of the true focus, in which the coordinates were 8.75, 1.00, 5.00.

Despite the success of the laboratory experiment, difficulty was experienced in focus determination in the field. Blast experiments (Fig. 7) with known focus and probe coordinates demonstrated extreme velocity variations and attenuation of the high frequency portion of the blast energy over short distances in slides in soft, clayey materials. In landslide material, a successful focus determination of a natural rock noise event has not yet been accomplished. Instrumental difficulties of one sort or another limited the number of hours of rock noise records successfully obtained on all four channels simultaneously. Rock noise events that were recorded on all channels could not be analyzed because of the effect of casing in the drill holes, or because of velocity differences resulting from the fact that probe emplacements were on either side of the water table or on either side of the slide boundary. Consistent velocities were obtained only in holes all above or all below the ground water table at small separations.

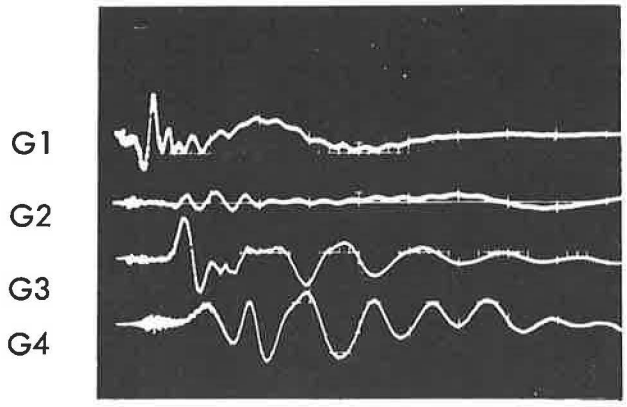

Figure 6. Typical determination of focus coordinates.

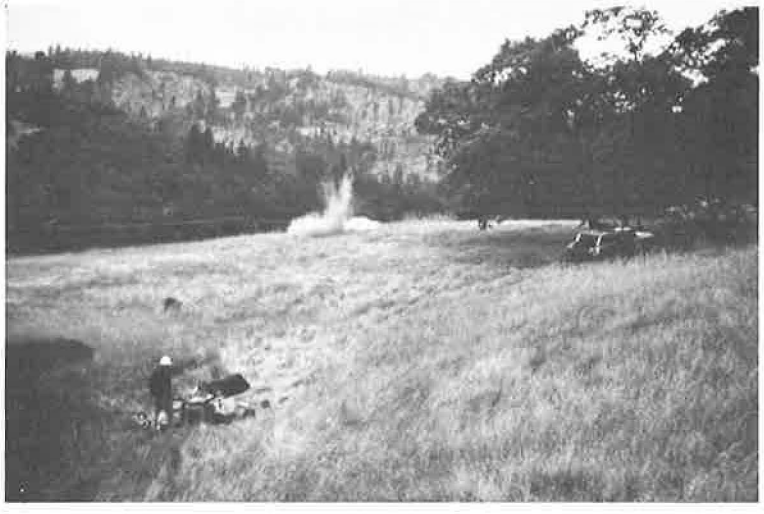

Figure 7. Blast experiment at Sylvandale slide.

DISCUSSION OF DATA

Sylvandale Slide

In August 1963, limited rock noise monitoring in a new freeway cut near Sylvandale on Highway 101 showed a very high rate of rock noise activity. Field investigation of the gently sloping hillside above the cut revealed large deep cracks throughout a large region. Subsequently large movements of approximately 30 ft have occurred and the limiting escarpments of a half-elliptical sliding mass roughly 100 ft long and 600 ft in maximum width have become evident. The slide (Fig. 8) appears to be a reactivated region of a large older landslide and is located in a sequence of shales between two ribs of resistant sandstone of the Franciscan Formation.

Considerable corrective work has been performed, most notably flattening of the highway cut slope and installation of drains. There is evidence of continuing minor movements in shear displacements on the latest cut face. However, the upper regions of the slide have shown no evidence of change since December 1963.

Figure 8. Sylvandale slide.

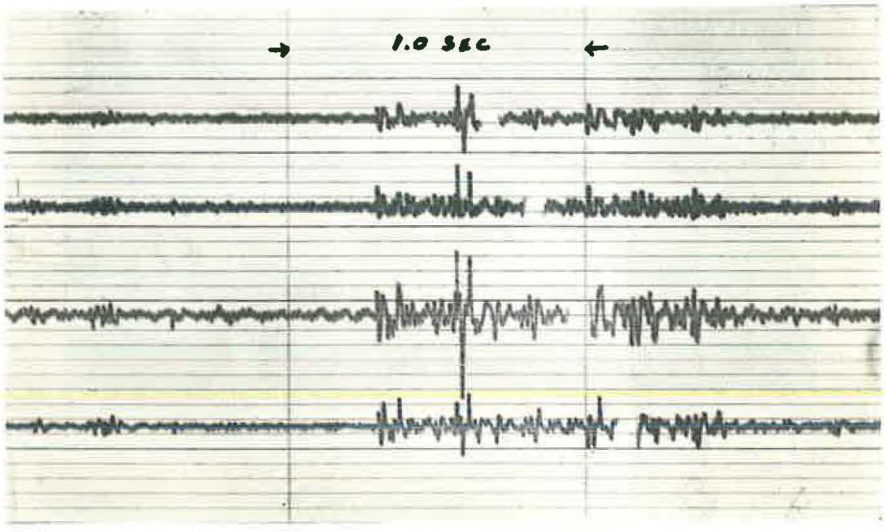

Figure 9. Rock noise record from northern slide extremity at Sylvandale, January 1964.

The slide was monitored a number of times for periods of several hours during the year following its discovery. The upper region of the slide, which now appears inactive, has been quiet since December 1963. Near the top of the cut face, high rock noise rates preceded large movements as the slide spread into previously undisturbed ground (Fig. 9).

Lands End Slide

This slide, located on the Golden Gate at the northwest extremity of San Francisco, has had a long history of activity consisting of intermittent major movements followed by periods of creep (see Fig. 10). The last major movement occurred in 1955.

Figure 10. Lands End slide, April 1964.

The slide is located in sandstone and Franciscan serpentine locally altered to clay. Slope indicators emplaced in the slide, under the direction of H. B. Seed, have shown that creep is presently continuing at a rate of up to ½ in./mo.

Rock noise surveys have been carried out intermittently at Lands End since May 1963. Probes have been positioned at various depths in cased slope indicator holes. The average rock noise rate has remained very high, from 25 to 40 SARN/min. The rate is independent of the duration of monitoring, indicating that in an actively creeping landslide, a 10-min monitoring period is sufficient to determine the rock noise rate. Some of the events were recorded coincidently with delay on two or more channels when spreads of less than 60 ft were employed. When two geophones were placed in a single hole, the majority of events appeared, with suitable delay, on both channels.

Highway Cut in British Columbia

Soon after excavation of the first bench of a large mountainside highway cut, in granite, a continuous crack opened up 300 ft above the highway. Inclined holes several feet long were drilled into the suspected projection of the surface crack and rock noise monitoring was performed in April 1964. This survey showed an extreme rate of rock noise, greater than 40 SARN/min. Subsequent to this survey, new cracks opened, minor rock falls occurred, and the safety of the cut became so questionable that a warning system was installed and continuous watch was initiated. A second rock noise survey, made a month later, showed a noise rate of less than 1 SARN/min, suggesting that the cut had stabilized at least temporarily. Although cracks have continued to open, a major rock fall has not occurred in the three months following this survey.

CONCLUSION

During the two years of this investigation, about 50 hr of rock noise recordings were made and some 15,000 noise events were examined in the laboratory. About 40 separate slides or cuts were monitored. We have reached the following conclusions concerning the applicability of the rock noise method to landslides and cut slopes.

1. There is no question that actively creeping landslides generate detectable audio frequency disturbances.
2. Because of the necessity to distinguish rock noise from extraneous sources of noise, such as raveling of the sides of boreholes, radio static, and telephone messages, a multichannel survey should be performed.
3. Most rock noises received by a probe in a landslide originate within a distance of 100 ft.

4. The rate of attenuation of high-frequency signals and the variation of wave velocities over short distances in soft landslide materials makes it difficult to determine the focus of a rock noise event. In rockslides focus determination is practical.

5. No rock noises have been detected in rock cliffs and steep rock cuts subject to frequent rock falls.

6. Rock noise monitoring does forewarn of accelerated movements in landslides and rockslides.

ACKNOWLEDGMENTS

The authors wish to extend their appreciation to the following: F. D. Beard, Liberty Mutual Insurance Company; Ben Lennert, Soils Engineer; Dan Moye, Visiting Lecturer in Geological Engineering, 1962-1963; Professor Stanley H. Ward; Dr. Richard La-Force; Marvin Ma Cauley, Geologist for the Materials and Research Laboratory, Department of Highways; W. D. Kovacs, graduate student in Soil Mechanics; Thomas A. Lang, Lecturer in Geological Engineering; Thomas Thompson, Lecturer in Geological Engineering; and the following students: Gary Glaser, Ron Gesley, Vince Howes, Robert Miller, Bob Bradbury, Roy Clifton and Jeff Kennedy.

REFERENCES

1. Obert, L. Use of Subaudible Rock Noises for Prediction of Rock Bursts. U. S. Bur. of Mines, RI 3555, 1941.
2. Obert, L., and Duvall, W. Use of Subaudible Noises for Prediction of Rock Bursts. Pt. II. U. S. Bur. of Mines, RI 3654, 1942.
3. Obert, L., and Duvall, W. Microseismic Method of Predicting Rock Failures in Underground Mining. Pt. I. General Methods, U. S. Bur. of Mines, RI 3797, 1945.
4. Obert, L., and Duvall, W. Microseismic Method of Predicting Rock Failures in Underground Mining. Pt. II. Lab. Exp., U. S. Bur. of Mines, RI 3903, 1945.
5. Obert, L., and Duvall, W. Microseismic Method of Determining the Stability of Underground Workings. U. S. Bur. of Mines Bull. 573, 1957.
6. Crandall, F. J. Determination of Incipient Roof Failures in Rock Tunnels by Micro-Seismic Detection. Jour. of Boston Soc. of Civ. Eng., Jan. 1955.
7. Persson, T., and Hall, B. Microseismic Measurement for Predicting the Risk of Rock Failures and the Need for Reinforcement in Underground Cavities. Royal Inst. of Tech., Stockholm, Sweden, 1958.
8. Beard, F. D. Predicting Slides in Cut Slopes. Western Construction, p. 72, Sept. 1961.
9. Obert, L., and Duvall, W. Seismic Methods of Detecting and Delineating Subsurface Subsidence. U. S. Bur. of Mines, RI 5882, 1961.
10. Boyum, Burton H. Subsidence Case Histories in Michigan Mines. Proc., Fourth Symp. on Rock Mech., Pennsylvania State Univ., 1961.
11. Mogi, Kiyoo. Study of Elastic Shocks Caused by the Fracture of Heterogeneous Materials and Its Relationship to Earthquake Phenomena. Bull. of Earthquake Res. Inst., Vol. 40, pp. 125-173, 1962.
12. Goodman, R. E. Subaudible Noise During Compression of Rock. GSA Bull. Vol. 74, No. 4, 1963.
13. Suzuki, T., Sasaki, K., Siohara, Z., and Hirota, T. A New Approach to the Prediction of Failure by Rock Noise. Proc., Fourth Internat. Conf. on Strata Control and Rock Mech., New York, May 4-8, 1964.

Treatment of Crushed Stone with Quaternary Ammonium Chloride

T. DEMIREL, M. H. FARRAR, and J. M. HOOVER, Iowa State University

ABRIDGMENT

•THE EFFECT of a quaternary ammonium salt on the stability of a base course material treated with varying percentages of the salt and exposed to the action of water was determined by investigating its shearing strength.

The quaternary ammonium salt used was dioctadeyl dimethyl ammonium chloride.

The granular base course material used was a crushed rock obtained from a quarry located in Taylor County, Iowa, classified as A-1-a. This material, although meeting the AASHO specifications for base courses, was very susceptible to the action of water, as indicated by its soaked CBR value of 33 at standard AASHO density.

Preliminary investigations were conducted to establish the maximum dry densities and optimum moisture contents. Curing studies were also conducted by air-drying the specimens to establish the residual moisture contents at which the soaked specimens would give the maximum immersed CBR.

The specimens for determination of shearing strength were molded by vibrational compaction to near Standard Proctor density at the optimum moisture contents. The specimens were confined in rubber membranes, and then were cured by air-drying. They were soaked vertically in water which worked into the soil from the bottom up for about 48 hr, and were tested by the unconsolidated-undrained triaxial shear test. The Mohr envelopes and their 95 percent confidence limits were evaluated using the least squares method developed by Balmer (1). The results are summarized in Table 1.

TABLE 1

EFFECT OF QUATERNARY AMMONIUM SALT ON APPARENT COHESION AND APPARENT ANGLE OF SHEARING RESISTANCE OF GRANULAR BASE COURSE MATERIAL[a]

Arquad 2HT Content (%)	Apparent Cohesion (psi)	Angle of Shearing Resistance (deg)
0	11.5±6.5	16.5±5
0.01	4 ±2	23.1±2.6
0.03	7.5±1.5	22.7±1.2
0.05	6 ±2	24.3±1.3

[a]Evaluated using total principal stresses determined by undrained, quick triaxial tests.

The apparent cohesion and apparent angle of shearing resistance (based on total stresses) are unlike the true apparent cohesion and angle of shearing resistance (based on effective stress), neither independent variables of the shearing resistance nor basic properties of a soil; they depend extensively on the pore pressure (neutral stress) developed within the stressed soil-water system. The determination of true apparent cohesion and angle of shearing resistance and their use require careful examination of

Paper sponsored by Committee on Physico-Chemical Phenomena in Soils.

neutral stresses which, in certain cases such as road base courses, may be unpredictable, undeterminable, and inconsistent due to the heterogeneous nature of the material and the variable nature of such field conditions as loading and seepage patterns. The apparent cohesion and apparent angle of shearing resistance, however, under prevailing conditions determine the shearing resistance of the material (soil-water system) according to Coulomb's empirical law of shearing resistance. For example, prevailing conditions for a material protected against the ingress of water do not allow the development of significant and fluctuating pore pressure, resulting in high and stable values of apparent cohesion and/or apparent angle of shearing resistance. In other words, these paramenters indicate the stability attained by a treatment. For these reasons and because of its simplicity the undrained quick test was used.

Waterproofing additives, by controlling the impregnation of the material by water, reduce and stabilize pore pressure development and thus eliminate high magnitudes and fluctuations of developed neutral stresses, and result in high shearing resistance and stability.

The addition of the quaternary ammonium salt to the granular base material caused a significant reduction in the fluctuations of both apparent cohesion and apparent angle of shearing resistance (Table 1). A possible explanation of the mechanism of waterproofing action of the quaternary ammonium salt on water susceptible granular material is that a granular material is made up of aggregate-size structural units with large pores between these units. The structural units are particles of gravel, sand, and silt cemented together by clay. When the material is untreated, water penetrates into the large pores and into the structural units, which may cause segregation of fines and may increase the pore pressure with the structual units. The water in large pores is assumed to have little effect on the neutral stresses affecting the shear strength of a granular material but the water within the pores of structural units does. Due to heterogeneity of the granular material augmented by the action of water (segregation of fines causing a sort of plug against the entrance of water) moisture adsorption and the pore pressures within these structural units of untreated material may vary, causing significant fluctuations in shearing strengths of different samples or of different parts of the base of a road. These fluctuations are evidenced by high values of 95 percent confidence limits.

When the material is treated the aggregation is increased due to coagulant action of the quaternary ammonium salts, leading to reduced segregation during compaction (better homogeneity), and the structural units are waterproofed against the penetration of water. Water then enters only the large pores. The pore pressure within the structural units is limited to a stable equilibrium value that is far less than the maximum pore pressure developed in soaked-untreated material.

The following conclusions are based on the data obtained.

Quaternary ammonium salts are effective additives for improving the shear strength of a water susceptible granular material under adverse moisture conditions. Without treatment the shear strength of the material varies greatly. The average shear strength of the untreated material is significantly lower than that of treated materials. There is little variation in the shear strength of treated material under extreme moisture conditions, eliminating the uncertainties otherwise inescapable and risky for design purpose.

REFERENCE

1. Balmer. ASTM, Proc., Vol. 52, pp. 1260-1271, 1952.

Consolidation Characteristics of Stabilized Clayey Soils

J. G. LAGUROS, Department of Civil Engineering, University of Oklahoma, Norman

ABRIDGMENT

•THREE typical clayey soils were stabilized with portland cement, lime, and sodium hydroxide, and their consolidation characteristics were compared with those of the natural soils.

The soils, whose clay content varied, contained kaolinite, illite, or montmorillonite as the clay mineral. They were compacted to standard proctor density at optimum moisture content, then cured for 28 days in near 100 percent relative humidity at room temperature and subsequently tested in a double drainage fixed type consolidometer up to 8 kg/cm^2 loads. Two sets of tests were run: the saturated and the unsaturated.

In all cases, the beneficial effect of stabilization was observed by the flattening of the e-log p curves. However, it was difficult to distinguish between the relative effects of stabilizing agents as the e-log p curves tended to fall within a narrow band whereas the 28-day unconfined compressive strengths indicated the differences very conclusively. This is explained by the fact that the unconfined compressive strength is a measure of a property well within the plastic range of the soil, but the consolidation test covered only a small part of this range. The rebound curves attest to this. Also, the rebound curve data obtained after the application of the 8 kg/cm^2 load indicated that the difference between the natural soils and the stabilized soils was minimized. Thus, consolidation seemed to have a stabilizing character, whose influence approached that of the stabilizing agents at high compressive loads only.

The application of the consolidation load caused a rearrangement of the particles and the geometry of the soil structure apparently changed. The change was large for the natural soil and small for its stabilized counterpart. The major contribution of stabilizing agents was to bring about an initial bonding which prevented the detrimental effect of thickness change in the soil-pavement components.

Consolidation, being a time-dependent phenomenon, presents a problem which is analyzed in terms of the coefficient of consolidation, C_v. The effects of stabilization were apparent when comparing C_v values of natural and stabilized soil mixes. Increases from about 40 to 400 percent were observed, with the kaolinitic clayey soil located in the lower range, the montmorillonitic in the upper range, and the illitic in between. However, the increase in the coefficients of consolidation appeared functionally related not to a specific property but rather to a composite parameter of the clayey soils. In the saturated consolidation tests, the C_v values remained constant for the incremental load system used but in the unsaturated consolidation tests they tended to decrease slightly with an increase in compression loads.

Paper sponsored by Committee on Physico-Chemical Phenomena in Soils.

Entrapped Air Effects on Soil Suction Measurements

R. N. YONG and R. S. CHAHAL, McGill University, Montreal, Quebec, Canada

ABRIDGMENT

•THE PARTICLE interaction characteristics in a soil-water system may be measured and described in terms of soil suction (pF) or moisture potential. Of the many methods available for measurement of soil suction, the two most common techniques utilize either the Richards pressure method (1949) or the Haines tension apparatus (1930). The characteristic soil suction or moisture potential curve obtained by the pressure technique may not represent the actual condition of the soil water as determined by the Haines tension method.

Because of the possibility of air bubbles nucleating in the soil water after release of pressure from the pressure technique, the corresponding tension in the water will not be equivalent to that obtained from actual initial tension measurements. The results of study on an initially unsaturated coarse silt fraction show that at a water content of 23 percent, the tension method indicated that the moisture potential was 8 cm of mercury, whereas the pressure method gave a value of 17 cm of mercury. The discrepancy becomes less with decreasing water contents. At 13 percent water content, the moisture potential derived was 24.5 cm and 27.4 cm of mercury for the tension and pressure methods, respectively. Experiments on a fine fraction silt showed that the discrepancy between the two techniques was less at the same water contents.

A theoretical expression is derived relating moisture potential with changes in pressure which may be related directly to the volume of entrapped air.

$$\frac{\partial v}{\partial \psi} = \frac{\frac{\partial \theta}{\partial \psi}(1+k)\,(B + J\alpha^{-1/3}) - \alpha}{B + J\alpha^{-1/3}}$$

where

ψ = moisture potential;
v = total volumetric water content (includes volumetric entrapped air content);
α = volumetric entrapped air content;
θ = actual volumetric water content;
k = fraction of volume of water filled with entrapped air or vapor bubbles;
$J = \frac{4\sigma}{3}\left(\frac{4\pi n}{3}\right)^{1/3}$, where σ is surface tension of water, and n is number of bubbles per unit volume of soil; and
$B = \psi + p$, (p = pressure).

In the theoretical development for air entrapment, the successful use of the equation derived depends on one's ability to provide values for volumetric entrapped air content and estimation of the compression of trapped air bubbles. This development is restricted because of the difficulty in measuring the rate at which the trapped air may be increasing or decreasing.

The results show clearly that soil moisture potential measurements obtained using either the pressure or tension technique do not lend themselves to the description of equivalent tensions in the soil water. For soils in the initially unsaturated state, the

Paper sponsored by Committee on Physico-Chemical Phenomena in Soils.

difference between actual and assumed tensions is maximum before air entry. Following air entry, this difference becomes progressively smaller. In the case of the initially saturated samples, because of the absence of initial air content, the values for actual and assumed tension correspond exactly until air entry. Following air entry, these values begin to diverge and remain divergent even at the lower ranges of water content.

The differences in tension recorded by the two techniques lead to the conclusion that the tensiometer method would provide a more realistic picture of the tension in the soil water. However, this technique is necessarily restricted to pressure differences below one atmosphere. The energy relationship between soil and water described in terms of soil suction or soil moisture potential is, in essence, a reflection of the tension in the soil water. Unless an accurate assessment of this phenomenon is made, predictions and correlations using soil suction measurements must be made with total awareness of the air entrapment effect. As long as the technique is specified, and comparisons are made within the same technique, the error involved in correlative studies may at best be given the role of a constant.